STOL TACTICAL AIRCRAFT INVESTIGATION

Volume II, Part II

A Lifting Line Analysis Method for Jet-Flapped Wings

Franklyn J. Davenport

Approved for public release; distribution unlimited.

FOREWORD

This report was prepared for the United States Air Force by The Boeing Company, Seattle, Washington in partial fulfillment of Contract F33615-71-C-1757, Project No. 643A. It is one of eight related documents covering the results of investigations of vectored-thrust and jet-flap powered lift technology, under the STOL Tactical Aircraft Investigation (STAI) Program sponsored by the Air Force Flight Dynamics Laboratory, Air Force Systems Command, Wright-Patterson Air Force Base, Ohio. The relation of this report to the others of this series is indicated below:

AFFDL TR-73-19	STOL TACTICAL AIRCRAFT INVESTIGATION	
Vol I	Configuration Definition: Medium STOL Transport with Vectored Thrust/Mechanical Flaps	
Vol II Part I	Aerodynamic Technology: Design Compendium Vectored Thrust/Mechanical Flaps	
Vol II Part II	A Lifting Line Analysis Method for Jet-Flapped Wings	This Report
Vol III	Takeoff and Landing Performance Ground Rules for Powered Lift STOL Transport Aircraft	
Vol IV	Analysis of Wind Tunnel Data, Vectored Thrust/Mechanical Flaps and Internally Blown Jet Flaps	
Vol V Part I	Flight Control Technology: System Analysis and Trade Studies for a Medium STOL Transport with Vectored Thrust and Mechanical Flaps	
Vol V Part II	Flight Control Technology: Piloted Simulation of a Medium STOL Transport with Vectored Thrust/Mechanical Flaps	
Vol VI	Air Cushion Landing System Study	

The work reported here was performed in the period June 1971 through January 1973 by the Aero/Propulsion Staff of the Research and Engineering Division, Aerospace Group, The Boeing Company. Mr. Franklyn J. Davenport served as Program Manager.

The Air Force Project Engineer for this investigation was Mr. Garland S. Oates, Air Force Flight Dynamics Laboratory, PTA, Wright-Patterson Air Force Base, Ohio.

This report was released within The Boeing Company as Document D180-14409-2, and submitted to the Air Force in June 1973.

This technical report has been reviewed and is approved.

E. J. Cross Jr.

E. J. Cross Jr., Lt. Col., USAF
Chief, Prototype Division
Air Force Flight Dynamics Laboratory

TABLE OF CONTENTS

LIST OF FIGURES (Continued)

LIST OF SYMBOLS

A	Aspect ratio, b^2/S
b	Wing span, ft
c	Local chord, ft
$\bar{c}$	Wing mean aerodynamic chord, ft
$c_{()}$	Section aerodynamic coefficient, as indicated by subscript. (Section coefficients are nondimensionalized by local extended chord and dynamic pressure as indicated in the text.)
$C_{()}$	Wing aerodynamic coefficient, as indicated by subscript.
D	Wing drag, lbs
d	Section drag, lbs/ft
e	Flap extension ratio
E	Wake "extension distance", ft
J	Jet flap thrust, lbs
L	Wing lift, lbs
ℓ	Section lift, lbs/ft, or wing rolling moment, ft-lbs (as indicated by context)
m	Section pitching moment, ft-lbs/ft, or wing pitching moment, ft-lbs
n	Yawing moment, ft-lbs
q	Dynamic pressure, $1/2\,\rho V^2$, lbs/sq ft (Sometimes based on other velocities, as indicated by text.)
S	Wing area, sq ft
V	Freestream velocity, ft/sec
w	Downwash velocity, ft/sec
Y	Side force, lbs

SECTION I

INTRODUCTION AND SUMMARY

1.1 Introduction

The U.S. Air Force's need for modernization of its Tactical Airlift capability led to establishment of the Tactical Airlift Technology Advanced Development Program (TAT-ADP), contributing to the technology base for development of an Advanced Medium STOL Transport (AMST).

The AMST must be capable of handling substantial payloads and using airfields considerably shorter than those required by large tactical transports now in the Air Force inventory. If this short field requirement is to be met without unduly compromising aircraft speed, economy, and ride quality, an advanced-technology powered-lift concept will be required.

The STOL Tactical Aircraft Investigation (STAI) is a major part of the TAT-ADP, and comprises studies of the aerodynamics and flight control technology of powered-lift systems under consideration for use on the AMST. Under the STOL-TAI, The Boeing Company was awarded Contract No. F33615-71-C-1757 by the USAF Flight Dynamics Laboratory to conduct investigations of the technology of the vectored-thrust and internally blown jet flap powered-lift concepts. These investigations included:

- o Aerodynamic analysis and wind tunnel testing
- o Configuration studies
- o Control system design, analysis, and simulation

This report presents the results of an analytical investigation of the aerodynamics of jet flapped wings, with emphasis on drag behavior in conditions where the classical assumption of an essentially planar system of wing, jet, and trailing vortex system no longer gives satisfactory results. The analysis method was intended to apply not only to wings with "internally blown" jet flaps, but also to wings with externally blown jet flaps or with upper surface blowing.

1.2 Summary

An analytical procedure was developed to calculate the spanwise load distribution, forces, and moments on wings embodying the jet flap powered lift concept. The procedure is programmed to be run on a CDC 6600 digital computer. It is capable of analyzing configurations having up to six separate "panels" of differing flap angle and jet momentum per side. The jet distribution and orientation can be varied so as to correspond either to internally blown flaps (momentum proportional to local wing chord, blowing normal to hinge line) or to externally blown flaps (momentum unrelated to wing chord, blowing direction parallel to the aircraft plane of symmetry).

The analysis uses a nonplanar trailing vortex system in order to determine the component of induced velocity antiparallel to the relative wind. That component, neglected in the analysis methods hitherto available, becomes important when the very large circulation lift levels typical of jet flaps are reached. Its effect is generally to reduce the lift corresponding to a given value of induced drag, so its neglect is unconservative.

Comparison of performance data predicted by this analysis with wind tunnel test results indicates that use of the nonplanar vortex system concept accounts, in several cases, for substantial drag increments which had previously defied explanation. However, as presently formulated, the procedure over-predicts drag at very large flap deflections. Also, some difficulties in the iteration process have been encountered where local jet momentum is very high (i.e., in externally blown cases) and the jet deflection angles are large.

It is the view of the author that nonplanar trailing vortex geometry is an essential element in the explanation of jet flap drag behavior, and that the method of this report deserves further development. It is felt that adjustment of the relation between jet momentum, angle of attack and jet angle to the lifting circulation and the trailing vortex geometry details can lead to a calculation procedure giving good results for the whole range of jet flap configurations of interest in the STOL field.

SECTION II

THEORY

2.1 Background

The theory of the jet flapped wing in two dimensions is complicated by the fact that it is a "mixed" boundary value problem. The customary requirement of classical airfoil theory, zero net normal flow at the airfoil surface, is only part of it. Downstream of the trailing edge, the same condition must be met for an unknown jet shape. In addition, the loading there must just suffice to turn the jet. This problem was solved by Spence[1,2] using "classical" mathematical methods and by Malavard[3] using the rheoelectric analogy, with essentially equivalent results.

The jet flapped wing of finite span is much less tractable. Maskell and Spence's[4] formulation of the problem could only be solved by drastic simplification, which amounted to reducing the wing-jet system to an elliptically loaded lifting line. Malavard[5] obtained some interesting solutions to the three-dimensional lifting surface problem using the rheoelectric analogy, but the inconvenience and special equipment required make that approach unsuitable for design purposes. More recently, Lopez and Shen[6] and Lissaman[7] have reported relatively convenient methods of analyzing jet flapped wings of arbitrary geometry.

All of these methods use linearized boundary conditions, and do not account for the streamwise component of induced velocity due to the vertical displacement of the trailing vortex system, as diagrammed in Figure 1. This streamwise component causes a reduction in lift, but no saving in drag, for any given value of the "bound" circulation on the wing. The drag polar can be significantly affected at the lift coefficient levels generated by the jet flap, especially in the case of partial span blowing. Furthermore, this effect implies an upper limit to aerodynamic (or "circulation") lift which is determined by span, as opposed to section characteristics. Helmbold's analysis[8], which accounts for the effect of roll-up on the angle of the vortices downstream, gives a limiting value of 1.9 times the aspect ratio for circulation lift. Lift and drag data for a blown wing at very high momentum coefficient, reported by Lockwood, Turner and Riebe[9], agree with this result.

2.2 Strip Analysis

The approach adopted here is to divide the wing into strips for which the section lift and moment coefficients depend only on the local angle of attack (α), flap deflection (δ_F), and momentum coefficient (C_J). This sacrifices some realism, especially for low aspect ratio configurations, but greatly simplifies the analysis and reduces computation time.

2.2.1 Vortex Structure

Each strip has an associated "horseshoe" vortex, as diagrammed in Figure 2. Induced velocities are calculated at control points located at the nominal quarter-chords of the centers of the strips, which coincide

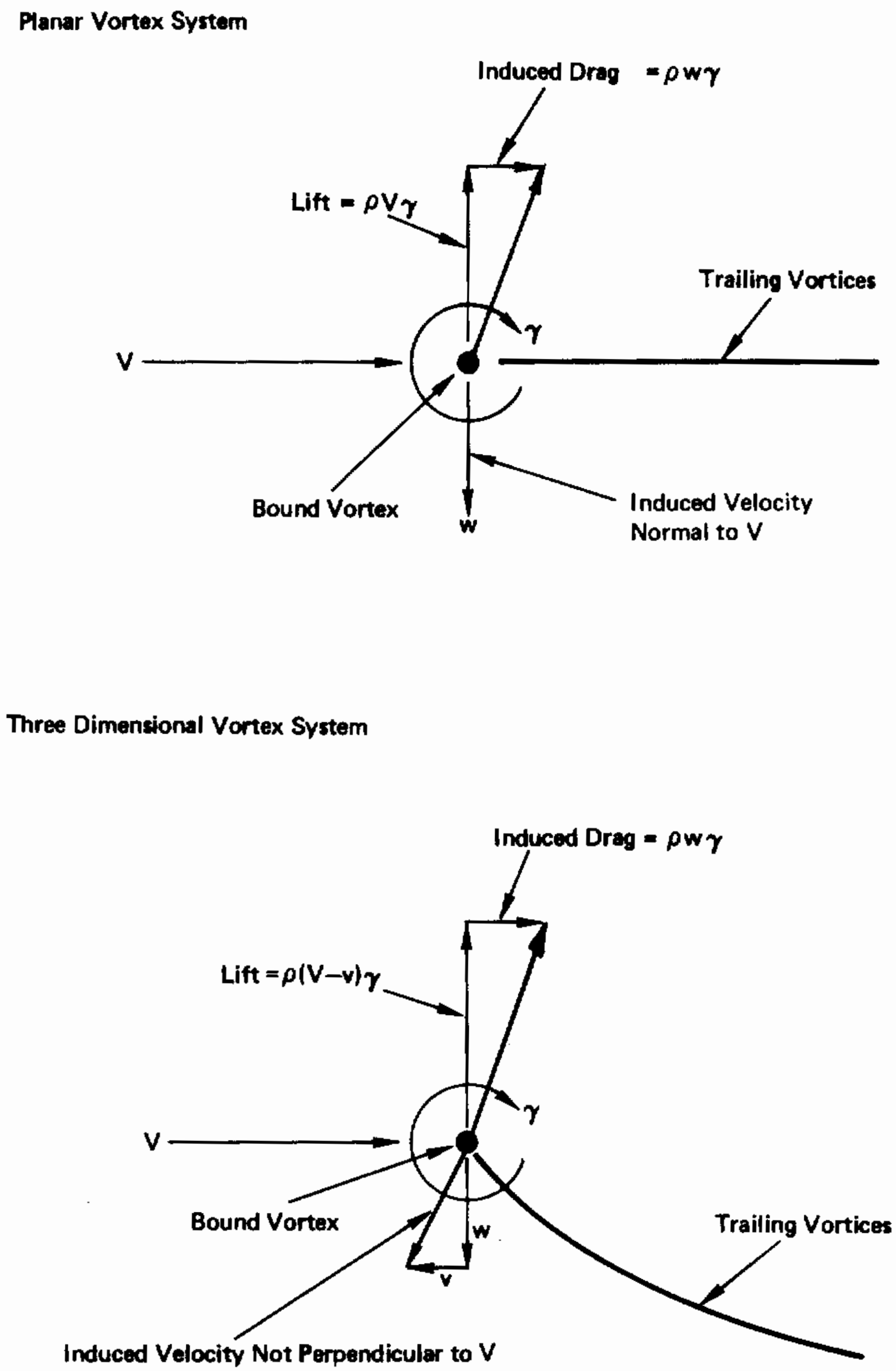

Figure 1: Effect of Vortex Wake Vertical Structure on Aerodynamic Forces

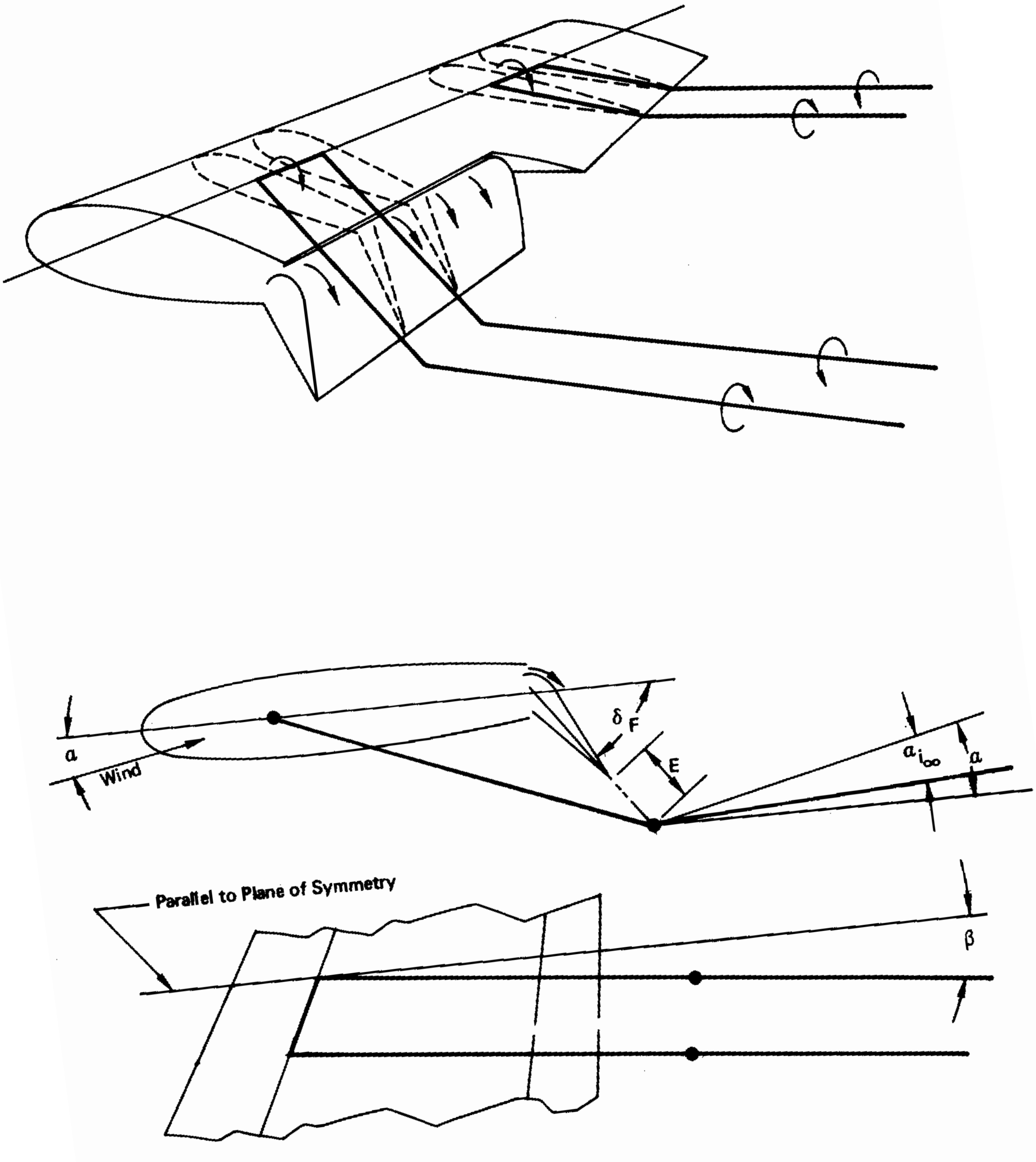

Figure 2: Vortex Structure

with the centers of the "bound" segments of the horseshoe. Each trailing vortex is divided into two segments. The first one represents the "near wake", the location of which is dominated by the section geometry and local blowing. It extends from the bound vortex line to a point extended some distance beyond the trailing edge of the flap. The extension distance (E) was determined empirically to give good drag correlation at varying c_J:

$$E/c = 1.2 \sqrt[4]{c_J} \tag{1}$$

The second segment of each trailed vortex represents the "far wake", extending to infinity downstream at an angle (α_{i_∞}) to the freestream wind direction, determined as follows:

1. A rough estimate of the local circulation lift coefficient (c_{ℓ_c}) is determined from the local c_J, δ_F, and α (assuming zero induced velocity) using the section lift function (discussed later), and corrected for finite span using the following formula, based on ordinary lifting line theory:

$$c_{\ell c} = c_{\ell c\,(NO\ DOWNWASH)} \frac{A}{A+2} \tag{2}$$

   A is the aspect ratio of the whole wing, and is assumed to be appropriate for this correction.

2. The wake angle is inferred from an approximation to the rolled-up vortex value implied by Helmbold's highly loaded wing theory[8]:

$$\alpha_{i_\infty} = 0.243 \sin^{-1}(c_{\ell c}/1.9A) \tag{3}$$

   (A derivation is given in Appendix I.)

2.2.2 Section Characteristics

"Jet" Lift vs "Circulation" Lift

The lift on a jet flapped wing includes both an aerodynamic (or "circulation") component and a direct jet thrust component. To determine trailing vortex strengths, it will be necessary to distinguish between them. Furthermore, it must be recognized that aerodynamic forces also act on the jet behind the wing, and thus contribute additionally to the circulation. Figure 3 indicates these relations.

The total section lift coefficient is

$$c_\ell = c_{\ell c,W} + c_J \sin(\alpha + \delta_F) \tag{4}$$

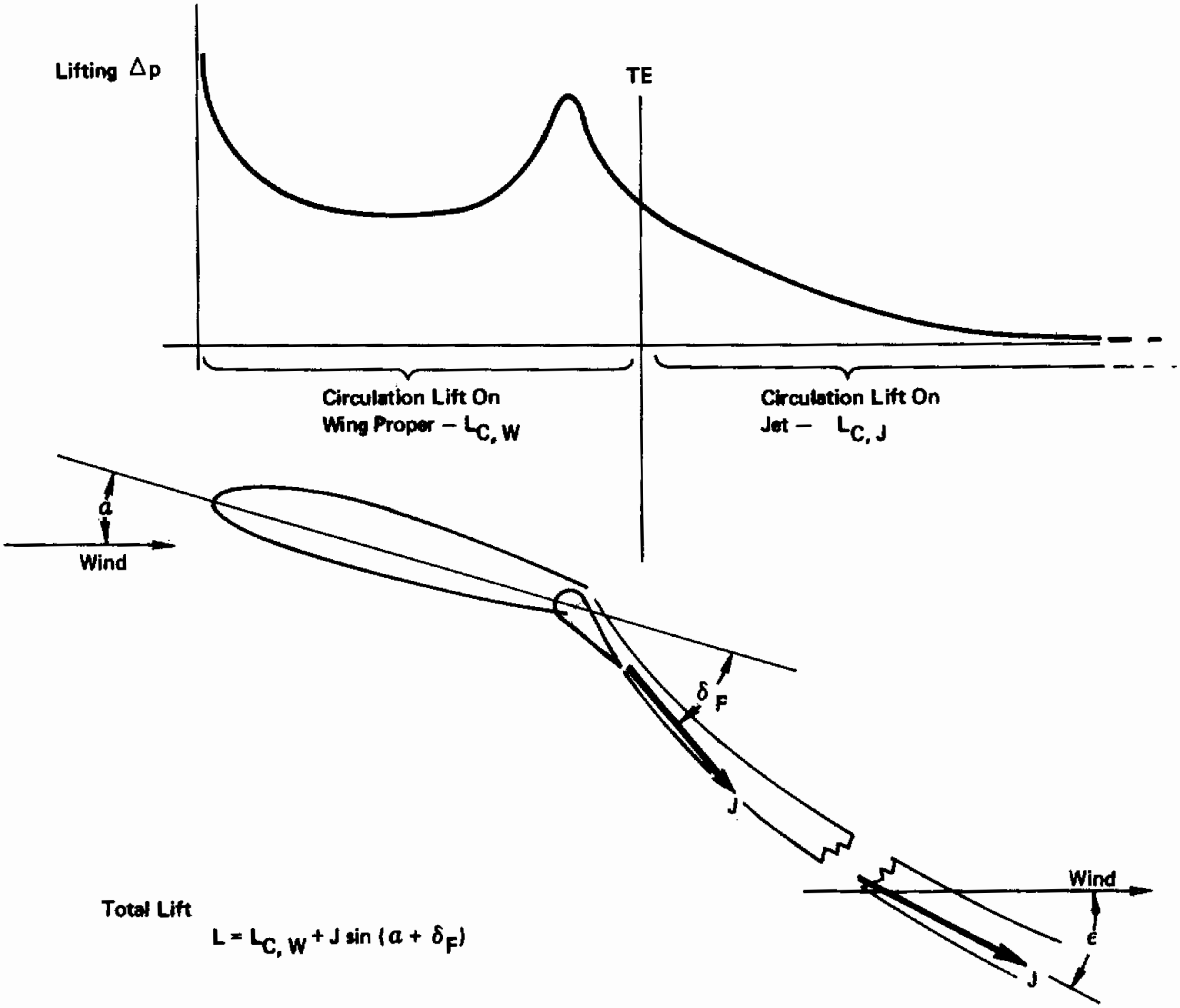

Total Lift

$$L = L_{C,W} + J \sin(\alpha + \delta_F)$$

or $$L = L_{C,W} + L_{C,J} + J \sin \epsilon$$

Figure 3: Section Lift Breakdown

The aerodynamic force on the jet must be just enough to turn the jet momentum vector to the far downstream angle ε, so

$$c_{\ell_{c,J}} = c_J \left[\sin(\alpha + \delta_F) - \sin \varepsilon \right] \tag{5}$$

Therefore, the "circulation" lift determining the vortex strength is

$$c_{\ell_c} = c_\ell - c_J \sin \varepsilon \tag{6}$$

The drag may be inferred from the extra streamwise momentum passing through the Trefftz plane:*

$$c_d = -c_J \cos \varepsilon \tag{7}$$

The section must, therefore, experience an aerodynamic drag coefficient

$$c_{d_{c,W}} = -c_J \left[\cos \varepsilon - \cos(\alpha + \delta_F) \right] \tag{8}$$

This force appears in the form of low pressures at the leading edge, which will be in a strong local upwash region.

In the two-dimensional case, there can be no trailing vortices and ε must be zero. Then, all the lift is circulation lift (in the sense that it is associated with bound vorticity) and all the jet thrust is recovered. The two-dimensional analyses used as the basis for the lift function used here compute $c_{\ell_{c,W}}$ on the basis that ε is zero. If it is not, the bound vorticity on the jet sheet goes down, implying a reduction in $c_{\ell_{c,W}}$. That reduction is ignored here.

To determine c_{ℓ_c}, ε must be specified as well as α, δ_F and c_J. In the present analysis, which uses an iterative procedure to establish the circulation of each horseshoe vortex element, the downwash velocity (w) at the lifting line (computed for the previous iteration) is assumed to be doubled far downstream. Ignoring the streamwise induced velocity component for this purpose,

---

*In the present analysis, friction or "profile" drag is neglected because the other components (jet thrust and downwash-rotated lift) will overwhelmingly dwarf it. Note also that the section coefficients are defined in terms of the direction and dynamic pressure (q) of the <u>local</u> relative wind. They must be resolved and adjusted for the freestream direction and q when total wing forces are computed.

$$\varepsilon = \tan^{-1}(2w/V) \tag{9}$$

In the initial determination of an approximate c_{ℓ_c} to define a trailing vortex far wake angle, ε was assumed to be zero. The subsequent correction of c_{ℓ_c} for aspect ratio should approximately correct for this.

Local Relative Wind Adjustments

The application of section data to three-dimensional wings is best done by resolving the flow into components normal and parallel to the lifting line, as shown in Figure 4. The effect of taper, which implies a different resolution at each chord station, will be neglected.

Consider a typical strip (indicated by shading). Its area will be $c_{ext}\ \delta y$, where c_{ext} is the local streamwise chord* and δy the width of the strip. Let the blowing thrust applied to the strip be denoted by δJ. Normally, the direction of the blowing thrust will either be streamwise (as in the case of externally blown or upper-surface blown flaps) or normal to a nozzle line, usually the flap hinge (as in the case of internally blown jet flaps).

Now construct a plane normal to the lifting line and passing through the control point of the strip. The "normal strip" (indicated by the broken lines) of width $\delta y'$ and length c'_{ext} will have the same area as the streamwise strip, except for a small error due to taper, which will be neglected. The normal component of jet thrust will be

$$\delta J_{NORMAL} = \delta J \cos \Lambda \tag{10}$$

for streamwise blowing, and

$$\delta J_{NORMAL} = \delta J \tag{11}$$

for blowing normal to the hinge line.

Let the component of the wind vector in the normal plane (including both freestream and induced components) be denoted by V_N. Let α and δ_F be measured in the normal plane.

The momentum coefficient for the normal strip will be

$$c_J = \frac{\delta J_{NORMAL}}{\frac{1}{2}\rho V_N^2\, \delta y'\, c'_{ext}} \tag{12}$$

*Including extension, or "Fowler flap" action.

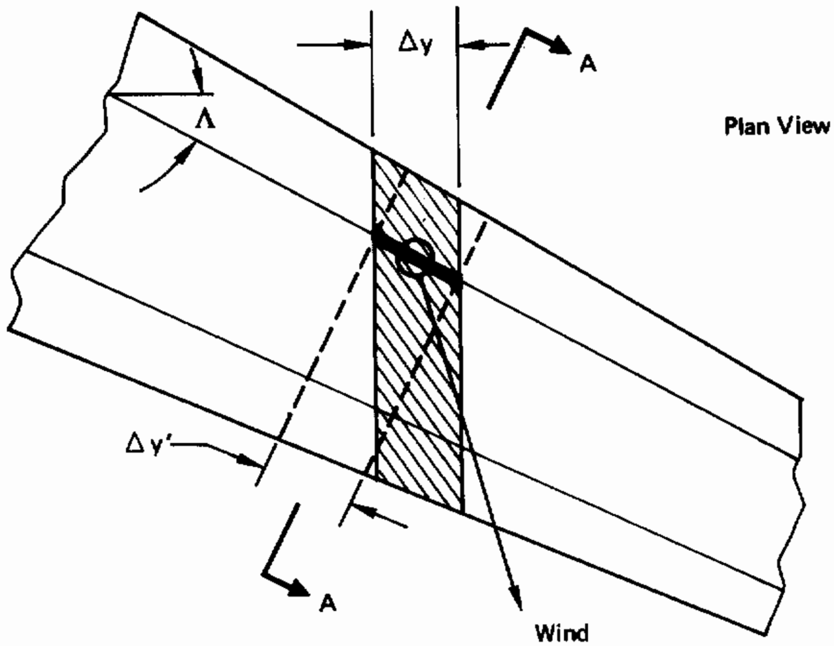

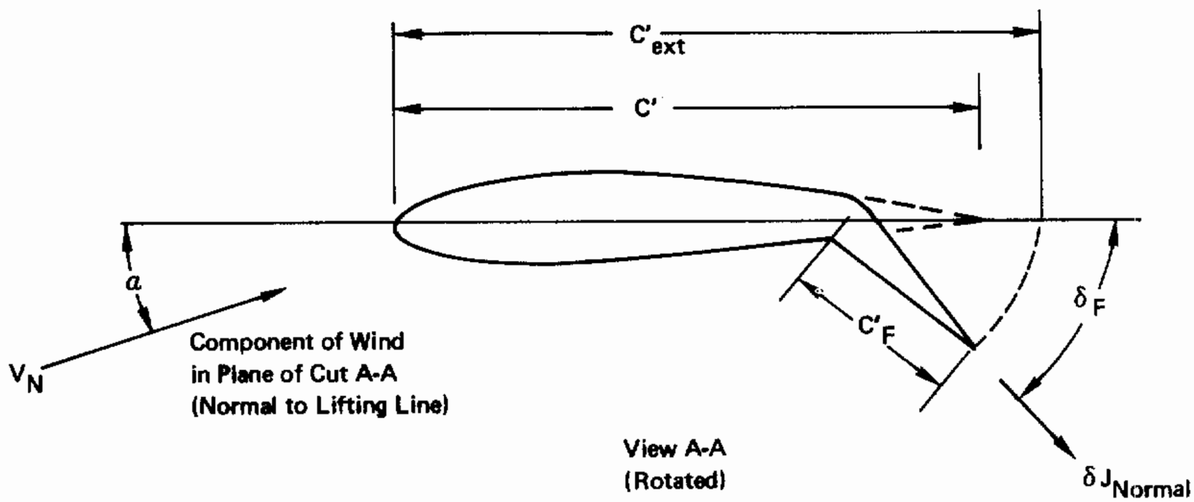

Figure 4: Relative Wind for Strip Analysis

The downstream angle of the jet, used to determine the circulation lift, must be revised to reflect sweep effects, replacing equation (9) above by the following:

$$\varepsilon = \tan^{-1}[2w/V\cos(\Lambda \mp \beta)] \tag{13}$$

where Λ and β are the sweepback and sideslip angles, respectively. The plus sign applies to the left wing, the minus sign to the right.

The circulation lift coefficient, c_{ℓ_c} (as defined in the preceding subsection), may then be calculated as a function of C_J, δ_F, α, ε, and c_F'/c_{ext}', using the section lift expression given in the following subsection. From c_{ℓ_c}, the bound circulation (γ) corresponding to the strip's loading may then be found:

$$\gamma = c_{\ell_c} V_N c_{ext}'/2 \tag{14}$$

The moment coefficient (c_m) of the loading on the normal strip about its quarter chord can also be extressed as a function of C_J, δ_F, α and c_F'/c_{ext}'. This contributes a couple, acting about the quarter chord of the normal strip, and parallel to the lifting line, equal to

$$\delta m_N = \tfrac{1}{2}\rho V_N^2 c_m c_{ext}'^2 \delta y' \tag{15}$$

2.3 Lift and Moment Functions

Initially, the circulation lift function used in the present analysis was simply an approximation to the curves published by Malavard[3]. It was found that this underpredicted measured changes in lift curve slopes and lift due to jet deflection. Some of the discrepancy could be ascribed to thickness effects, since Malavard's electric analogy data were for a zero thickness airfoil. Wygnanski[10] suggests that entrainment effects, absent in any potential flow analysis, would also amplify lift.

The approach taken here was simply to adjust the coefficients in the section lift formula to give good agreement with the data of Lockwood, Turner, and Riebe[9]. The following expression is used for the total lift:

$$c_{\ell_c} = c_{\ell_o} + \Delta c_{\ell_J} \tag{16}$$

where

$$c_{\ell_o} = 2\pi\left[\alpha + \left(0.32 + 1.155\,\frac{c_F'}{c_{ext}'}\right)\delta_F\right] \tag{17}$$

is the lift for zero jet momentum, and

$$\Delta c_{\ell_J} = (2.76\,\delta_F + 1.092\alpha)\,c_J^{0.68} + (\alpha + \delta_F)\,c_J \tag{18}$$

is the extra lift (both aerodynamic and jet thrust) due to the jet.

The moment coefficient (about the leading edge) is determined by an approximation to Spence's thin airfoil results[1,2]:

$$c_{m_{LE}} = c_{m_{LE,0}} + \Delta c_{m_{LE,J}} \tag{19}$$

where

$$c_{m_{LE,0}} = -\frac{\pi}{2}\alpha - \left(4.62\sqrt{\frac{c_F'}{c_{ext}'}} - 2.93\,\frac{c_F'}{c_{ext}'}\right)\delta_F \tag{20}$$

and

$$c_{m_{LE,J}} = -0.2F\alpha - F\delta_F\, e^{-1.189\, c_F'/c_{ext}'} \tag{21}$$

in which

$$F = 1.25\,c_J + 1.5\left(1 - e^{-1.204\,c_J}\right) \tag{22}$$

The moment coefficient referred to the quarter c_{ext}' point is then

$$c_m = c_{m_{LE}} + c_\ell/4 \tag{23}$$

Figure 5 shows how the above formulae compare to the relations given by Malavard and Spence.

<u>Section "Model"</u>

Judgment must be used in specifying the flap deflection angle so that the lifting effectiveness of the actual flap design to be analyzed will be fairly represented by the simple c_ℓ vs δ_F relation. Figure 6 indicates the "model" represented by that function. The correct representation of multiple segment flaps and the influence of jet spreading on the effective angle of the jet at the trailing edge are beyond the scope of this report.

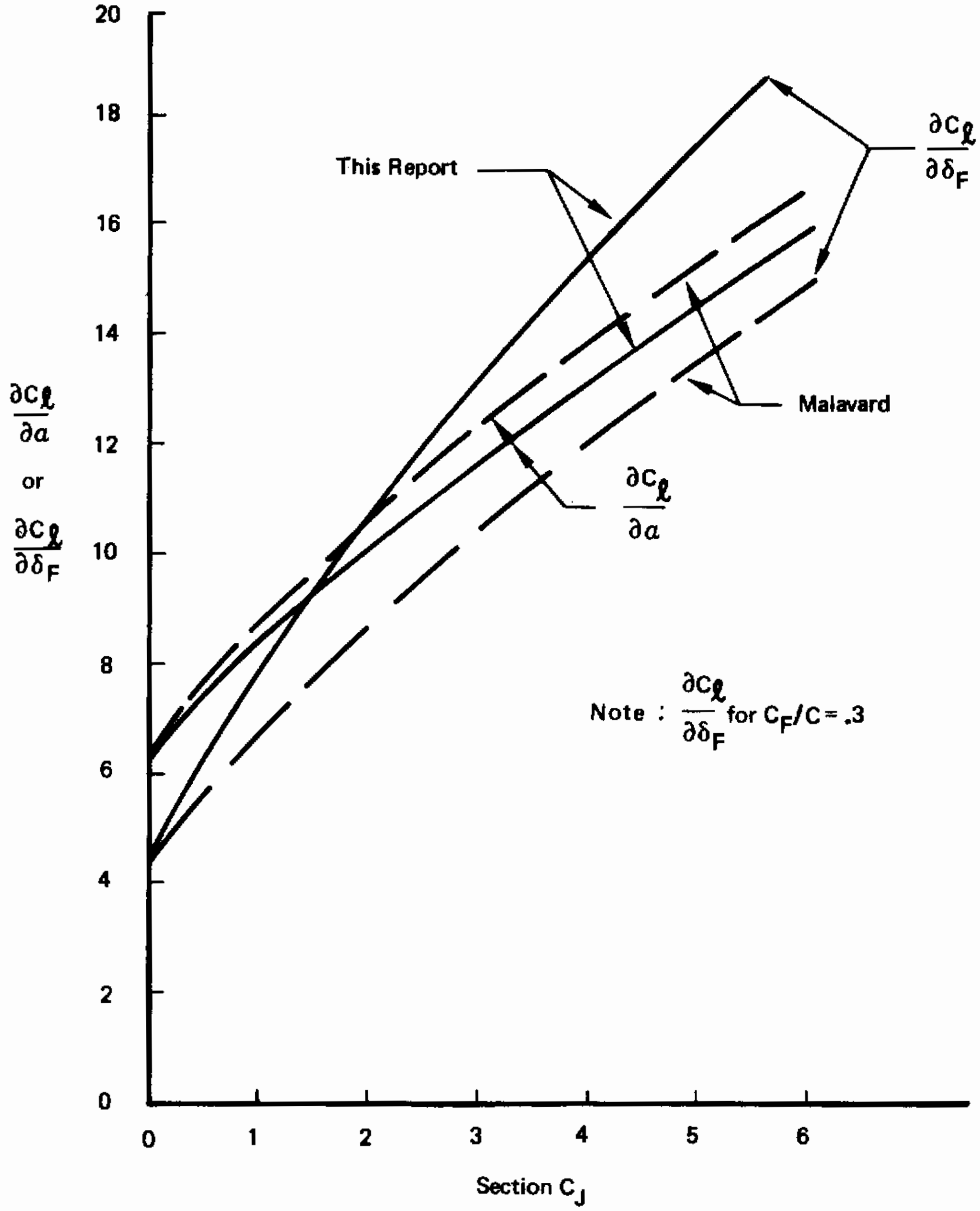

Figure 5: Section C_ℓ and C_m

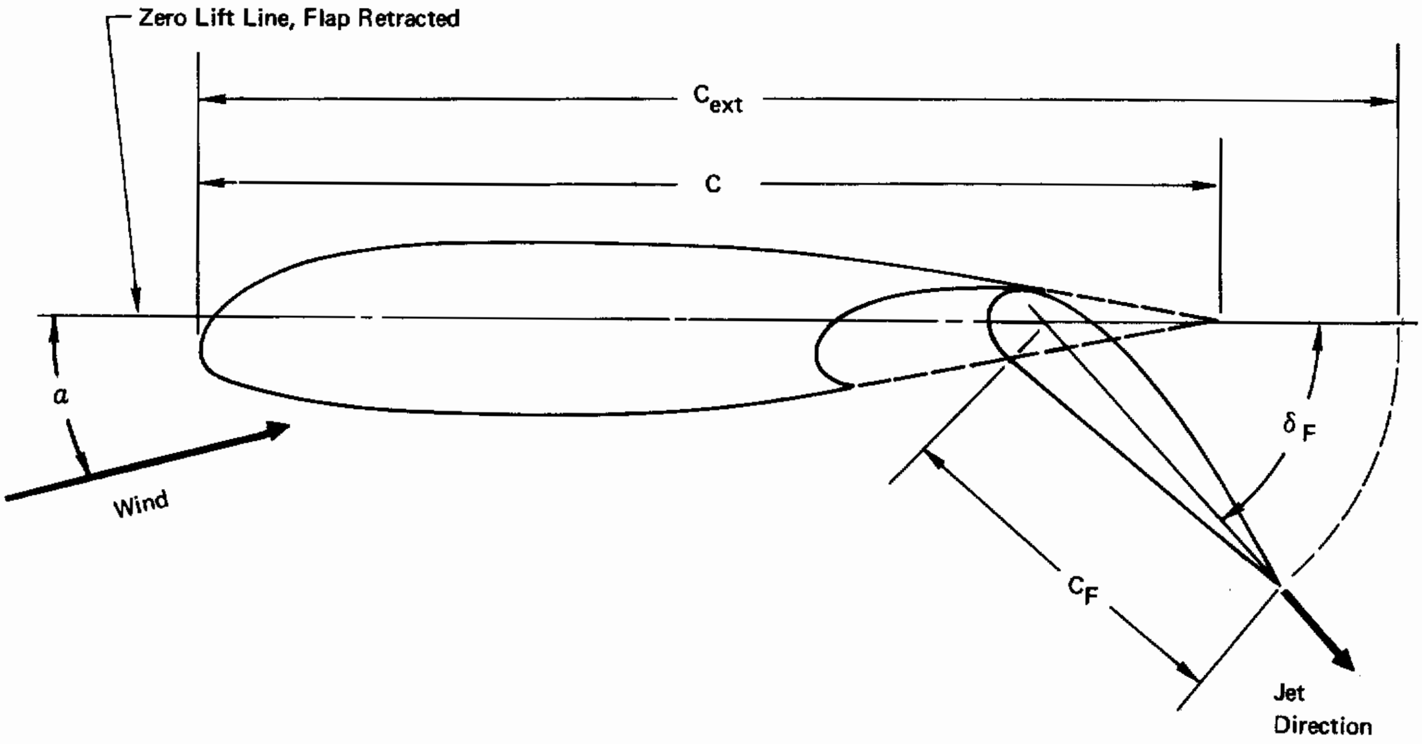

Figure 6: Section Geometry Conventions

SECTION III

ANALYSIS PROCEDURE

3.1 Wing Description

Basic Reference Geometry

The procedure presently programmed applies to trapezoidal wings having a plane of symmetry, although these restrictions are not essential to the analysis. Unsymmetrical blowing and flap deflection/extension are permitted. The chord line at the center of the wing lies on the x-axis, and the origin is at its 25% point. Figure 7 shows the relation of the wing to the coordinate axes.

The wing is completely defined by the parameters given in Table I. All dimensions are expressed in semi-spans, so the area of the wing is

$$S_w = 4/A \tag{24}$$

Its root chord is

$$c_r = 4/A(1+\lambda) \tag{25}$$

and the mean aerodynamic chord (for moment reference purposes) is

$$\bar{c} = \frac{2c_r^2(1+\lambda+\lambda^2)}{1.5\,S_w} \tag{26}$$

The x and z coordinates of the quarter mean chord are then

$$x_{\bar{c}/4} = \frac{c_r - \bar{c}}{c_r(1-\lambda)} \tan\Lambda$$

$$z_{\bar{c}/4} = \frac{c_r - \bar{c}}{c_r(1-\lambda)} \tan\Gamma \tag{27}$$

except when $\lambda = 1$, in which case

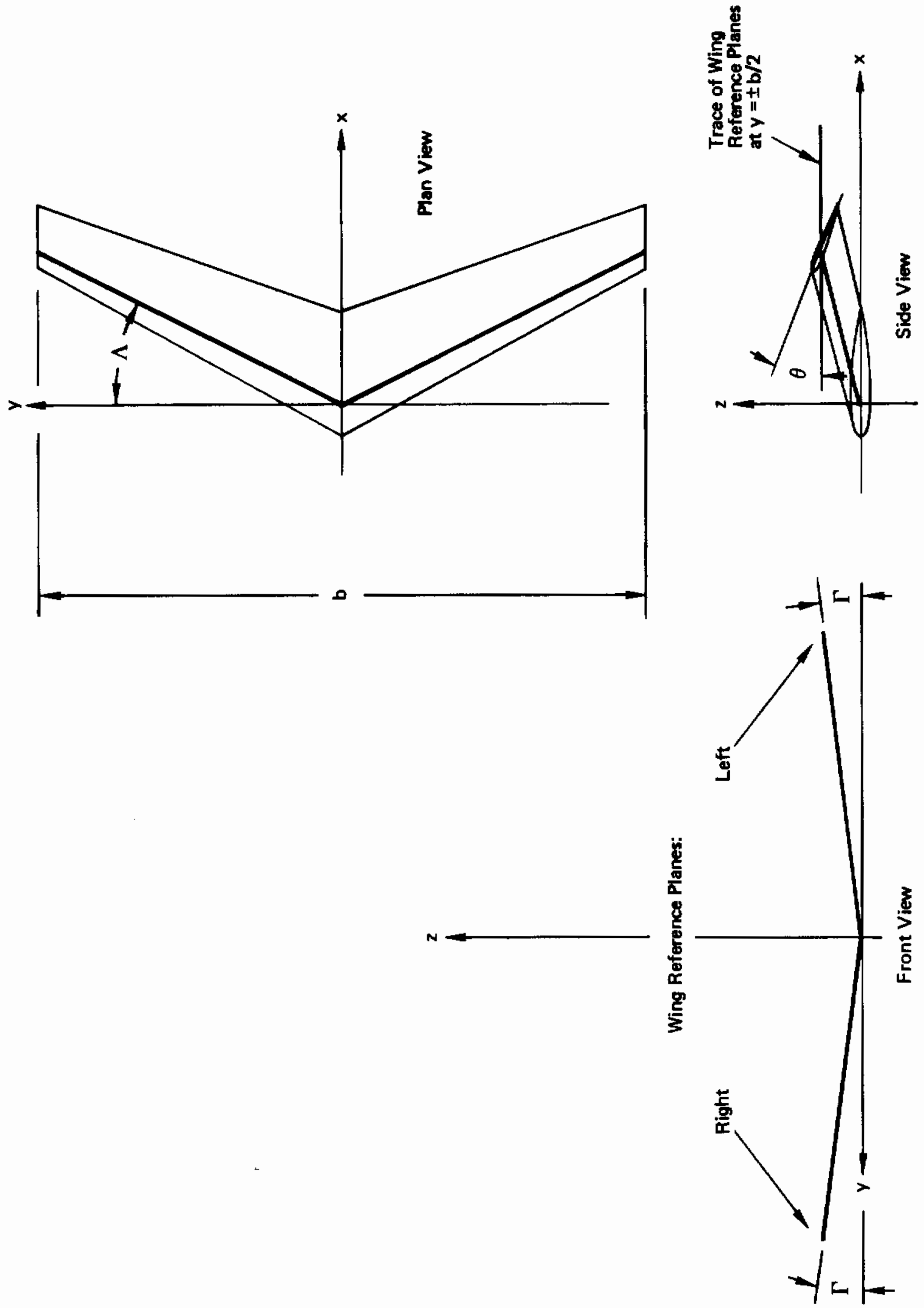

Figure 7: Coordinate Axes and Wing Reference Planes

TABLE I

WING DESCRIPTION PARAMETERS

PARAMETER	SYMBOL
Aspect Ratio	A
Sweepback Angle	Λ
Taper Ratio	λ
Dihedral Angle	Γ
Tip Twist	θ
Number of Panels	n_{max}
Span Station of Inboard End of n^{th} Panel	y_{end_n}
Flap Chord Ratio (Based on Nominal Chord) of n^{th} Panel	$(c_F/c)_n$
Flap Deflections Right and Left Wing, n^{th} Panel	$\delta_{F_{R,n}}, \delta_{F_{L,n}}$
Flap Extension Ratios (C_{ext}/c) Right and Left Wing, n^{th} Panel	$e_{F_{R,n}}, e_{F_{L,n}}$
Blowing Type: a) "Internal" Constant c_J over panel or b) "External" Constant J per unit span	(No Symbol)
Blowing Direction: a) Normal to hinge line or b) Streamwise.	(No Symbol)

$$x_{c/4} = 0.5 \tan \Lambda$$

$$z_{c/4} = 0.5 \tan \Gamma \qquad (28)$$

Several unit vectors which will be useful later are defined next: $\bar{N}_R$ and $\bar{N}_L$ are unit vectors normal to the right and left wing reference planes, given by

$$\bar{N}_{(\,)} = 0\bar{i} \mp \bar{j} \sin\Gamma + \bar{k} \cos\Gamma \qquad (29)$$

where the upper sign applies to the right wing, and $\bar{i}$, $\bar{j}$, $\bar{k}$ are unit vectors in the x, y, and z directions, respectively. B_R and B_L are unit vectors parallel to the lifting lines, given by

$$\bar{B}_{(\,)} = \pm\bar{i} \sin\Lambda + \bar{j} \cos\Lambda \cos\Gamma \pm \bar{k} \cos\Lambda \sin\Gamma \qquad (30)$$

(The sign conventions chosen here give the $\bar{B}$ vectors the same sense as the bound circulation.) As discussed previously, section characteristics are considered to apply in the plane normal to the wing - that is, normal to $\bar{B}$. It will also be convenient to define the unit vectors perpendicular to both $\bar{B}$ and $\bar{N}$, pointing "downstream" in the plane normal to the wing. Since $\bar{B}$ and $\bar{N}$ are already mutually perpendicular,

$$\bar{D}_{(\,)} = \bar{N}_{(\,)} \times \bar{B}_{(\,)} \qquad (31)$$

Trailing-Edge Device Geometry

The wing is divided into "panels" corresponding to the divisions of the trailing-edge flaps or blowing arrangements. Up to six panels may be used. The number six was chosen to provide the capability to analyze a four-engine externally blown flap configuration. Flap deflection and extension are independently specified, according to the conventions stated in Section II. The flap chord ratio, referred to the extended chord, for the n^{th} panel is

$$(c_F/c_{ext})_{(),n} = (c_F/c)_n / e_{F_{(),n}} \tag{32}$$

Because the wing is analyzed in slices 0.04 semi-spans wide, the ends of the panels must fall on span stations which are integral multiples of 0.04. The nominal area of the n^{th} panel is denoted by S_n, and is calculated according to the procedure given in Subsection 3.3 (Eq. 40).

3.2 Flight Condition

The additional data required for complete statement of the problem are the descriptions of the relative wind and the jet blowing. Since all calculations are nondimensional, the freestream velocity is taken as unity. The freestream vector, $\bar{U}$, is given by

$$\bar{U} = \bar{i}\cos\alpha_W\cos\beta - \bar{j}\cos\alpha_W\sin\beta + \bar{k}\sin\alpha_W \tag{33}$$

where α_W and β are the wing angle of attack and angle of sideslip.

The total thrust of the blowing system is defined by the wing thrust coefficient, C_{J_W}, referred to freestream dynamic pressure and the area of the whole wing. The distribution of the thrust among the panels is defined by $f_{B_{R,n}}$ and $f_{B_{L,n}}$. These are weighting factors apportioning the jet thrust among the panels; e.g.,

$$J_{(),n} = J_W f_{B_{(),n}} \tag{34}$$

Thus, a "panel C_J" can be calculated:

$$C_{J_{(),n}} = f_{B_{(),n}} C_{J_W} \frac{S_W}{S_n} \tag{35}$$

where S_n is the area of the wing panel corresponding to the n^{th} spanwise flap portion, and S_W is the area of the whole wing. Deflection angles of the jets are taken to be equal to those of the corresponding flaps.

3.3 Determination of Strip Parameters

Geometry

Twenty-five equal-span strips are used on each wing. The points on the lifting line at the edges of the strips have the vector coordinates

$$\bar{P}_{(),i} = \pm \frac{i\,\bar{B}_{()}}{25\cos\Lambda\cos\Gamma} \tag{36}$$

where i is the "index" of the point, beginning with 1 at the centerline, and going up to 26 at the tip.

The control point for the i^{th} strip is thus at

$$\bar{Q}_{(),i} = (\bar{P}_{(),i} + \bar{P}_{(),i+1})/2 \tag{37}$$

The nominal chord of the i^{th} strip, measured at its center, is

$$c_i = c_r[1-(.04i-.02)(1-\lambda)] \tag{38}$$

The corresponding extended chords are

$$c_{ext_{(),i}} = e_{F_{(),n}}\, c_i \tag{39}$$

where n is determined by the panel on which the i^{th} strip lies. The nominal area of the i^{th} strip is

$$S_{s_i} = 0.04\, c_i \tag{40}$$

The nominal area of the n^{th} panel is thus

$$S_n = \sum_i S_{s_i} \tag{41}$$

where the range of i covers the strips in the panel.

Blowing

The thrust coefficients applicable to each strip, referred to free-stream dynamic pressure and to the extended strip area, are

$$C_{JS_{(),i}} = C_{J_{(),n}} / e_{F_{(),n}} \tag{42}$$

for "internal" blowing. For "external" blowing

$$C_{JS_{(),i}} = \frac{C_{J_{(),n}} S_n}{m_n S_{Si} e_{F_{(),n}}} \tag{43}$$

where m_n is the number of strips in the panel.

The jet behind a particular strip will actually induce lift on the adjacent strips, and the absence of a jet behind an unblown strip will reduce the induced lift on an adjacent blown strip. Furthermore, large abrupt changes in strip characteristics cause rapid spanwise variations of loading which slow the convergence of the iteration procedure. It has, therefore, been found expedient to "smear" the edges of the jet by transferring 1/3 of the jet momentum on any strip at the edge of a panel to the adjacent strip on the next panel.

Wind

The total wind at the i^{th} control point on the indicated side is

$$\bar{V}_{(),i} = \bar{U} + \bar{W}_{(),i} \tag{44}$$

$\bar{W}$ will be available from computations executed in a previous iteration, details of which will be given later.

The magnitude of the wind velocity normal to the lifting line is

$$V_{N_{(),i}} = |\bar{V}_{(),i} \times \bar{B}_{()}| \tag{45}$$

The angle of attack, measured in the normal plane, is

$$\alpha_{(),i} = \sin^{-1}\left(\frac{\bar{V}_{(),i} \cdot \bar{N}}{V_{N_{(),i}}}\right) + \theta Q_{Y_{R,i}} \tag{46}$$

The thrust coefficient used for section C_ℓ and C_m calculation is then

$$C_J = C_{JS_{(),i}} / V_{N_{(),i}}^2 \tag{47}$$

for blowing normal to the hinge line, or

$$C_J = C_{JS_{(),i}} \cos\Lambda / V_{N_{(),i}}^2 \tag{48}$$

for streamwise blowing. (Equations 46 and 47 follow directly from equations 10-12.)

The downstream jet angle (ε) referred to in Equation 13 is taken to be

$$\varepsilon_{(),i} = \tan^{-1}\left[2W_{Z_{(),i}} \;/\; \cos(\Lambda \mp \beta)\right] \tag{49}$$

Next, $c_{\ell_{c(),i}}$ and $c_{m(),i}$ are computed using the results of Equations 45, 46 (or 47), 48 and 32 in the lift and moment functions of Subsection 2.3.

The circulation of the ith horseshoe vortex is then

$$\gamma_{(),i} = \left(c_{\ell_{c_{(),i}}} \; V_{N_{(),i}} \; c_{ext_{(),i}} \; \cos\Lambda\right)/2 \tag{50}$$

3.5 Iteration Procedure

The set of vortex strengths constituting a solution is found by successive approximation. The first set is calculated assuming zero induced velocity at all control points. Substitution of each new set of γ's directly into the equations for induced velocities will <u>not</u>, however, lead to a solution. That procedure is unstable, giving a rapidly diverging sequence of vortex strengths. Instead, the iteration process is "damped" by use of a weighted average of the previous two solutions for the next trial:

$$\gamma_{NEW(),i} = d_{(),i}\,\gamma_{(),i} + \left(1 - d_{(),i}\right)\gamma_{OLD(),i} \tag{51}$$

The damping factors (different for each strip) are determined by the process described in Appendix III.

In cases where very powerful blowing is applied over narrow portions of the span, such as externally blown flaps, the abrupt change in circulation between adjacent wing panels was sometimes found to drive the computed local induced velocities and flow angles to values where the nonlinearities of the analysis would prevent convergence of the iterations. A smoothing procedure was therefore added. This process leaves the computed results almost unaffected where convergence is obtained anyway, and extends the range of conditions for which answers can be obtained to substantially higher local C_J values. The smoothing procedure is also given in Appendix III.

After each set of γ's is calculated, it is checked against the previous set. When the maximum difference of any one from the corresponding OLD is less than one percent of the average of all the γ's, the solution is considered satisfactory and iterations cease. Computation of final output data (overall force and moment coefficients, load distributions, etc.) is then started.

3.6 Induced Velocities

Induced velocities are computed from aerodynamic influence coefficients and the weighted average vortex strengths:

$$\overline{W}_{(\,),i} = \sum_{j=1}^{25} \left[\gamma_{NEW_{R,j}} \overline{T}_{R,(\,),i,j} + \gamma_{NEW_{L,j}} \overline{T}_{L,(\,),i,j} \right] \quad (52)$$

The aerodynamic influence coefficients are simply the velocities induced at the control points by the horseshoe vortices of the various strips, computed for unit circulation. For instance, $\overline{T}_{R,L,i,j}$ is the velocity vector at the i^{th} control point of the left wing due to the j^{th} vortex on the right wing, for $\gamma_{R,j} = 1$.

Influence Coefficient Calculation

The $\overline{T}$'s are the sums of contributions of straight line vortex segments, computed according to the Biot-Savart law. (Appendix III gives details.) Figure 8 shows the segment arrangements and notation, using $T_{R,L,i,j}$ as an example. $\overline{P}$ and $\overline{Q}$ have already been defined by Equations 36 and 37. $\overline{H}_{R,n}$ is the unit vector parallel to the semi-infinite segments of the far wake portion of the vortices trailing from the n^{th} panel. It is given by

$$\begin{aligned} \overline{H}_{R,n} = \bar{i} \cos(\alpha_W - \alpha_{i_\infty R,n}) \cos\beta \\ + \bar{j} \cos(\alpha_W - \alpha_{i_\infty R,n}) \sin\beta \\ + \bar{k} \sin(\alpha_W - \alpha_{i_\infty R,n}) \end{aligned} \quad (53)$$

where $\alpha_{i_\infty R,n}$ is computed for the panel by the procedure given in Paragraph 2.2.1 above.

The corner points near the trailing edge are found from

$$\overline{K}_{R,j} = \overline{P}_{R,j} + \overline{E}_{R,j} \quad (54)$$

and

$$\overline{L}_{R,j} = \overline{P}_{R,j+1} + \overline{E}_{R,j} \quad (55)$$

where

$$\begin{aligned} \overline{E}_{R,j} = c_{JS_{R,j}} \left\{ 0.75 - \left(\frac{c_F}{c}\right)_n + \left[\left(\frac{c_F}{c}\right)_n + \frac{E}{c}\right] \cos\delta_{F_{R,n}} \right\} (\bar{i} + \bar{j} \tan\beta) \\ + \bar{k}\, c_{JS_{R,j}} \left[\left(\frac{c_F}{c}\right)_n + \frac{E}{c}\right] \sin\delta_{F_{R,n}} \end{aligned} \quad (56)$$

The quantity E/c in Equation 56 is the effective chord extension due to blowing given by Equation 1. Large abrupt variations in $\overline{K}$ and $\overline{L}$ at transition points between panels have been found to cause anomalies in the computed loadings and to slow the convergence process. Therefore, the $\overline{L}$ at the outboard end of a panel and the $\overline{K}$ at the inboard end of the adjacent one are averaged, and the common value used for both.

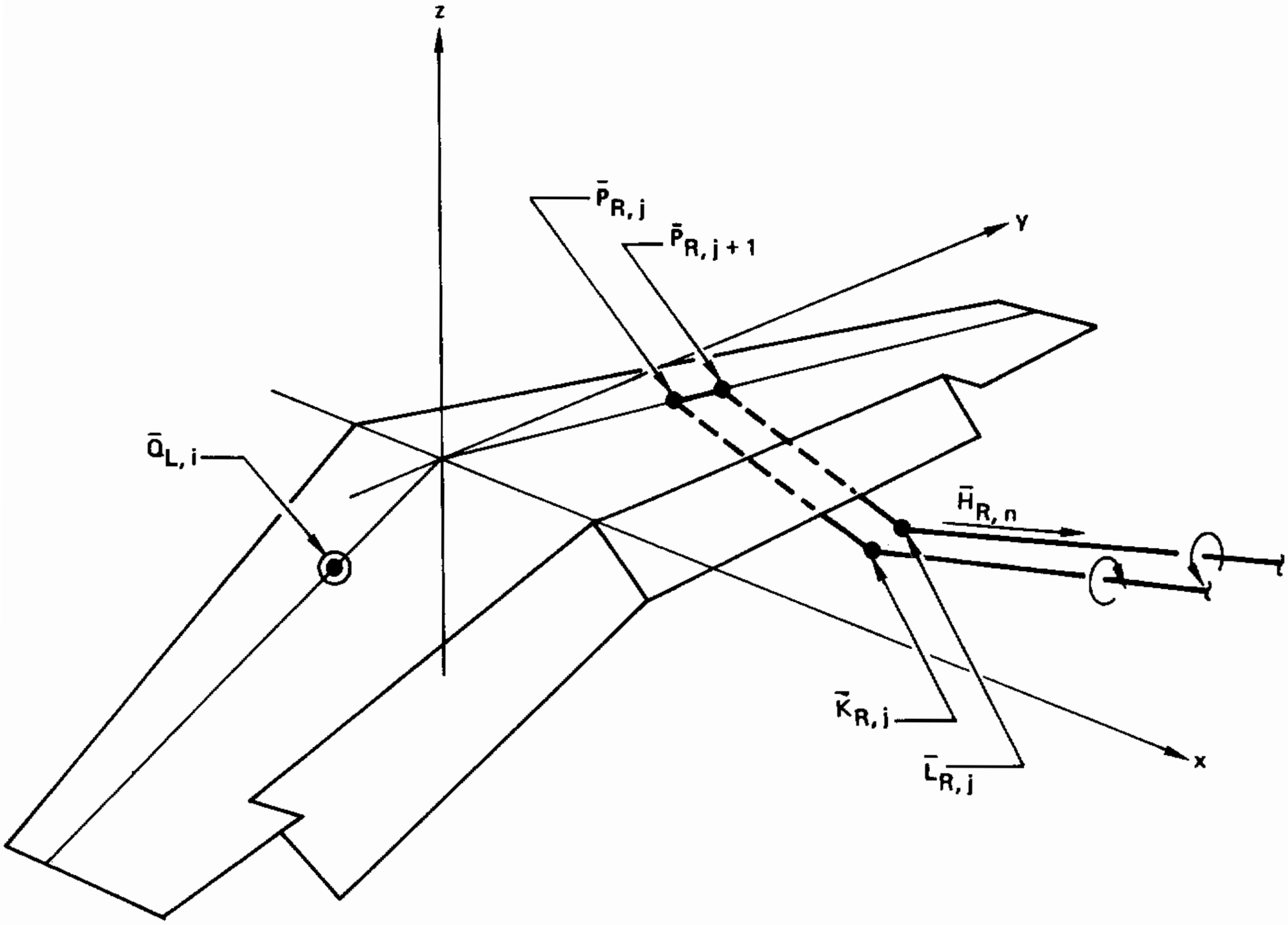

Figure 8: Vortex Segments for Influence Coefficient Calculations

The velocity $\overline{T}_{R,L,i,j}$ is then the sum of the contributions of:

1) The semi-infinite segment from infinity downstream to $\overline{K}_{R,j}$.
2) The segment from $\overline{K}_{R,j}$ to $\overline{P}_{R,j}$.
3) The segment from $\overline{P}_{R,j}$ to $\overline{P}_{R,j+1}$.
4) The segment from $\overline{P}_{R,j+1}$ to $\overline{L}_{R,j}$.
5) The segment from $\overline{L}_{R,j}$ to infinity downstream.

If the control point in question were on the right wing, $\overline{T}_{R,R,i,j}$ would be found using $Q_{R,i}$ instead of $Q_{L,i}$, and the bound vortex segment (the 3rd) would be omitted, since its contribution must vanish. The $T_{L,R}$'s and $T_{L,L}$'s are found using the same procedure, with obvious changes of subscript.

3.7 Forces and Moments

Vortex Forces

The aerodynamic forces on the wing and jet, which give rise to the vortex system in the first place, may be inferred using the Kutta-Joukowski theorem:

$$\delta \overline{F} = \rho(\overline{V} \times \overline{\Gamma})\delta \ell \tag{57}$$

where $\delta\overline{F}$ is the force acting on a segment of bound vortex, ρ is the fluid density, $\overline{V}$ is the wind vector across the vortex segment (assumed constant, since the segment is short), $\overline{\Gamma}$ is the circulation vector of the segment, and $\delta\ell$ its length. Nondimensionalizing forces by freestream dynamic pressure and semispan squared, the force on the i^{th} segment will be

$$\overline{F}_{(\,),i} = 2[\,\overline{V}_{(\,),i} \times (\gamma_{(\,),i}\,\overline{B}_{(\,)})]\delta\ell \tag{58}$$

and the segment length will be

$$\delta\ell = 0.04\sqrt{1+\tan^2\Lambda+\tan^2\Gamma} \tag{59}$$

The total aerodynamic force acting on the wing/jet system is therefore

$$\overline{F}_{TOT} = \sum_{i=1}^{25}\left(\overline{F}_{\ell,i} + \overline{F}_{L,i}\right) \tag{60}$$

Jet Forces

Part of the direct jet forces acting on the wing are actually included in the vortex forces acting on the wing-jet combination. The jet forces, as defined here, correspond to the jet momentum far downstream of the wing, as indicated in Figure 9. The nondimensional jet force increment will be

$$\delta J_{(),i} = c_{JS_{(),i}} S_{s_i} e_{F(),n} \tag{61}$$

The vector contribution of the strip jet force will then be

$$\bar{J}_{(),i} = \delta J_{(),i}\left[\bar{N}_{()} \sin(\varepsilon_{(),i} - \alpha_{(),i}) + \bar{D}_{()} \cos(\varepsilon_{(),i} - \alpha_{(),i})\right] \tag{62}$$

for blowing normal to the hinge line, or

$$\bar{J}_{(),i} = \delta J_{(),i} \left\{\cos\Lambda\left[\bar{N}_{()} \sin(\varepsilon_{(),i} - \alpha_{(),i}) + \bar{D}_{()} \cos(\varepsilon_{(),i} - \alpha_{(),i})\right] + \bar{B} \sin\Lambda\right\} \tag{63}$$

for streamwise blowing.

The total jet force will be

$$\bar{J}_{TOT} = \sum_{i=1}^{25} \left(\bar{J}_{R,i} + \bar{J}_{L,i}\right) \tag{64}$$

Moments

Each strip contributes a moment increment in two ways:

1) The product of the force on the strip and its distance from the moment center.

2) The couple associated with the section C_m.

The i^{th} strip's section C_m contributes

$$\bar{M}_{s_{(),i}} = c_{m_{(),i}} V^2_{N(),i} S_{s_i} c_i e^2_{F(),n} \bar{B} \cos\Lambda \tag{65}$$

where $C_{m(),i}$ was computed at the same time as $C_{\ell c(),i}$ according to the formulae given in Subection 2.3. (The M_s's are referred to the freestream dynamic pressure times the semispan cubed.)

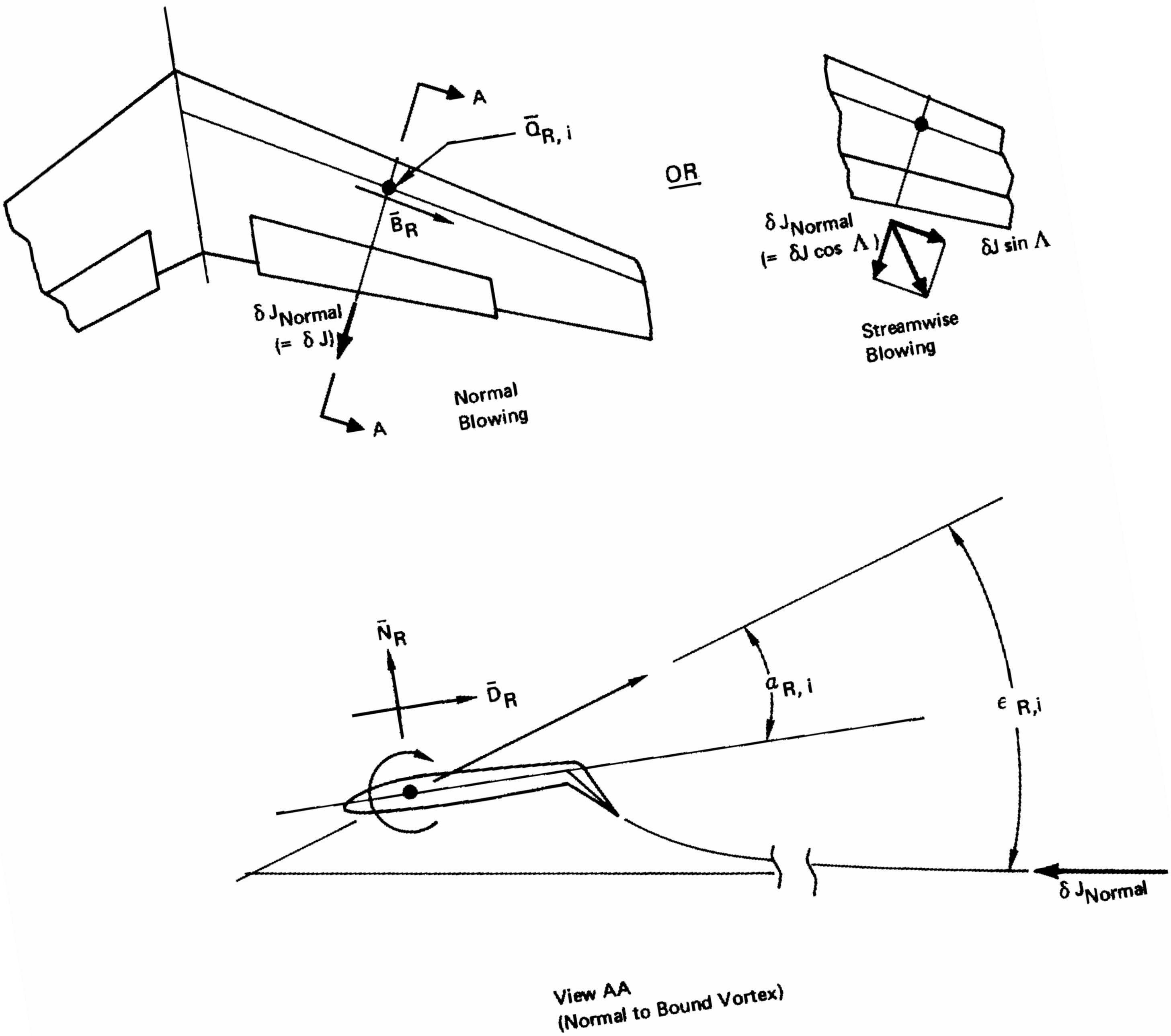

Figure 9: Jet Force Determination

The total moment about the origin of coordinates is, therefore,

$$\bar{M}_{TOT} = \sum_{i=1}^{25} [\bar{M}_{R,i} + \bar{M}_{L,i} + \bar{Q}_{R,i} \times (\bar{F}_{R,i} + \bar{J}_{R,i}) + \bar{Q}_{L,i} \times (\bar{F}_{L,i} + \bar{J}_{L,i})] \tag{65}$$

Force and Moment Coefficients

The forces and moments are then expressed in the customary coefficient form. First, they are resolved in the stability axis system. Unit vectors in the x, y and z stability axis directions are given by

$$\begin{aligned} \bar{S}_X &= -\bar{i}\left(\frac{U_x}{\sqrt{U_x^2 + U_z^2}}\right) - \bar{k}\left(\frac{U_z}{\sqrt{U_x^2 + U_z^2}}\right) \\ \bar{S}_Y &= \bar{j} \\ \bar{S}_Z &= \bar{S}_X \times \bar{S}_Y \end{aligned} \tag{66}$$

The three force coefficients are then

$$C_L = -\bar{F}_{TOT} \cdot \bar{S}_Z / S_W \tag{67}$$

$$C_D = -\bar{F}_{TOT} \cdot \bar{S}_X / S_W \tag{68}$$

$$C_Y = \bar{F}_{TOT} \cdot \bar{S}_Y / S_W \tag{69}$$

The moments must be transferred to the quarter m.a.c. as well as resolved:

$$C_m = [\bar{M}_{TOT} + (\bar{i}\, x_{\bar{c}/4} + \bar{k}\, z_{\bar{c}/4}) \times \bar{F}_{TOT}] \cdot \bar{S}_Y / \bar{c}\, S_W \tag{70}$$

$$C_\ell = [\bar{M}_{TOT} + (\bar{i}\, x_{\bar{c}/4} + \bar{k}\, z_{\bar{c}/4}) \times \bar{F}_{TOT}] \cdot \bar{S}_X / 2\, S_W \tag{71}$$

$$C_n = [\bar{M}_{TOT} + (\bar{i}\, x_{\bar{c}/4} + \bar{k}\, z_{\bar{c}/4}) \times \bar{F}_{TOT}] \cdot \bar{S}_Z / 2\, S_W \tag{72}$$

SECTION IV

EXAMPLES OF APPLICATION

4. General

This section presents applications of the method to a variety of problems for which wind tunnel test data is available for comparison. The configurations range from the somewhat academic case of a rectangular wing with uniform internal trailing edge blowing but zero flap chord to the very practical case of a swept back wing with double slotted flaps and external underwing blowing.

4.1 "Pure" Internally Blown Jet Flaps

Lockwood, Turner, and Riebe[9] reported results of tests on a rectangular wing of aspect ratio 8.4 with full span trailing edge blowing. The semi-span model was constructed by truncating the trailing edge of a symmetrical wing and installing an air supply tube, as shown in the sketch at the top of Figure 10. This tube fed a plenum exhausting through a nozzle tangent to the tube. The jet was forced to follow the outside surface of the tube by the Coanda effect until it reached a sharp corner, the location of which was used to set the jet deflection angle. The "flap chord" was, therefore, effectively zero.

This model was tested to very large momentum coefficients (up to 56), and gave results corroborating the limitation of circulation lift predicted by Helmbold[8]. Figure 10 shows measured drag polars for this model at $C_J \cong 7$, at several jet angles. The test results are given both as reported in Reference 9 and as adjusted for the pressure deficiency on the base of the wedge used to set the jet deflection.* "Classical" jet flap theory gives, for elliptical lift distribution,

$$C_D = -C_J + \frac{C_L^2}{\pi A + 2C_J} \qquad (73)$$

(This neglects the contribution of parasite drag, which is negligible in comparison to the range of drag values generated by induced and jet effects present here.) This equation agrees very well with the adjusted test data for low jet deflection angles. However, at $_J$ = 56° and 86°, the test results break sharply away from the classical parabola. The fact that the planform and blowing distribution are rectangluar, rather than elliptical, does not explain this behavior, since:

1) The differences are much too large; and

2) The effect of the planform difference (assuming that the loading retains the same shape as the lift builds up) would be to produce another <u>parabolic</u> polar, corresponding to a reduced aspect ratio.

*The correction was determined using a base pressure coefficient equal to that required to give $C_D = -C_J$ at zero lift and $\delta_J = 0$.

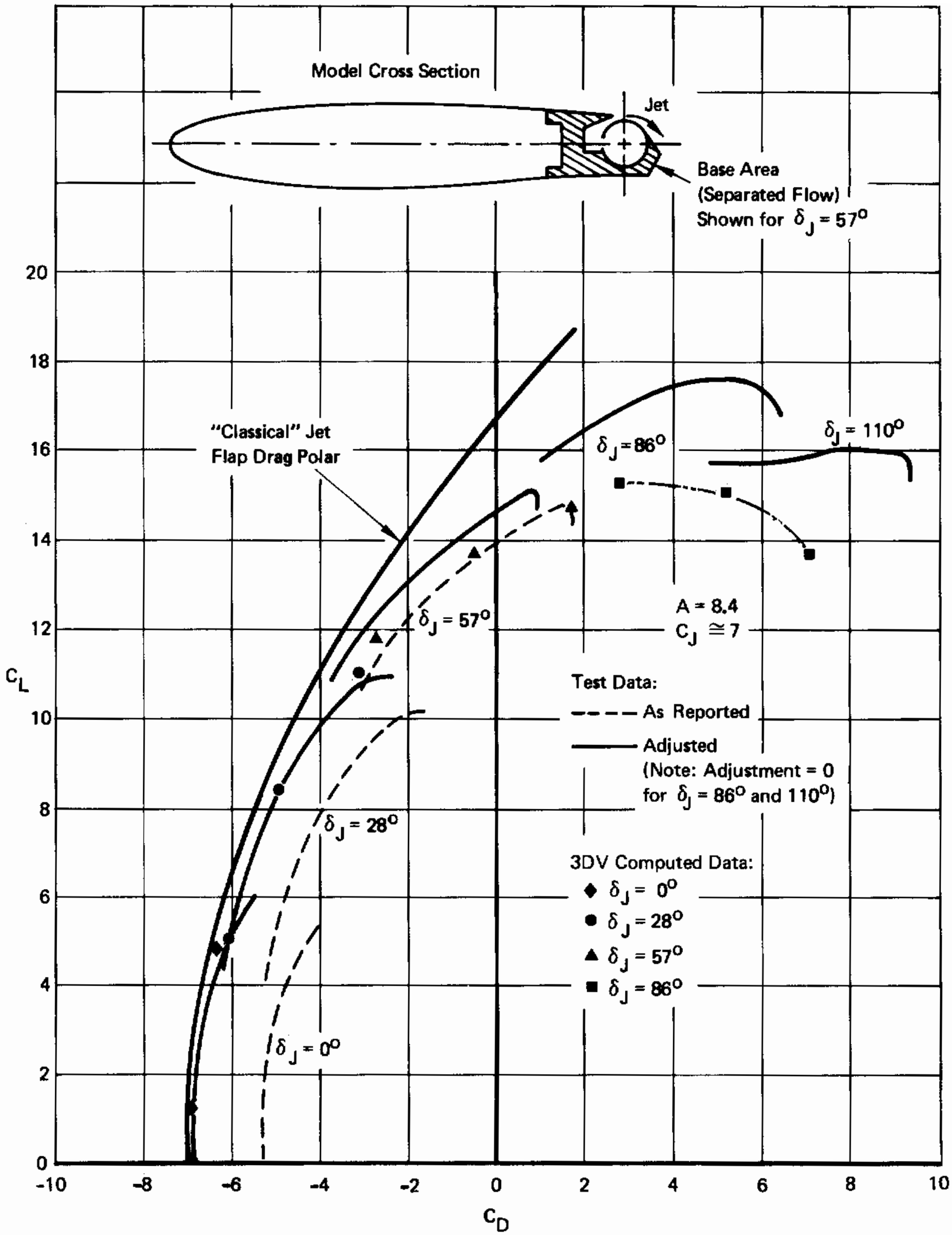

Figure 10: Drag of a Rectangular Jet Flapped Wing With Full Span Blowing (Ref. 9)

The deviation from parabolic form at high C_L is similar to that given by Helmbold's theory (already cited), in which the anti-streamwise induced velocity due to the tilt of the trailing vortices reduces the lift at a given circulation value, without reducing induced drag. This effect should be even more striking in the jet flap case, where blowing at high C_J carries the vortex system steeply down behind the wing.

The method of this report (which will henceforth be referred to as the 3DV method, for "3-Dimensional Vortex") includes this effect, and as a result is successful in predicting the break-away from parabolic shape, as will also be seen on Figure 10. The loss in lift at the largest angle tested (δ_J = 110°) is prematurely predicted, indicating that further refinement of the analytical relation between C_J, δ_J, and vortex system geometry is required. No such loss could have been predicted by a theory based on a planar vortex system, however.

Figure 11 shows C_L vs α for the same conditions. Here, the need for improvement of the vortex geometry model is reflected in the reduction of computed lift curve slope at δ_J = 86° to zero and below, which the test data indicate is approached only at δ_J = 110° or beyond. Agreement at lower jet angles is fair, indicating that refinement of the $C_L - \delta_J - \alpha - C_J$ relation is also needed.

4.2 Partial Span Jet Flaps

The same model was also tested by Gainer[11], with blowing over the inboard half of the span, at δ_J = 57°.* His results indicate that the three-dimensional trailing vortex structure is even more essential in the analysis of systems using partial span flaps. Figure 12 shows the polar obtained at C_J = 1.79. In this case, the difference between the test results and the "classical" jet flap polar is dramatic. Here, a substantial fraction of the added drag may be ascribed to the short span of the heavily loaded inboard portion of the wing. This effect accounts, however, for only half the measured additional drag at C_L = 5.0. The 3DV method predicts nearly the full increment indicated by the adjusted test data.

Figure 13 shows the calculated spanwise circulation distribution for the C_L = 6.15 condition. The lift and drag of a planar-vortex system having this distribution of bound vorticity were computed using a method based on Rauscher's analysis[12]. The jet forces were added vectorially as indicated by the diagram at the upper right of the figure to determine the "classical" drag corrected for span load distribution effects.

The failure of this model to achieve C_L's above 5.0 is attributed to stall of the outboard portion of the wing, where, of course, there is not jet to produce low trailing edge pressures to maintain attachment of the upper surface flow. The 3DV computer program fails to predict this stall, of course, since it is based on potential flow section characteristics.

*Gainer includes the jet-deflection-setting wedge's contribution to the chord, giving a slightly higher reference area and reducing the nominal aspect ratio from 8.4 to 8.3.

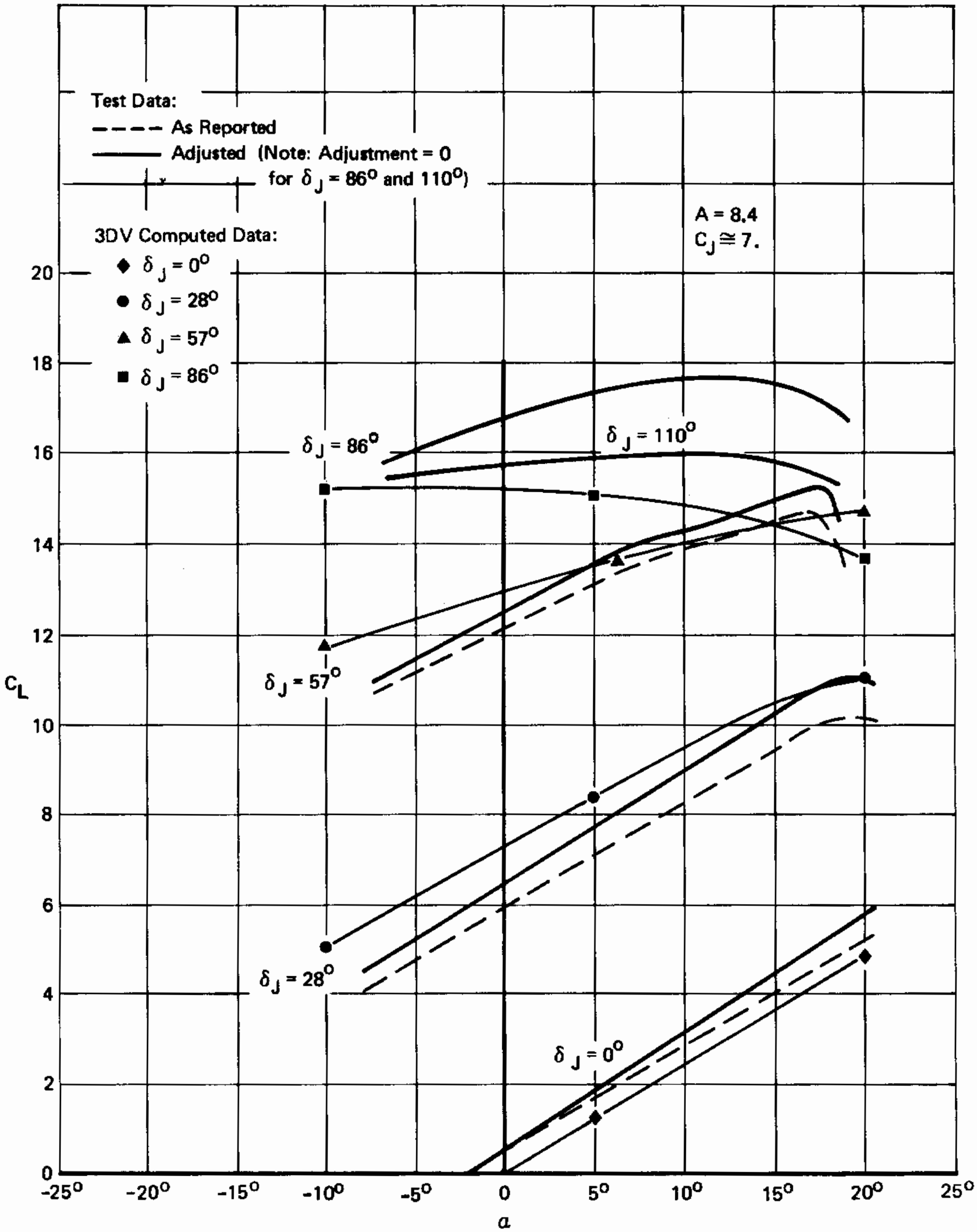

Figure 11: Lift of a Rectangular Jet Flapped Wing With Full Span Blowing (Ref. 9)

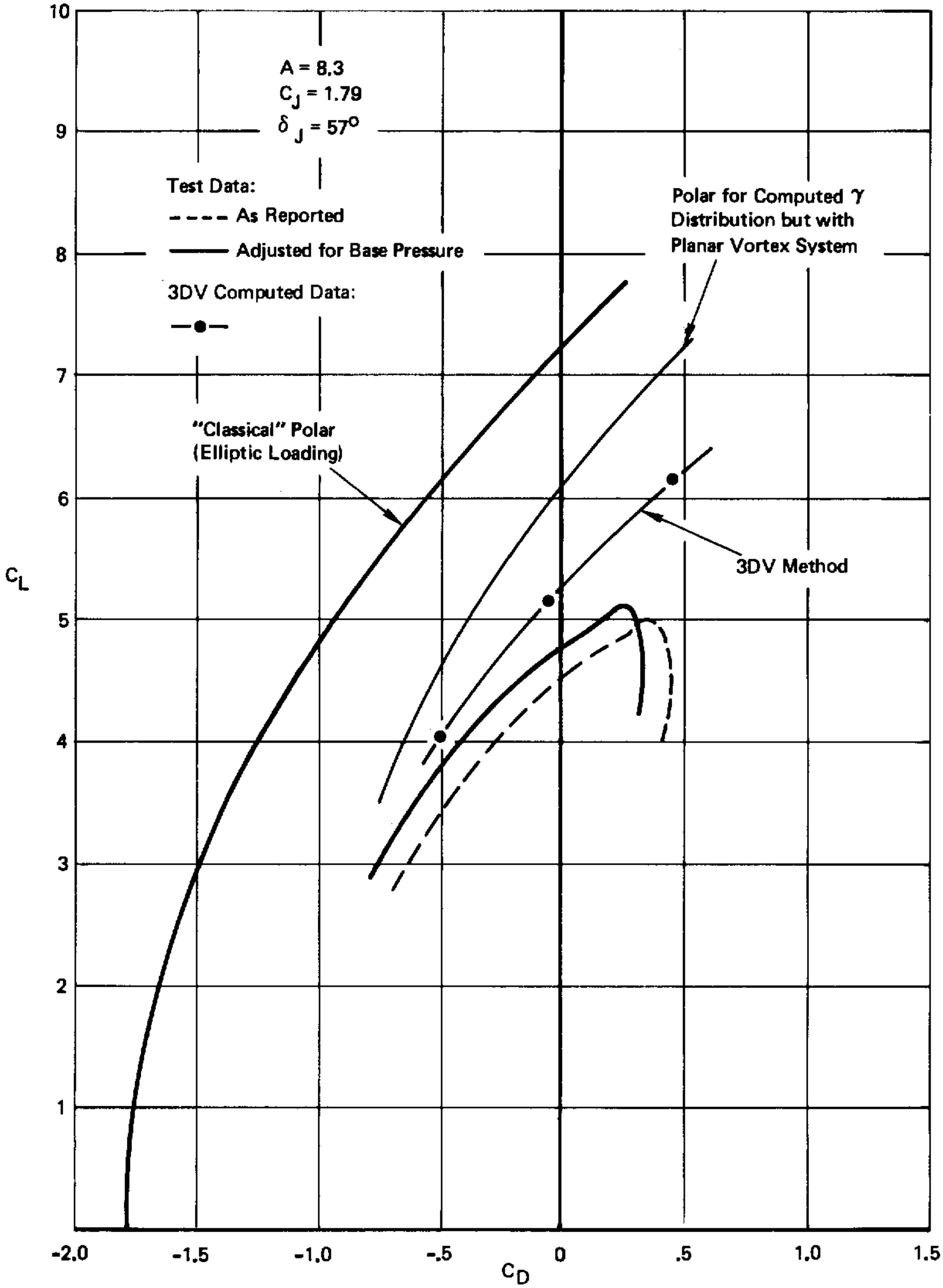

Figure 12: Drag of a Rectangular Jet Flapped Wing With Blowing Over the Inboard Half Span (Ref. 11)

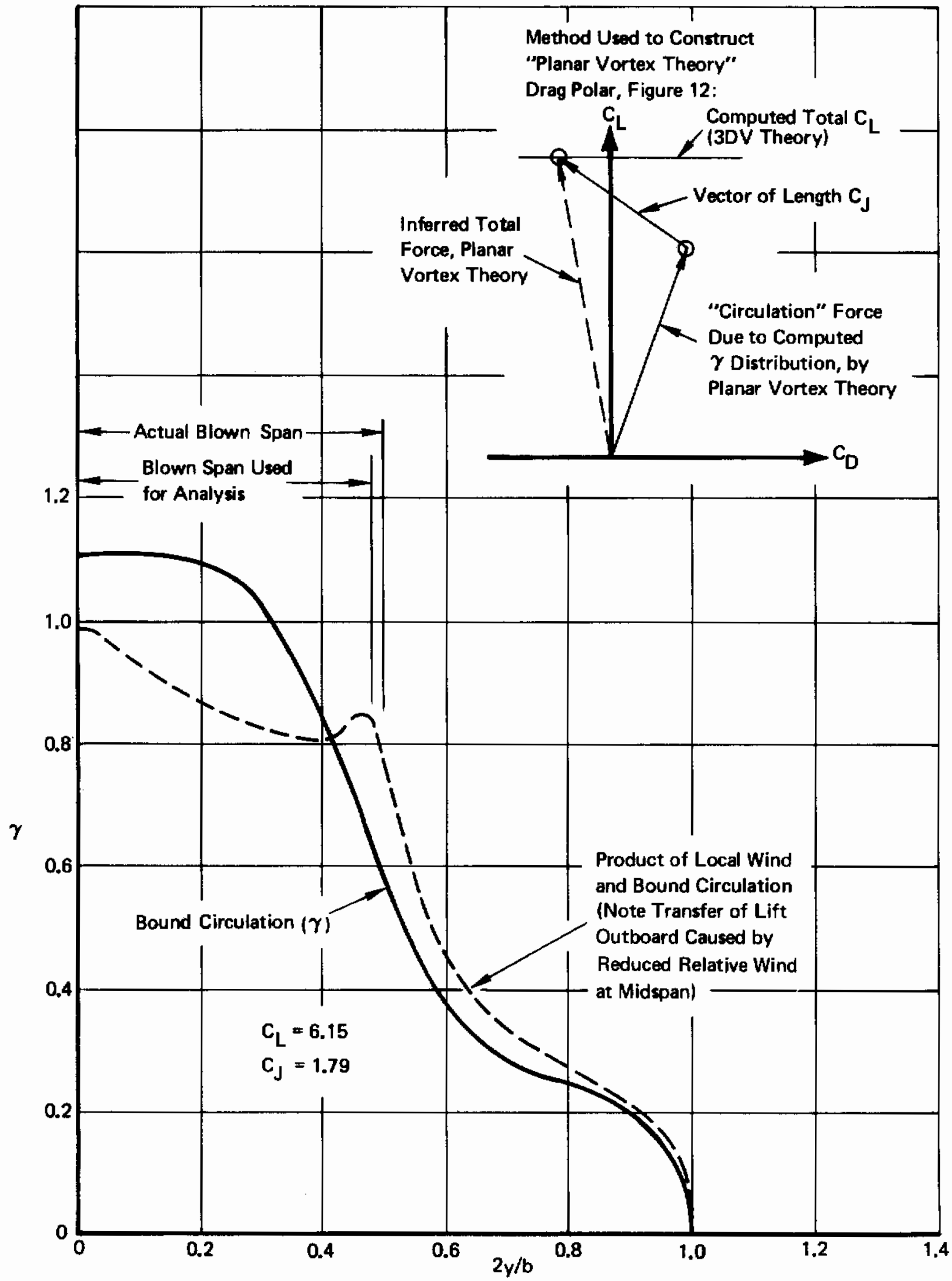

Figure 13: Circulation and Lift Distribution for Rectangular Jet Flapped Wing With Blowing Over the Inboard Half Span

Figure 14 compares measured and predicted lift curves. Again, the need for refinement of the $C_L - \alpha - \delta_J - C_J$ relation for section characteristics is indicated.

4.3 Jet Flap AMST Model

A model representative of a tactical transport equipped with internally blown trailing edge flaps was tested in the STOL TAI program, and the results reported in Volume IV of the present series by Monk, Lee and Palmer[13]. This model was more realistic than the somewhat academic device discussed in the preceding subsections, in that the wing was interrupted by a cargo-transport fuselage, the jet was blown over a 75% span flap of substantial chord, and nacelles were installed.

Figure 15 shows the measured longitudinal aerodynamic characteristics of this model for two jet flap angles at $C_J = 0.6$.

Lift, drag, and moment values were also computed using the 3DV program. Body carry-over effects were assumed to be adequately simulated by an unblown flap of the same chord and deflection as the jet flap, covering the portion of span between the inboard ends of the actual flaps. (The topic of body carry-over for powerful high lift systems deserves a study in itself, and was not investigated in this study.) The flap angle used for computation was 5° higher than the model geometric value, because the jet was nearly parallel to the flap upper surface, which was substantially steeper than the centerline reference.

Agreement is good at $\delta_F = 40°$. However, at $\delta_F = 80°$, drag and nose-down moment are underestimated, and the lift is too high. The drag deficiency indicates that not enough 3DV effect was registered at $\delta_F = 80°$. In the previous case, at about 10 times the jet strength, the 3DV effects were exaggerated at high angles. The need for refinement of the relation of C_J to jet geometry is again apparent.

4.4 Comparison with the EVD (Lopez-Shen) Method

To provide a comparison of the 3DV method with recent jet flap analyses using more sophisticated techniques than the classical analysis, it was applied to a case already analyzed by Lopez and Shen[6]. This was a model tested by the Royal Aircraft Establishment and reported by Butler, Guyett, and Moy[14]. This model had a full span jet flap of 9% chord, but the blowing was interrupted at the center by a fuselage. The wing section was an NACA 4424 profile, resulting in a jet angle about 20° steeper than the nominal centerline reference angle of the flap.

Figure 16 shows drag polars at 3 C_J's for 30° flap deflection (about 50° jet deflection), as measured by the RAE and as predicted by the 3DV method. Agreement is quite good. The "EVD" (elementary vortex, Douglas) method applied to the $C_J = 2.13$ case underpredicts drag substantially. (Ref. 6 did not give EVD drag results for the other C_J values.) This further substantiates the need for a three-dimensional vortex representation.

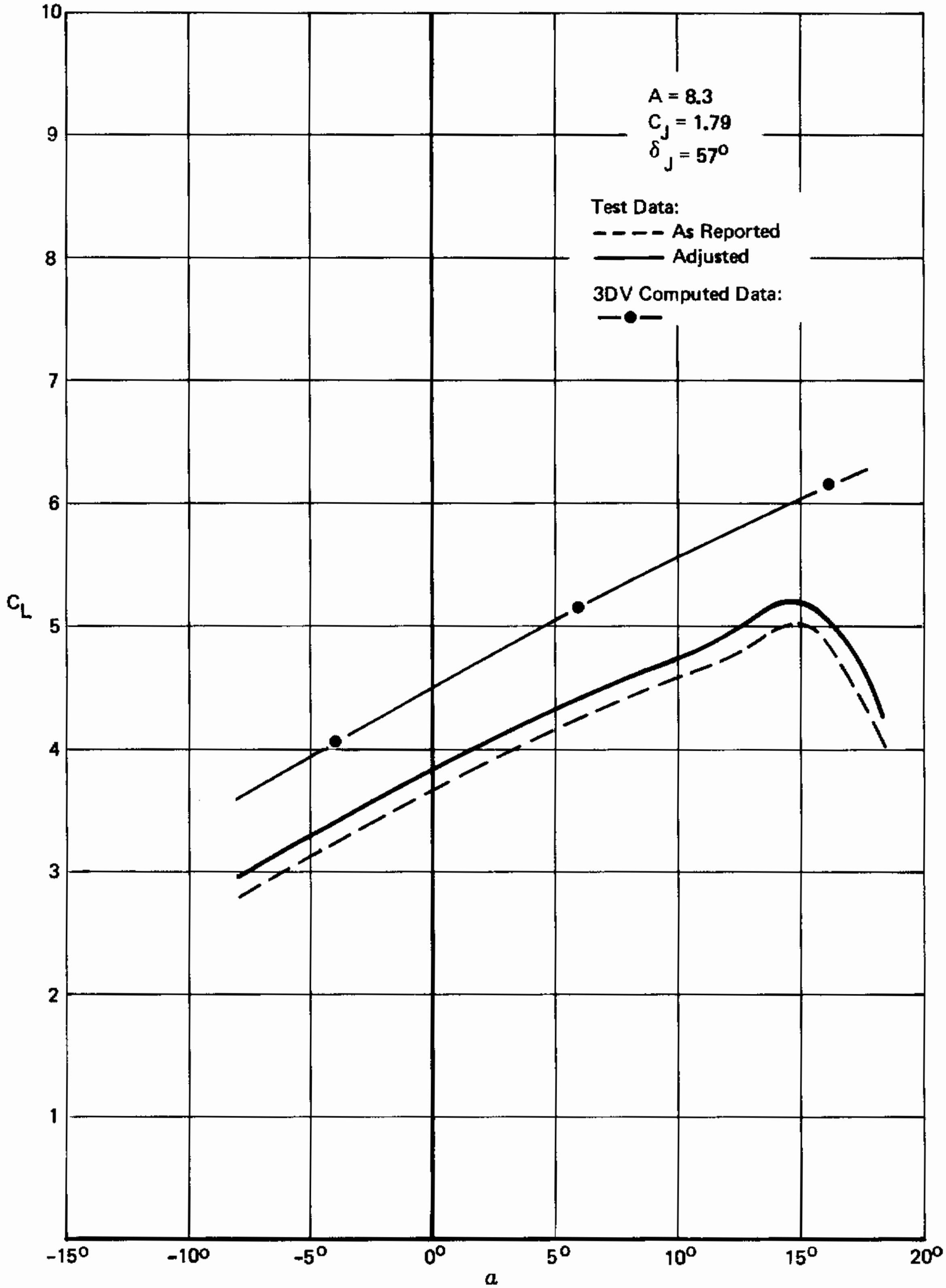

Figure 14: Lift of a Rectangular Jet Flapped Wing With Inboard Half Span Blowing (Ref. 11)

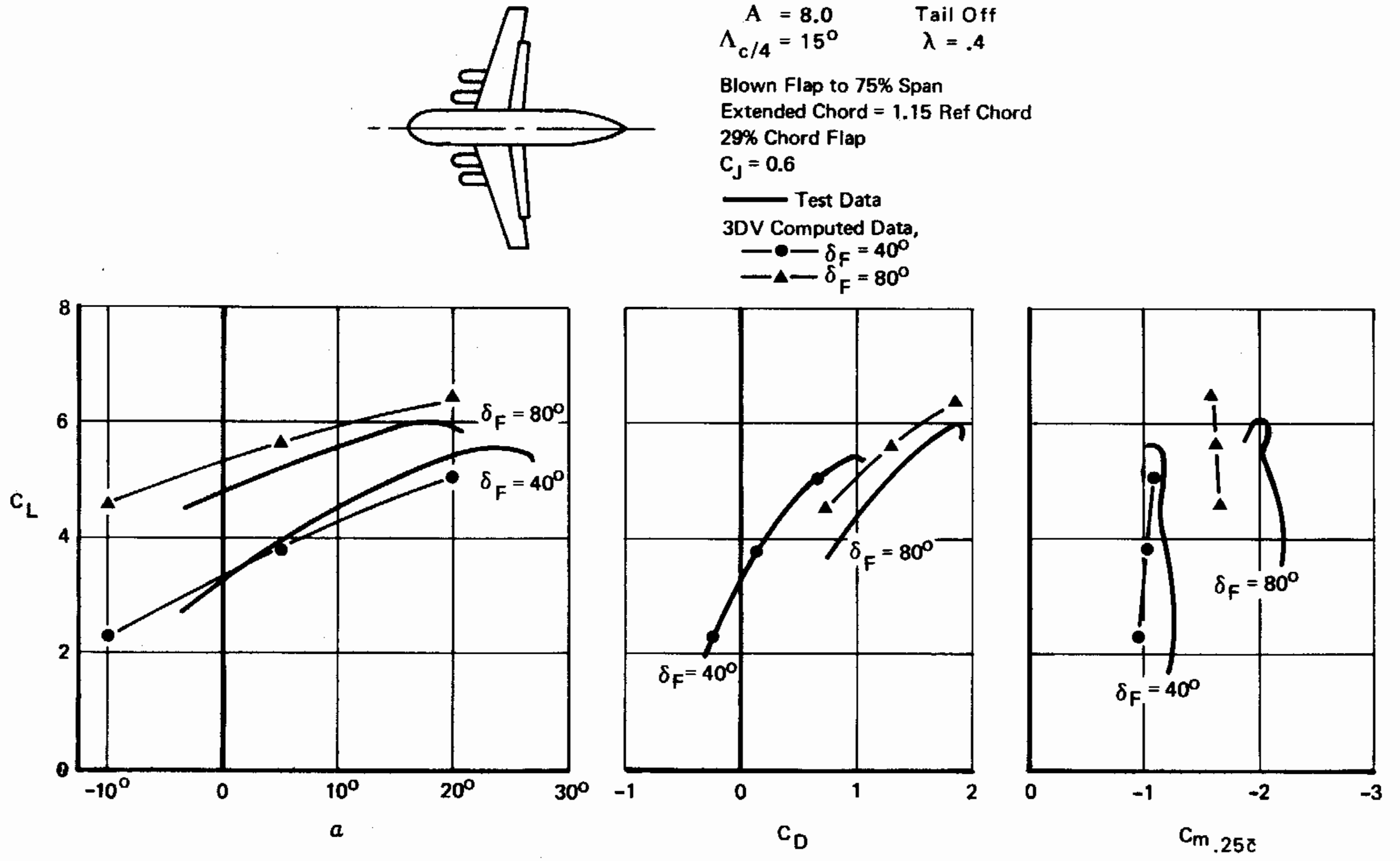

Figure 15: Longitudinal Aerodynamic Characteristics of a Jet Flapped AMST Model at C_J = 0.6 (Ref. 13)

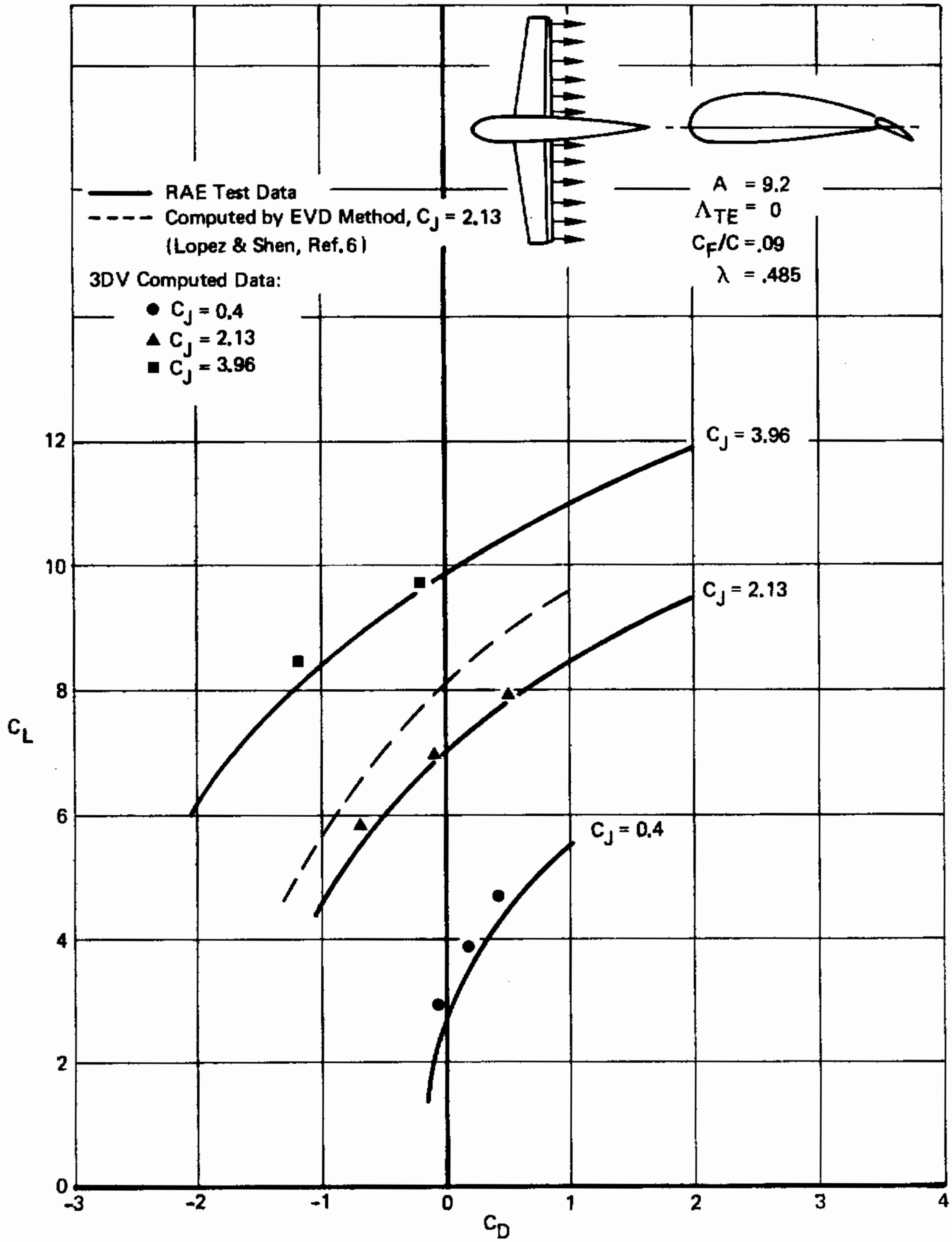

Figure 16: Drag Correlation of 3DV and EVD Methods, RAE Jet Flap Model, $\delta_F = 30^o$ ($\delta_J = 50^o$)

Figure 17 shows lift and pitching moment for the same test conditions. Both methods give good correlation at the lower C_J values. (In fact, the precision of the 3DV data's agreement at $C_J = 0.4$ is fortuitous. Since no representation of airfoil camber is included in the C_L vs α function, α's are only good to within an additive constant.) The 3DV method predicts a reduction in lift curve slope at higher angles of attack. This is due to the reduction of dynamic pressure at the wing caused by the anti-streamwise component of induced velocity. This prediction is borne out by the test results. It is not indicated by the EVD method.

Moment correlation of the EVD method is better. However, no attention has yet been devoted to "calibration" of the $C_m - C_J - \delta_F - \alpha$ relation in the 3DV program.

4.5 Externally Blown Flap

Parlett, Greer, Henderson and Carter[15] report the results of testing a swept-wing cargo transport type of configuration equipped with full span triple-slotted flaps blown by underwing nacelles. Figure 18 shows this model in the "spread engine" arrangement. (It was also tested with the engines in dual pods.)

The 3DV program was applied to this case to determine its capability to handle problems of maximum complexity. For analytical purposes, each wing was divided into five panels. The center panel represented the inboard wing plus the body "carry-over" region, the second and fourth panels represented the portions of the wing blown by the engines, and the third and fifth the remainder of the wing.

The C_J used for calculation was reduced to reflect "turning losses" as measured statically. The ratio of total force experienced by the model to thrust developed by the nacelles alone was 0.83 at 40° flap angle. Therefore, $C_J = 1.55$ was used for the 3DV analysis where the test was run at $C_J = 1.87$.

Figure 19 shows computed and measured tail-off longitudinal characteristics for this case. The test data show a break in the lift curve at $\alpha = 10°$, indicating flow separation over some part of the wing, most likely the outboard region, judging from the corresponding drift of the pitching moment toward more positive values.

The predicted lift curve slope (below the aforementioned partial separation) is too low, although the absolute lift level is close at $\alpha = 10°$. The pitching moment is roughly correct at low C_L, but does not, of course, register the pitch up. The drag agreement is excellent below stall. Again, refinement of the lift function is clearly needed, but these results were considered quite encouraging.

Test data were also given for $C_J = 3.74$. Computation attempted for this case failed to converge, however. In this case, a section C_J nearly equal to 9 is reached behind the outboard nacelle. The exact

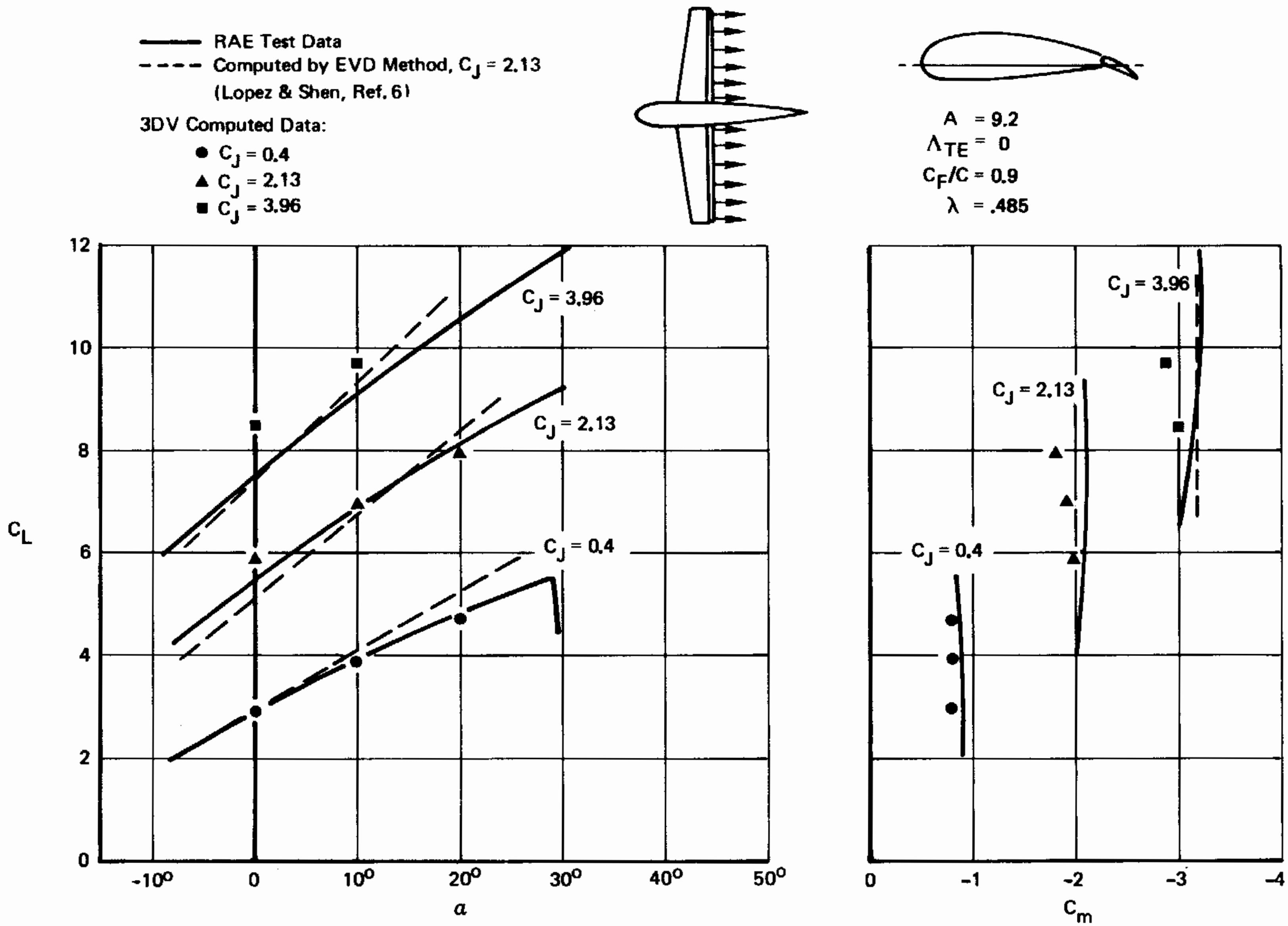

Figure 17: Lift and Moment Correlation of 3DV and EVD Methods, RAE Jet Flap Model $\delta_F = 30^o$ $(\delta_J = 50^o)$

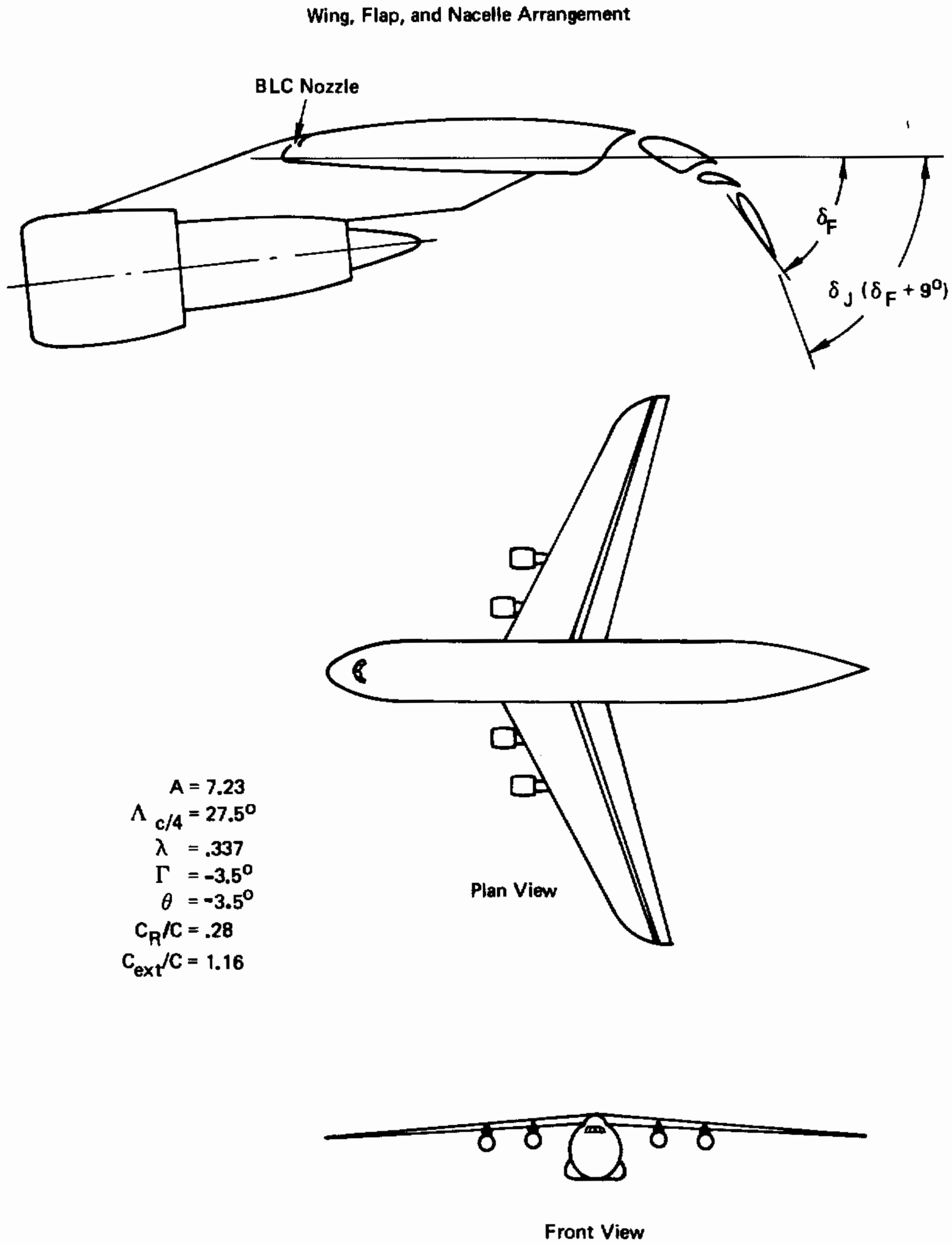

Figure 18: Externally Blown Flap Wind Tunnel Model (Ref. 15)

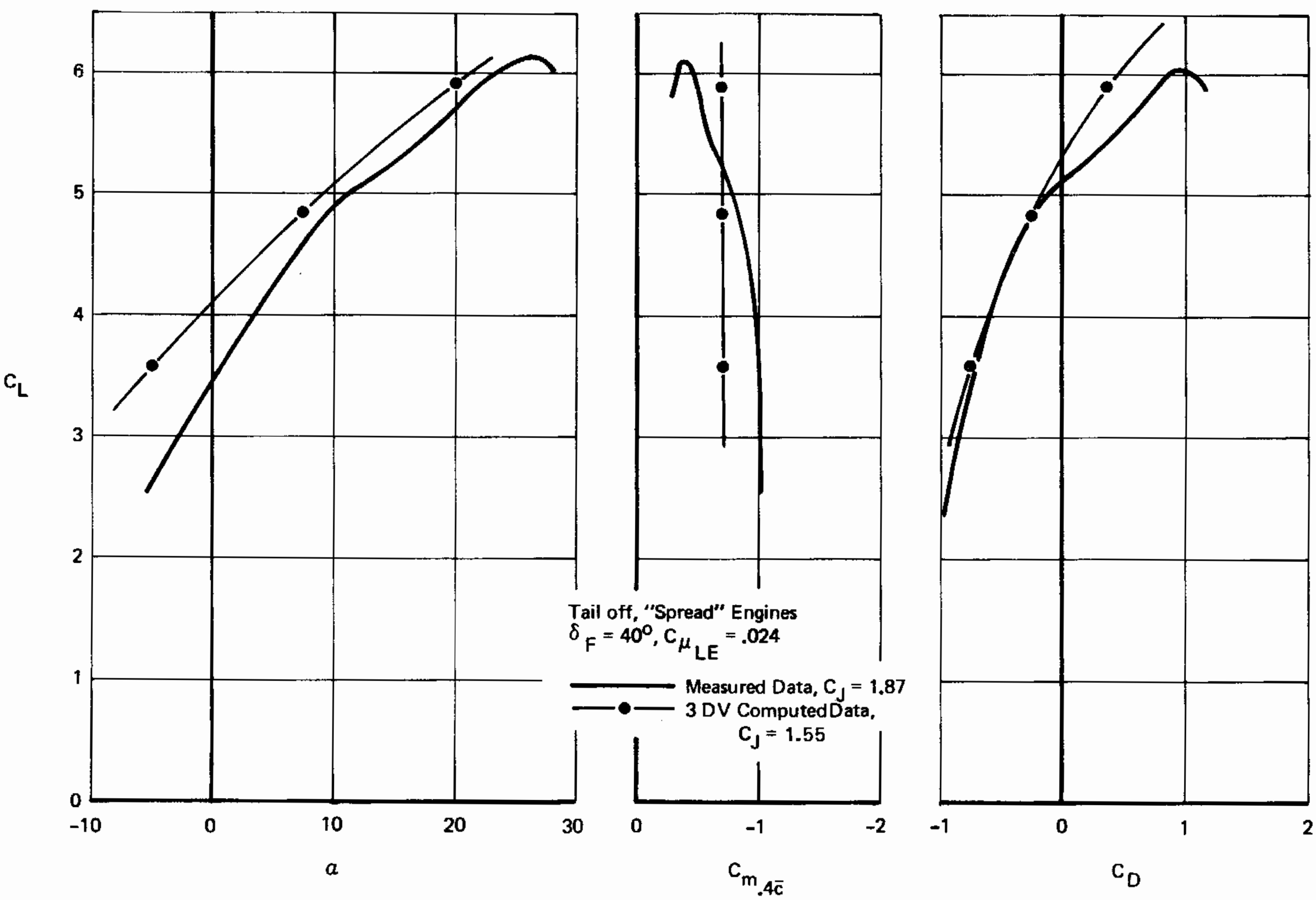

Figure 19: Longitudinal Characteristics of an Externally Blown Flap Configuration (Ref. 15)

mechanism by which the rapid local variation of section C_J prevents convergence is not understood, and must be resolved if this analysis is to reach its full potential usefulness.

Engine-out calculations were also run. Lateral characteristics are compared to test data in Figure 20. No engine-out tests were run with the vertical tail removed, so the comparison is somewhat ambiguous. The predicted rolling moment due to engine failure is on the conservative side until stall occurs. This implies that the 3DV method (as presently formulated) underestimates the spanwise extent of the influence of the still-operating inboard engine. Additional work is therefore indicated.

Because the model had a vertical tail, comparison of yawing moment and sideforce are dubious. However, if the difference in sideforce is attributed entirely to the fin, then the yawing moment can be corrected as indicated, to give good agreement. (Admittedly, the scale of the C_Y plot given by Reference 15 is too small to be read accurately, but the correction should be good to about 0.01 in C_n.)

4.6 Concluding Remarks

The 3DV method is able to predict the drag of jet flapped wings at high blowing coefficients and jet angles better than any method not containing the essential feature of a nonplanar trailing vortex system.

Refinement of the section $C_\ell - \alpha - C_J - \delta_F$ relation is needed to improve lift prediction. The usefulness of the method would be improved by resolution of difficulties in the solution procedure so that EBF systems can be analyzed at higher C_J's than presently possible.

Further study of the spanwise lift distribution due to locally concentrated blowing is also needed.

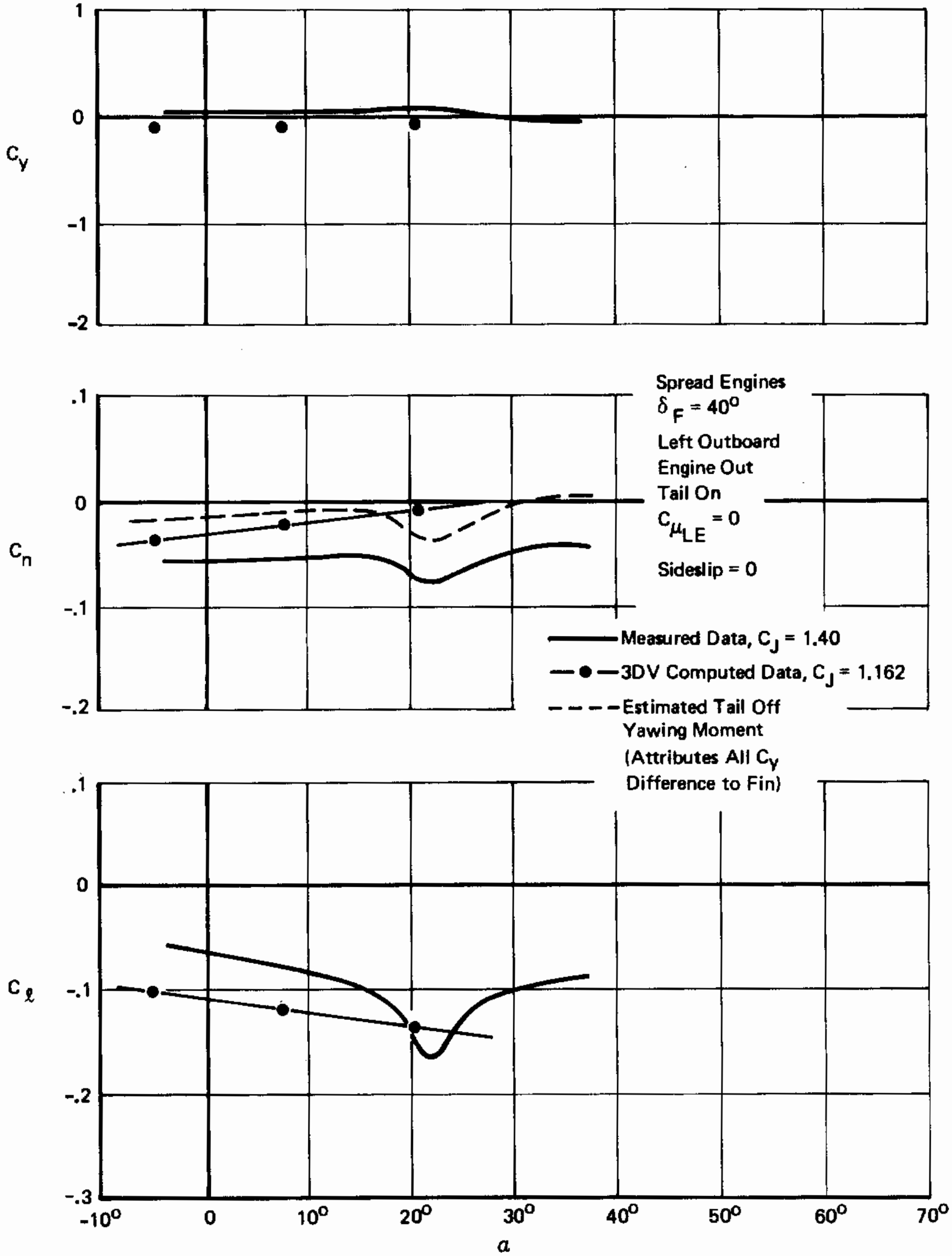

Figure 20: Engine Out Lateral Characteristics of Externally Blown Flap Configuration (Ref. 15)

APPENDIX I

DOWNWASH ANGLE OF A HIGHLY LOADED WING

The vortex system trailed behind a wing will be inclined to the freestream wind vector because of the downwash field of the wing. The angle of inclination will be greatest near the wing, but as the influence of the bound vortex diminishes with distance downstream, the angle approaches the value due to the trailing vortices alone.

Consider an elliptically loaded wing of span b and midspan circulation Γ_0 in a stream of velocity U and density ρ. The downwash velocity w induced at the wing by the trailing vortex system will be

$$w = \Gamma_0 / 2b \tag{I-1}$$

Far downstream, the induced velocity will be twice as great, and the downwash (and vortex inclination) angle will be

$$\varepsilon = \sin^{-1}(\Gamma_0 / Ub) \tag{I-2}$$

The velocity w will be inclined to U by at least this angle, so the wind component at the wing in the freestream direction will be reduced to

$$V = U - w \sin \varepsilon$$

or

$$V = U\left[1 - \frac{1}{2}\left(\frac{\Gamma_0}{Ub}\right)^2\right] \tag{I-3}$$

The lift on the wing is

$$L = \frac{\pi b}{4} \rho V \Gamma_0 \tag{I-4}$$

so

$$C_L = \frac{\pi A}{2}\left(\frac{\Gamma_0}{Ub}\right)\left[1 - \frac{1}{2}\left(\frac{\Gamma_0}{Ub}\right)^2\right] \tag{I-5}$$

where A is the wing aspect ratio (b^2/area).

This formula implies an upper limit to C_L of

$$C_{L_{LIM}} = \frac{\pi A}{3}\sqrt{\frac{2}{3}} = 0.855A \qquad \text{(I-6)}$$

reached when Γ_0/Ub equals $\sqrt{2/3}$. However, Lockwood's data[9] indicate that jet flapped wings can attain circulation C_L's more than twice this "limiting" value.

Helmbold[8] pointed out that this problem is resolved if the rolling up of the trailing vortex system is considered. Vortex sheets are generally unstable, and tend to roll up into pairs of more-or-less concentrated vortex cores. Momentum conservation arguments show that the sheet from an elliptically loaded wing should roll up into a pair of concentrated vortices of strength Γ_0 at a spacing of $\pi b/4$ from each other. Each one induces a downwash velocity on the other, given by

$$w' = 2\Gamma_0/\pi^2 b \qquad \text{(I-7)}$$

so they must be inclined to the freestream at the angle

$$\varepsilon' = \sin^{-1}\left(2\Gamma_0/\pi^2 bU\right) \qquad \text{(I-8)}$$

Helmbold then infers a relation between C_L and ε' through an argument based on energy conservation in the Trefftz plane. The same relation can be obtained in terms of conditions at the wing itself by assuming that the downwash velocity at the wing is still the value given by Equation I-1, but the inclination is reduced from ε to ε'.

The wind at the bound vortex is then

$$V' = U - w \sin\varepsilon' \qquad \text{(I-9)}$$

or

$$V' = U\left[1 - \left(\frac{\Gamma_0}{\pi bU}\right)^2\right] \qquad \text{(I-10)}$$

The lift coefficient will then be

$$C_L = \frac{\pi A}{2}\,\frac{\Gamma_0}{bU}\left[1 - \left(\frac{\Gamma_0}{\pi bU}\right)^2\right] \qquad \text{(I-11)}$$

The corresponding limit to C_L is

$$C_{L_{LIM}} = \pi^2 A / 3\sqrt{3} = 1.8994A \qquad \text{(I-12)}$$

This value agrees well with Lockwood's observed maximum circulation C_L. The "rolled up" vortex inclination angle, ε', is therefore used as the far wake inclination angle in the present analysis.

The equation relating ε' and C_L is awkward:

$$C_L = \frac{\pi^3 A}{4} \sin \varepsilon' \left(1 - \frac{\pi^2}{4} \sin^2 \varepsilon'\right) \qquad \text{(I-13)}$$

It was found more convenient to approximate the inverse of this relation by

$$\varepsilon' = 0.243 \sin^{-1}\left(C_L / 1.8994A\right) \qquad \text{(I-14)}$$

This expression is accurate within one percent over the whole range of C_L's, from 0 to 1.8994A.

APPENDIX II

VELOCITY DUE TO A VORTEX SEGMENT

The Biot-Savart law gives the incremental velocity due to an element $d\bar{s}$ of a vortex filament of circulation Γ, at a point whose position from the element is $\bar{r}$:

$$d\bar{v} = \frac{\Gamma}{4\pi|\bar{r}|^3} \quad d\bar{s} \times \bar{r} \tag{II-1}$$

Integrated over a straight line segment of constant circulation, this gives

$$|\bar{v}| = \frac{\Gamma}{4\pi h} \left(\cos\theta_1 - \cos\theta_2\right) \tag{II-2}$$

where h, θ_1 and θ_2 are as diagrammed in the sketch below, drawn in the plane containing the vortex segment and the point.

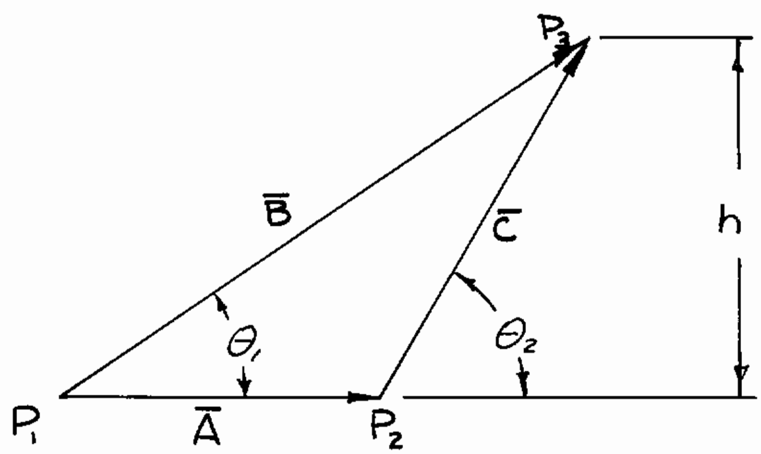

The direction of the induced velocity would be "out of the paper" for the circulation sense indicated by the arrow.

The procedure as programmed, therefore, computes the induced velocity vector, for unit Γ, using the vector cordinates of the segment ends ($\bar{P}_1$ and $\bar{P}_2$) and of the point ($\bar{P}_3$), as follows:

1) Define

$$\begin{aligned} \bar{A} &= \bar{P}_2 - \bar{P}_1 \\ \bar{B} &= \bar{P}_3 - \bar{P}_1 \\ \bar{C} &= \bar{P}_3 - \bar{P}_2 \end{aligned} \tag{II-3}$$

2) The unit vector parallel to $\bar{v}$ is

$$\bar{U}_v = \frac{\bar{A} \times \bar{B}}{|\bar{A} \times \bar{B}|} \qquad \text{(II-4)}$$

3) The cosines are given by

$$\cos \theta_1 = \frac{\bar{A} \cdot \bar{B}}{|\bar{A}||\bar{B}|}$$

and (II-5)

$$\cos \theta_2 = \frac{\bar{A} \cdot \bar{C}}{|\bar{A}||\bar{C}|}$$

4) The perpendicular distance is

$$h = |\bar{B}| \sin \theta_1 = \frac{|\bar{A} \times \bar{B}|}{|\bar{A}|} \qquad \text{(II-6)}$$

5) $\bar{v}$ is then the product of $|\bar{v}|$ from Equation II-2 and $\bar{U}_v$.

In the case of a semi-infinite vortex, $\bar{P}_1$ and $\bar{P}_3$ are as before, but $\bar{A}$ is defined as a unit vector parallel to the vortex, and replaces $\bar{P}_3$ as an input. Then Steps 3 and 4 become:

3) The cosines are

$$\cos \theta_1 = \frac{\bar{A} \cdot \bar{B}}{|\bar{B}|}$$

and (II-7)

$$\cos \theta_2 = 1$$

4) The perpendicular distance is

$$h = |\bar{A} \times \bar{B}| \qquad \text{(II-8)}$$

APPENDIX III

DAMPING FACTORS AND SMOOTHING

1. Damping Factors

The vortex strengths are determined by a set of weakly nonlinear equations. The nonlinearity is introduced by the inclusion of streamwise induced velocities in the determination of angle of attack and in the relation between circulation and lift coefficient. To obtain damping factors which would result in economical convergence of the successive approximations, consider the situation when nonlinearities are ignored. The equations defining the vortex strengths are then of the form

$$C_{L_i} = C_{L_\delta}\delta + C_{L_\alpha}\left(\alpha - \sum_j \gamma_j W_{ij}\right) \qquad \text{(III-1)}$$

and

$$\gamma_i = C_{L_i}\, c\, V/2 \qquad \text{(III-2)}$$

where C_{L_α} and C_{L_δ} are (local) partial derivatives of section C_L* with angle of attack and flap deflection, γ_i the circulations, W_{ij} the change in α at the ith station due to unit circulation at the jth station, and α, δ, c and V are geometric angle of attack, flap deflection, chord, and wind across the lifting line. (All of the latter four may differ at various stations, but are independent of the γ's.)

Define

$$K_{ij} = \frac{1}{2} C_{L_\alpha} c V W_{ij} \qquad \text{(III-3)}$$

Then the equations for the γ's can be written

$$\gamma_i + \sum_j K_{ij}\gamma_j = R_i \qquad \text{(III-4)}$$

where R_i includes all the terms not containing γ's. To solve this set of equations by iteration, an initial set of γ's is assumed, and a subsequent one computed using Equation III-4, rearranged:

$$\gamma_i = R_i - \sum_j K_{ij}\gamma_{j_{OLD}} \qquad \text{(III-5)}$$

*"Circulation" C_L that is.

The next set of trial γ's will then be given by

$$\gamma_{i_{NEW}} = d_i \gamma_i + (1 - d_i)\gamma_{i_{OLD}} \qquad \text{(III-6)}$$

where the d_i's are the damping factors we seek.

The K_{ij}'s generally follow the following pattern:

1) For i = j, K_{ij} is a large positive number.

2) For i = j, K_{ij} is a negative number. Unless i and j are nearly equal, K is a small negative number.

This implies that the solution will be dominated by the terms for which i = j, In the limit, neglecting all other terms, that would imply

$$\gamma_i \cong \frac{R_i}{1 + K_{ii}} \qquad \text{(III-7)}$$

For what value of d_i will this result be obtained for $\gamma_{i_{NEW}}$, starting from an arbitrary set of $\gamma_{i_{OLD}}$'s? Replacing the summation in III-5 by the single term $\gamma_i K_{ii}$, substituting the result in III-6 and equating to III-7 gives

$$d_i R_i + \gamma_{i_{OLD}}\left[1 - d_i(1 + K_{ii})\right] = \frac{R_i}{1 + K_{ii}} \qquad \text{(III-8)}$$

If d_i is taken to be

$$d_i = \frac{1}{1 + K_{ii}} \qquad \text{(III-9)}$$

then Equation III-8 is satisfied identically, and the coefficient of $\gamma_{i_{OLD}}$ vanishes.

To apply this to the actual case, K_{ii} is interpreted as

$$K_{ii} = -\frac{\partial \gamma_i}{\partial \gamma_{i_{OLD}}} \qquad \text{(III-10)}$$

This is calculated by computing a set of γ's based on zero induced velocities, then finding the change due to the velocities induced by a very small increment in γ.

In practice, the d_i's so computed have been found to be too large, leading to divergence. However, values in the range of 0.8 to 0.9 of the theoretical d_i's usually work very well. To prevent divergence in the case of anomalies caused by possible large differences between the computed derivatives and those correct for the "near solution" environment, the maximum difference between γ_{iOLD} and γ_{iNEW} is tracked. If this "excess" increases between successive iterations, the d_i's are all multiplied by 0.8 for subsequent trials.

2. Smoothing

The smoothing procedure begins by a transformation of the spanwise coordinate:

$$\bar{y} = \sin^{-1} y \qquad \text{III-11}$$

Fourier cosine series are then determine for the circulation:

$$\gamma(\bar{y}) = \sum B_n \cos(n\pi\bar{y}/2) \qquad \text{III-12}$$

Each side is done independently, which implies a series for which the B's vanish for even values of n. The result is that the smoothed ($\bar{y}$) must have zero slope on the airplane centerline, which is only necessarily true for symmetrical cases. However, the slope at the centerline is generally small, even when symmetry is not present, in the flight conditions of interest for STOL. No serious distortion of the results is therefore expected.

The coefficients of the series are determined by numerical integration of the expression

$$B_n = \frac{4}{\pi}\int_0^{\pi/2} \gamma(\bar{y}) \cos(n\pi\bar{y}/2)\, d\bar{y} \qquad \text{III-13}$$

Smoothing is then done by determining a new circulation function using only the first six terms of the series:

$$\gamma_{SMOOTH}(\bar{y}) = \sum_{\substack{n=1 \\ (Odd)}}^{11} B_n \cos(n\pi\bar{y}/2) \qquad \text{III-14}$$

This procedure is based on concepts used in classical lifting-line theory, as presented, for example, by Rauscher[12]. The transformation and the use of Fourier series are "natural" for the problem: In the case of elliptic loading, all the Fourier coefficients except the first one vanish. Furthermore, when the wake angle is low, the lift is determined entirely by the first coefficient:

$$C_L = \frac{\pi}{8} B_1 A \qquad \text{III-15}$$

and the induced drag coefficient is given by

$$C_{D_i} = \frac{C_L^2}{\pi A}\left[1 + 3\left(\frac{B_3}{B_1}\right)^2 + 5\left(\frac{B_5}{B_1}\right)^2 + \dots\right] \qquad \text{III-16}$$

APPENDIX IV

COMPUTER PROGRAM

1. General

The analysis procedure has been coded for automatic computation in FORTRAN IV language for the CDC 6600 digital computer.

2. Program Structure

The program consists of a main program, FLAPZ2, and four subroutines, VICTOR, WASH, CEEL and SMOOTH. Communication between the main program and the subroutines is mostly by means of argument; COMMON is used only for subroutine SMOOTH. Figure 21 is a block diagram of the main program.

2.1 Subroutines

2.1.1 VICTOR

Subroutine VICTOR is a package of three-dimensional vector operations, with arguments $\bar{A}$, $\bar{B}$, $\bar{C}$, D and E. Different entry points are provided for different operations, as tabulated below:

Entry	Operation
VPLUS	$\bar{C} = \bar{A} + \bar{B}$
VMINE	$\bar{C} = \bar{A} - \bar{B}$
VCROSS	$\bar{C} = \bar{A} \times \bar{B}$
VDOT	$D = \bar{A} \cdot \bar{B}$
VMAG	$D = \lvert A \rvert, \; E = \bar{A} \cdot \bar{A}$
SCALM	$\bar{C} = D\bar{A}$
SCALD	$\bar{B} = \bar{A}/D$

2.1.2 WASH

Subroutine WASH computes the velocity vector due to a unit-strength straight line vortex segment of finite or semi-infinite length. Its arguments are $\bar{P}$, $\bar{A}$, $\bar{Q}$ and $\bar{W}$.

Entry WASH finds the velocity $\bar{W}$ at $\bar{Q}$ due to a vortex extending from $\bar{P}$ to infinity, in a direction parallel to $\bar{A}$.

Entry SEG finds $\bar{W}$ at $\bar{Q}$ due to a vortex extending from $\bar{P}$ to $\bar{A}$.

2.1.3 CEEL

Subroutine CEEL computes "circulation lift" and section pitching moment in accordance with the formulae of Section 2.3, Equations 16-23.

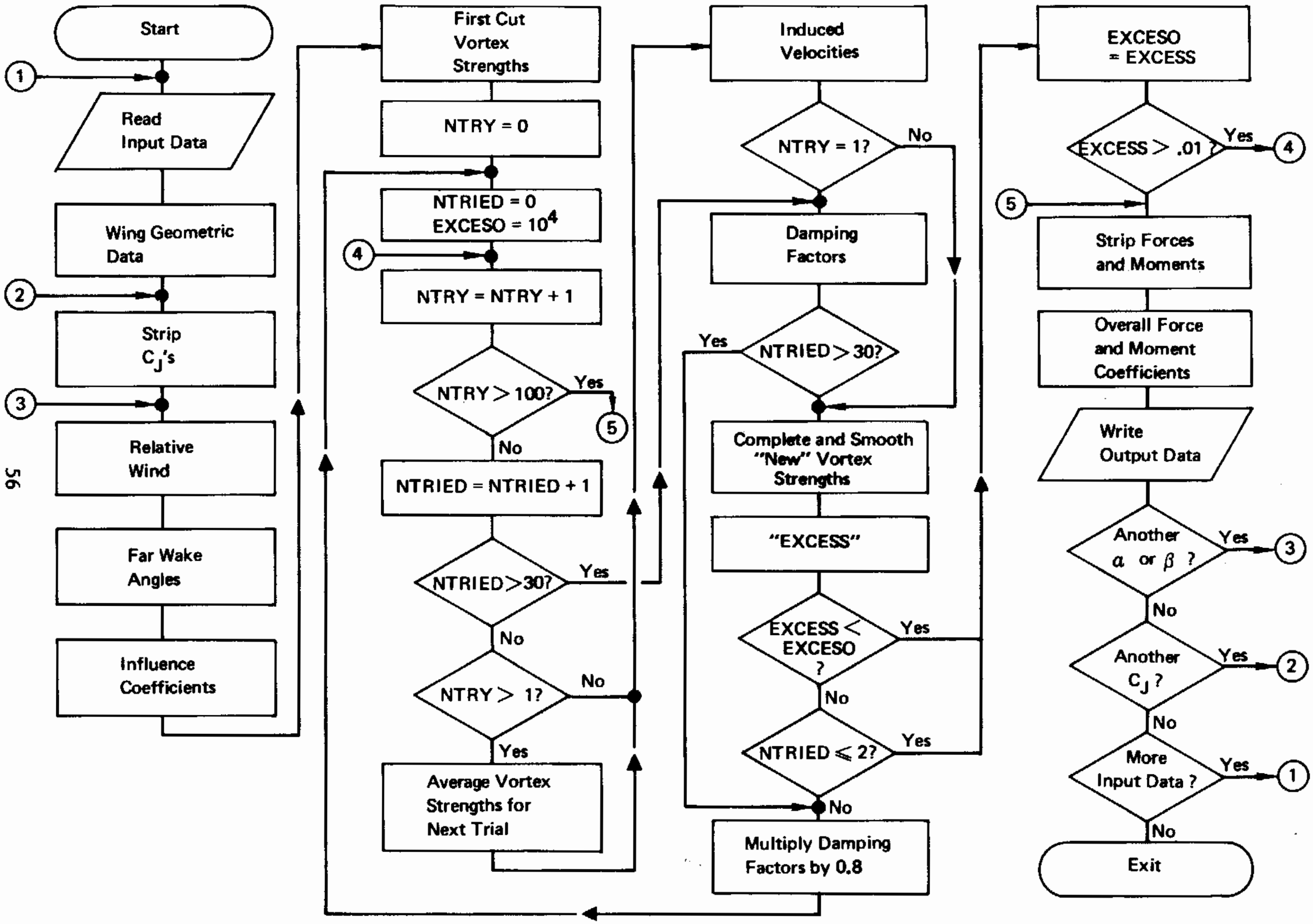

Figure 21: FLAPZ2 Program Block Diagram

2.1.4 SMOOTH

Subroutine SMOOTH contains the smoothing procedure given in Appendix III. The argument, G, is the array of γ's (either left or right wing) to be smoothed. The array of smoothed γ's is transmitted back to the main program by the same argument.

COMMON contains arrays F and T which are, respectively, weighting factors for the numerical integration used in computing the Fourier coefficients, and the values of the transformed coordinate, $\bar{y}$, corresponding to the control point locations. These are computed in the main program.

3.0 Program Listing

The FORTRAN coding of the program is listed on Pages 61 through 97. A partial table of correspondence between FORTRAN variable names and the quantities referred to in the main body of the report is given in Table II.

4. Input Data

4.1 Format

A complete set of input data comprises thirteen punched cards. Card 1 is simply 70 columns of free-form alphameric data which is printed as a heading at the beginning of each output case.

Cards 2 through 13 contain numerical data in "10-field, seven-digit" floating point format. That is, the first 70 columns of each card are divided into 10 equal seven-column "fields". Each field must either contain a number <u>with a decimal point</u> (location optional) or blanks only. Columns 71 and 72 are not used. Columns 73 through 80 are available for card identification.

4.2 Data Sequence

Card 1:	Title	
Card 2:	Field 1	Aspect Ratio
	Field 2	Sweep Angle (degrees)
	Field 3	Taper Ratio
	Field 4	Dihedral (degrees)
	Field 5	Twist (degrees)
	Field 6	Blowing Direction Number (Any number $\geq 0.$ means blowing parallel to x-axis. A number $< 0.$ means blowing normal to hinge line.)
Card 3:	Fields 1 to 5	Span stations of <u>inboard</u> ends of flap panels 2 through 6. If less than 6 panels are used, remaining values should be 1.0.

TABLE II

VARIABLE NAME CORRESPONDENCE

	FORTRAN Name	Text Symbol
Wing Descriptors:		
	AR	A
	DIHDRL	Γ
	SWEEP	Λ
	TAPER	λ
	FB	y_{end}
	CF	c_F/c
	FFR, FFL	e_F
	DFR,DFL	δ_F
	TWIST	θ
Derived Wing Data:		
	ESS	S_w
	CR	c_r
	CBAR	$\bar{c}$
	XCBAR	$x_{\bar{c}/4}$
	ZCBAR	$z_{\bar{c}/4}$
	UNR,UNL	$\bar{N}$
	ABØNDR,ABØNDL	$\bar{B}$
	DØWNR,DØWNL	$\bar{D}$
	PR,PL	$\bar{P}$
	QR,QL	$\bar{Q}$
	CNØM	c
	CHDR,CHDL	c_{ext}
Vortex System Data:		
	TEIR,TEIL	$\tilde{K}$
	TEØR,TEØL	$\bar{L}$
	EHR,EHL	$\bar{H}$
Vortex Strengths:		
	GØR,GØL	γ_{OLD} or γ_{NEW}
	GR,GL	γ
Blowing Data:		
	CJW	C_{J_W}
	BLØR,BLØL	f_B
	CJPR,CJPL	C_J
	CJR,CJL	C_{J_S}

TABLE II (Continued)

	FORTRAN Name	Text Symbol
Velocities and Influence Coefficients:		
	U	$\bar{U}$
	TRR,TRL,TLR,TLL	$\bar{T}$
	WR,WL	$\bar{W}$
Forces and Moments:		
	FØR,FØL	$\bar{F}$
	TF	$\bar{F}_{TOT}$
	FJR,FJL	$\bar{J}$
	TJF	$\bar{J}_{TOT}$
	TØTM	$\bar{M}_{TOT}$
	CLIFT	C_L
	CDRAG	C_D
	CSIDE	C_y
	CPITCH	C_m
	CRØLL	C_ℓ
	CYAW	C_n

Card 4:	Fields 1 to 6	Flap chord ratios.*
Card 5:	Fields 1 to 6	Right wing flap extension ratios.*
Card 6:	Fields 1 to 6	Left wing flap extension ratios.*
Card 7:	Field 1	Number of sideslip angles to be analyzed. (Maximum 9.0, minimum 1.0.)
	Fields 2-10	Sideslip angles. (At least one value <u>must</u> be given.)
Card 8:	Field 1	Number of angles of attack to be analyzed. (Maximum 9.0, minimum 1.0.)
	Fields 2-10	Angles of attack. (At least one value <u>must</u> be given.)
Card 9:	Fields 1 to 6	Right wing panel blowing factors.*
Card 10:	Fields 1 to 6	Left wing panel blowing factors.*

Note: The panel blowing factors give the <u>relative</u> blowing thrust for the panels, and are normalized by the program to give a sum equal to 1.0. Therefore, any convenient numbers having the correct relative magnitudes will work. To indicate constant local C_J (as for "internal" blowing) use negative numbers. Otherwise, constant thrust per unit span is assumed.

Card 11:	Fields 1 to 6	Right wing flap deflection.*
Card 12:	Fields 1 to 6	Left wing flap deflection.*
Card 13:	Field 1	Number of C_J's to be analyzed. (Minimum 1., maximum 8.)
	Fields 2-9	C_J's
	Field 10	Next case card number. (See explanation below.)

The following case (if any) may be defined either by a complete set of cards or by a partial set, beginning with the card indicated by the "next case card number". The intent of this arrangement is to permit analysis of a hierarchy of case parameters, with C_J the most easily varied, flap deflection next, blowing distribution third, relative wind fourth, and wing description the most trouble to vary.

*For Cards 4, 5, 6, 9, 10, 11 and 12, if less than six flap panels are used, the extra columns are ignored.

```
      PROGRAM FLAPZ2(INPUT,OUTPUT,TAPE5=INPUT,TAPE6=OUTPUT)
C
C     DIMENSIONS, ETC.
C
      COMMON   F(25),  T(25)
      DIMENSION       UNR(3)          ,UNL(3)          ,FFR(6)     ,FFL(6)         ,
     1                BLOR(6)         ,BLOL(6)         ,DFR(6)     ,DFL(6)         ,
     2                PR(26,3)        ,PL(26,3)        ,QR(25,3)   ,QL(25,3)       ,
     3                ABONDR(3)       ,ABONDL(3)       ,GRITE(3)   ,GLEFT(3)       ,
     4                FFSR(25)        ,FFSL(25)        ,DOWNR(3)   ,DOWNL(3)       ,
     5                CHDR(25)        ,CHDL(25)        ,DR(25)     ,DL(25)         ,
     6                CJPR(6)         ,CJPL(6)         ,CJR(25)    ,CJL(25)        ,
     7                TEIR(25,3)      ,TEIL(25,3)      ,AREX(3)    ,ALINX(3)       ,
     8                TEOR(25,3)      ,TEOL(25,3)      ,EHR(25,3),EHL(25,3,        ,
     9                TRR(25,25,3)    ,TRL(25,25,3)    ,GR(25)     ,GL(25)         ,
     X                TLR(25,25,3)    ,TLL(25,25,3)    ,GOR(25)    ,GOL(25)        ,
     1                DAMPR(25)       ,DAMPL(25)       ,WR(25,3)   ,WL(25,3)       ,
     2                DYNPR(25)       ,DYNPL(25)       ,AJETR(25),AJETL(25,        ,
     3                VELR(25)        ,VELL(25)        ,BETAR(25),BETAL(25,        ,
     4                ALFAR(25)       ,ALFAL(25)       ,TW(25),
     5                FOR(25,3)       ,FOL(25,3)       ,FJR(25,3),FJL(25,3,        ,
     6                DLOADR(25)      ,DLOADL(25)      ,SLOADR(25),SLOADL(25),
     7                UPLODR(25)      ,UPLODL(25)      ,CMR(25)    ,CML(25)    ,
     8                SECCLR(25)      ,SECCLL(25)      ,SECCDR(25),SECCDL(25)
      DIMENSION W1(3),  W2(3),   W3(3),   W4(3),   W5(3),  ROTORG(3)
      DIMENSION       TITLE(10)       ,XIN(10)         ,DV1(3)     ,DV2(3)         ,
     1BETA(9)      ,ALEF(9)         ,CJ(8)           ,U(3)       ,TEMP(3)        ,
     2TEMP1(3)     ,TEMP2(3)        ,CUE(3)          ,P1(3)      ,P2(3)          ,
```

```
     3P3(3)         ,P4(3)          ,AYE(3)         ,TJM(3)    ,TJF(3)         ,
     4TF(3)         ,TM(3)          ,TSM(3)         ,FJET(3)   ,
     5SAX(3)        ,SAY(3)         ,SAZ(3)         ,TOTF(3)   ,TOTM(3)        ,
     6FB(7)         ,CF(6)          ,NDIV(7)        ,LL(25)    ,CNOM(25)       ,
     7CFS(25)       ,SP(6)          ,BLOS(6)
      LOGICAL  CON,  SYM
      NJS=1
      NAS=1
      NBS=1
      PI=3.14159263
      DTOR=PI/180.
      UNL(1)=0.
      UNR(1)=0.
      CALL DATE(DATE1,  DATE2)
      NPAGE =0
      NEXT=1
      DG=.00001
C
C     INPUTS
C
1     READ(5,101) TITLE
101   FORMAT(10A7)
2     READ(5,102) AR,  SWEEP,  TAPER, DIHDRL, TWIST, BLOWDR
102   FORMAT(10F7.0)
      AR19=1.9*AR
      DO 41 I=1,25
41    TW(I)=TWIST*DTOR*(.04*I-.02)
3     READ(5,102) XIN
```

```
      FB(1)=0.
      FB(7)=1.
      DO 51 J=2,6
51    FB(J)=XIN(J-1)
4     READ(5,102 ) CF
5     READ(5,102) FFR
55    READ(5,102) FFL
6     READ(5,102) XIN
      NB=IFIX(XIN(1))
      DO 56 J=1,NB
56    BETA(J)=XIN(J+1)
7     READ(5,102) XIN
      NA=IFIX(XIN(1))
      DO 57 J=1,NA
57    ALFF(J)=XIN(J+1)
8     READ(5,102) BLOR
9     CONTINUE
      IF(NEXT.NE.10)GO TO 58
      DO 14 N=1,6
14    BLOR(N)=BLOR(N)*SUMB
58    CONTINUE
      READ(5,102)BLOL
10    READ(5,102) DFR
11    READ(5,102) DFL
12    READ(5,102) XIN
      NJ=IFIX(XIN(1))
      DO 62 J=1, NJ
62    CJ(J)= XIN(J+1)
```

```
C
C     WING GEOMETRY
C
      SWP=SWEEP*DTOR
      SNSW= SIN(SWP)
      CSSW= COS(SWP)
      TNSW= TAN(SWP)
      TNDI= TAN(DIHDRL*DTOR)
      DO 301  K=1,3
      PR(1,K)=0.
301   PL(1,K)=0.
      SNDI=SIN(DIHDRL*DTOR)
      DO 302  I=1,25
      PR(I+1,1)= .04*TNSW*I
      PL(I+1,1)= PR(I+1,1)
      PR(I+1,2)= .04*I
      PL(I+1,2)= -.04*I
      PR(I+1,3)= .04*TNDI*I
302   PL(I+1,3)= PR(I+1,3)
      ESS=4./AR
      DO 303  I=1, 25
      DO 303  K=1, 3
      QR(I,K)=(PR(I,K)+PR(I+1,K))/2.
303   QL(I,K)=(PL(I,K)+PL(I+1,K))/2.
      DO 21   N=1,  25
21    T(N)  =  ASIN(QR(N,2))
      F(1)=.5*(T(1)+T(2))
      DO 22   N=2, 24
```

```
22    F(N) = .5*(T(N+1)-T(N-1))
      F(25)= .5*(T(25)-T(24)) +.5*(PI/2.-T(25))
C
C     NORMALS    AND       BOUND VORTEX VECTORS
C
      UNR(2)=-SNDI
      UNL(2)= SNDI
      DO 305 K=1,3
      GRITE(K) = PR(2,K)
305   GLEFT(K) =-PL(2,K)
      UNR(3)=SQRT(1.-SNDI**2)
      UNL(3)=UNR(3)
C
C     SPANWISE DIVISIONS
C
      DO 306  L=2,6
306   NDIV(L)= IFIX((FB(L)  +.001)/.04) +1
      NDIV(1)=1
      NDIV(7)=26
      CALL VMAG(GLEFT, DV1, DV2, GBM, GBM2)
      FCTR = 1./GBM
      CALL  SCALM(GLEFT, DV1, ABONDL,  FCTR, DUM)
      CALL  SCALM(GRITE, DV1, ABONDR, FCTR, DUM)
      CR=  4./(AR*(1.+TAPER))
C
C     ASSIGN  PANEL  INDICES TO STATIONS
C
      CBAR=CR**2*(1.+TAPER+TAPER**2)/(1.5*ESS)
```

```
      IF(TAPER.NE.1.)GO TO 307
      XCBAR=.5*TNSW
      ZCBAR=.5*TNDI
      GO TO 308
307   CONTINUE
      ARM=(CR-CBAR)/(CR*(1.-TAPER))
      XCBAR=ARM*TNSW
      ZCBAR=ARM*TNDI
308   CONTINUE
      DO 310  L=1,6
      INDIO = NDIV(L)
      INDIU = NDIV(L+1)-1
      DO 310  I=INDIO, INDIU
310   LL(I)= L
      NPAN=LL(25)
      CALL VCROSS(ABONDR, UNR, DOWNR, DUMA, DUMC)
      CALL VCROSS(ABONDL, UNL, DOWNL, DUMA, DUMC)
      NPANP1 =NPAN+1
C
C     FLAP ANGLES, CHORDS, ETC.
C
      DO  410 J=1,25
      LLJ=LL(J)
      DR(J)= DFR(LLJ)*DTOR
      DL(J)= DFL(LLJ)*DTOR
      FFSL(J)=FFL(LLJ)
      CFS(J)=CF(LLJ)
      ETA=.04*J -.02
```

```
      FFSR(J)=FFR(LLJ)
      CNOM(J)=CR*(1.-ETA*(1.-TAPER))
      CHDR(J)=CNOM(J)*FFR(LLJ)
410   CHDL(J)=CNOM(J)*FFL(LLJ)
C     NOMINAL PANEL AREAS
C
      DO 411  L=1,NPAN
      SP(L)=0.
      I1=NDIV(L)
      I2=NDIV(L+1)-1
      IF(I2.LT.I1) GO TO  411
      DO  412  I=I1,I2
412   SP(L)=SP(L) +CNOM(I)/25.
411   CONTINUE
C
C     BLOWING DISTRIBUTION - NORMALIZATION  OF FACTORS
C
      SUMB=0.
      DO 421 L=1,NPAN
421   SUMB= SUMB+BLOL(L)+BLOR(L)
      IF(SUMB.EQ.0.)SUMB=1.
      DO 422 L=1,NPAN
      BLOL(L)= BLOL(L)/SUMB
      BLOR(L)= BLOR(L)/SUMB
422   BLOS(L)= 2.*BLOR(L)
C
C     OVERALL  CJ
C
```

```
450   CJ3= CJ(NJS)
C
C     LOCAL  CJ S   (PANELS  FIRST)
C
      DO  431  L=1,NPAN
      IF(SP(L).EQ.0.) GO TO  432
      CJPL(L)= BLOL(L)*CJ3*ESS/SP(L)
      CJPR(L)= BLOR(L)*CJ3*ESS/SP(L)
      GO TO  431
432   CJPL(L)=0.
      CJPR(L)=0.
431   CONTINUE
C
C     CJ S AT INDIVIDUAL STATIONS (REFERRED TO ACTUAL CHORDS)
C
      DO 435   I=1, 25
      LLI=LL(I)
      ENSTA = NDIV(LLI+1)- NDIV(LLI)
      CJL(I)=0.
      CJR(I)=0.
      IF(ENSTA.LT.1.) GO TO 435
      IF(SUMB.LT.0.)  GO TO 436
      CJL(I)=   SP(LLI)*CJPL(LLI)/(ENSTA*.04*CHDL(I))
      CJR(I)=   SP(LLI)*CJPR(LLI)/(ENSTA*.04*CHDR(I))
      GO TO 435
436   CJL(I)=CJPL(LLI)/FFL(LLI)
      CJR(I)=CJPR(LLI)/FFR(LLI)
435   CONTINUE
```

```
C
C     SMOOTH CJ VARIATION AT PANEL ENDS
C
      CJSPR=CJR(1)/3.
      CJSPL=CJL(1)/3.
      CJR(1)= CJR(1)-CJSPR+ CJSPL*FFR(1)/FFL(1)
      CJL(1)= CJL(1)-CJSPL+ CJSPR*FFL(1)/FFR(1)
      IF (NPAN.LT.2) GO TO 470
      DO 460 N=2,NPAN
      NN=NDIV(N)
      CJSPR = CJR(NN)/3.
      CJSPL = CJL(NN)/3.
      CJSPR1= CJR(NN-1)/3.
      CJSPL1= CJL(NN-1)/3.
      CJR(NN)= CJR(NN)-CJSPR + CJSPR1*CHDR(NN-1)/CHDR(NN)
      CJL(NN)= CJL(NN)-CJSPL + CJSPL1*CHDL(NN-1)/CHDL(NN)
      CJR(NN-1) = CJR(NN-1) -CJSPR1  + CJSPR*CHDR(NN)/ CHDR(NN-1)
460   CJL(NN-1) = CJL(NN-1) -CJSPL1  + CJSPL*CHDL(NN)/ CHDL(NN-1)
470   CONTINUE
C
C     RELATIVE  WIND
C
500   BATER=BETA(NBS)*DTOR
      SNB= SIN(BATER)
      CSB= COS(BATER)
      TNB= TAN(BATER)
      ALFER=ALEF(NAS)*DTOR
      SNA= SIN(ALFER)
```

```
      CSA= COS(ALFER)
      CSSMB=COS(SWP-BATER)
      CSSPB=COS(SWP+BATER)
      U(1)=CSA*CSB
      U(2)=-CSA*SNB
      U(3)= SNA
      WMIN=-.95*U(1)
C
C     SYMMETRY  TEST
C
      SYM=.TRUE.
      IF(BATER.NE.0.) SYM=.FALSE.
      DO 501   L=1,6
      IF(BLOR(L).NE.BLOL(L)) SYM=.FALSE.
      IF(DFR(L).NE.DFL(L)) SYM=.FALSE.
      IF(FFR(L).NE.FFL(L)) SYM=.FALSE.
501   CONTINUE
C
C     TRAILING EDGE POINTS
C
      DO 551  J=1, 25
      LLJ= LL(J)
      CELL=CF(LLJ)+ 1.2*CJL(J)**.25
      EPL=CNOM(J)*(.75-CF(LLJ)+CELL*COS(DL(J)))
      CELR=CF(LLJ)+ 1.2*CJR(J)**.25
      EPR=CNOM(J)*(.75-CF(LLJ)+CELR*COS(DR(J)))
      TEIL(J,1) = PL(J,1) +EPL
      TEOL(J,1) = PL(J+1,1) +EPL
```

```
      TEIR(J,1) = PR(J,1) +EPR
      TEOR(J,1) = PR(J+1,1)  +EPR
      TEIL(J,2) = PL(J,2) -EPL*TNB
      TEOL(J,2) = PL(J+1, 2) - EPL*TNB
      TEIR(J,2) = PR(J,2) -EPR*TNB
      TEOR(J,2) = PR(J+1,2)  - EPR*TNB
      EPL= CHDL(J)* CELL  *SIN(DL(J))/FFL(LLJ)
      EPR= CHDR(J)* CELR  *SIN(DR(J))/FFR(LLJ)
      TEIL(J,3) =PL(J,3)-EPL
      TEOL(J,3) =PL(J+1,3) -EPL
      TEIR(J,3) =PR(J,3)-EPR
      TEOR(J,3) =PR(J+1,3) -EPR
551   CONTINUE
C
C     SMOOTH TRAILING EDGE POINT VARIATION AT PANEL ENDS
C
      DO 510 K=1,3
      TEIR(1,K)=(TEIR(1,K)+TEIL(1,K))/2.
510   TEIL(1,K)=TEIR(1,K)
      DO 531 N=2, 25
      NN=N
      DO 531 K=1,3
      TEIR(NN,K)= (TEIR(NN,K)+ TEOR(NN-1,K))/2.
      TEOR(NN-1,K)=TEIR(NN,K)
      TEIL(NN,K)= (TEIL(NN,K)+ TEOL(NN-1,K))/2.
531   TEOL(NN-1,K)=TEIL(NN,K)
530   CONTINUE
C
```

```
C     TRAILING  VORTFX  DIRECTION COSINES
C
      CALL VCROSS(  U, ABONDL, TEMP, DUMA,  DUMBC)
      CALL VMAG (TEMP, DV1, DV2, WNORL, WNORL2)
      CALL VDOT (U, UNL, DV1, WNWCPL, DUMBC)
      ALLEFT =  ASIN(WNWCPL/WNORL)
      CALL VCROSS ( U,  ABONDR, TEMP, DUMA,  DUMC )
      CALL VMAG (TEMP, DV1, DV2, WNORR, WNORR2)
      CALL VDOT (U, UNR,  DV1,  WNWCPR, DUMBC)
      SPANF= AR/(AR+2.)
      ALRITE=  ASIN(WNWCPR/WNORR)
      DO 561  L=1,NPAN
      CEFL=CF(L)/FFL(L)
      DLEFT=  DFL(L)*DTOR
      CJLEFT= CJPL(L)/(WNORL2*FFL(L))
      DRITE=  DFR(L)*DTOR
      CJRITE= CJPR(L)/(WNORR2*FFR(L))
      CEFR=CF(L)/FFR(L)
      CALL CEEL(ALLEFT, CJLEFT, DLEFT, CEFL, 0., CLLEFT,  DUMA)
      CALL CEEL(ALRITE, CJRITE, DRITE, CEFR, 0., CLRITE,  DUMA)
      CLLEFT= CLLEFT*WNORL2/FFL(L)
      CLRITE= CLRITE*WNORR2/FFR(L)
C
C     AT THIS POINT, WE HAVE A PANEL CL  BASED ON NOMINAL PANEL AREA
C     AND FREE STREAM  Q.   NOW FIND A WAKE VORTEX ANGLE BASED ON THE
C     WHOLE-WING  ASPECT RATIO.
C
      CLLEFT = CLLEFT*SPANF
```

```
      CLRITE = CLRITE*SPANF
      IF(CLRITE.GT.AR19)CLRITE=.99*AR19
      IF(CLLEFT.GT.AR19)CLLEFT=.99*AR19
      DELTAR =  ASIN(CLRITE/(1.9*AR))/4.17
      DELTAL =  ASIN(CLLEFT/(1.9*AR))/4.17
      COSADL = COS(ALFER-DELTAL)
      COSADR = COS(ALFER-DELTAR)
      ALINX(1)=  COSADL*CSB
      ALINX(2)=  COSADL*SNB
      ALINX(3)=  SIN(ALFER-DELTAL)
      AREX(1)=  COSADR*CSB
      AREX(2)=  COSADR*SNB
      AREX(3)=  SIN(ALFER-DELTAR)
      I1= NDIV(L)
      I2= NDIV(L+1)-1
      IF(I2.LT.I1) GO TO 561
      DO 562  I= I1,  I2
      DO 562  K=1,3
      EHL(I,K) = ALINX(K)
562   EHR(I,K) = AREX(K)
561   CONTINUE
C
C     COMPUTE RIGHT  WING  INFLUENCE COEFFICIENTS
C
      DO  699 I=1, 25
      DO 601  K=1,3
601   CUE(K) =  QR(I,K)
      DO 698  J=1,25
```

```
      DO 602  K=1,3
      P1(K) =TEIR(J,K)
      P2(K) =PR(J,K)
      AYE(K) =EHR(J,K)
      P3(K) =PR(J+1,K)
602   P4(K) =TEOR(J,K)
      CALL WASH(P1, AYE, CUE, W1)
      CALL SEG(P1, P2, CUE, W2)
      CALL SEG(P3, P4, CUE, W3)
      CALL WASH(P4, AYE, CUE, W4)
      DO 603  K=1,3
      TRR(I,J,K) =  W2(K)+ W3(K) + W4(K) - W1(K)
      P1(K)= TEOL(J,K)
      P2(K)= PL(J+1,K)
      AYE(K)=EHL(J,K)
      P3(K) =PL(J, K)
603   P4(K) =TEIL(J, K)
      CALL WASH(P1, AYE, CUE, W1)
      CALL SEG (P1, P2 , CUE, W2)
      CALL SEG (P2, P3 , CUE, W3)
      CALL SEG (P3, P4 , CUE, W4)
      CALL WASH(P4, AYE, CUE, W5)
      DO  604  K=1, 3
604   TLR(I,J,K) = W2(K)+W3(K) + W4(K) +W5(K) - W1(K)
698   CONTINUE
      IF(SYM) GO  TO  699
C
C     COMPUTE LEFT WING  INFLUENCE  COEFFICIENTS
```

```
C
      DO  605  K=1, 3
605   CUE(K)= QL(I,K)
      DO  699  J=1, 25
      DO 606  K=1,3
      AYE(K)=FHR(J, K)
      P1(K)= TEIR(J, K)
      P2(K)= PR(J, K)
      P3(K)= PR(J+1, K)
606   P4(K)= TFOR(J, K)
      CALL  WASH(P1, AYE,  CUE, W1)
      CALL  SEG (P1, P2,   CUE, W2)
      CALL  SEG (P2, P3,   CUE, W3)
      CALL  SEG (P3, P4,   CUE, W4)
      CALL  WASH(P4, AYE,  CUE, W5)
      DO   607   K=1, 3
      TRL(I, J, K) = W2(K)+ W3(K) +W4(K) +W5(K) -W1(K)
      AYE(K) = FHL(J,K)
      P1(K) = TEOL(J, K)
      P2(K) = PL(J+1, K)
      P3(K) = PL(J, K)
607   P4(K) = TEIL(J, K)
      CALL  WASH(P1, AYE, CUE, W1)
      CALL  SEG (P1, P2,  CUE, W2)
      CALL  SEG (P3, P4,  CUE, W3)
      CALL  WASH(P4, AYE, CUE, W4)
      DO  608   K=1, 3
608   TLL(I, J, K) =  W2(K) +W3(K) + W4(K) -W1(K)
```

```
699   CONTINUE
C
C     FIRST CUT VORTEX STRENGTHS - RIGHT WING
C
      DO    799    J= 1,  25
      CJCALL = CJR(J)/WNORR2
      CFCALL = CFS(J)/FFSR(J)
      IF(BLOWDR.GE.0.)  CJCALL =CJCALL*CSSW
      CALL CEEL(ALRITE, CJCALL, DR(J), CFCALL,  0., CLRR, DCM)
      GRR=.5*CHDR(J)*CSSW*CLRR*WNORR
      GOR(J)=GRR
      GR(J)=GRR
C
C     FIRST CUT VORTEX STRENGTHS - LEFT  WING
C
      CJCALL = CJL(J)/WNORL2
      CFCALL = CFS(J)/FFSL(J)
      IF(BLOWDR.GE.0.) CJCALL= CJCALL*CSSW
      CALL CEEL(ALLEFT, CJCALL, DL(J), CFCALL, 0., CLRL, DCM)
      GLR= .5*CHDL(J)*CSSW*CLRL*WNORL
      GL(J)= GLR
      GOL(J)  = GLR
799   CONTINUE
      CALL SMOOTH(GL)
      CALL SMOOTH(GR)
      CALL SMOOTH(GOL)
      CALL SMOOTH(GOR)
      IONCE=0
```

```
      ICON=0
      NTRY=0
750   CONTINUE
C
C     INITIALIZE  ITERATION PARAMETERS
C
      NTRIED = 0.
      EXCESO=10000.
      CON=.FALSE.
801   CONTINUE
      NTRY=NTRY+1
      IF(NTRY.EQ.1) GO TO 802
      IF(NTRY.GT.100) GO TO 85
      NTRIED =NTRIED +1
      IF(EXCESS.GT.0.2) GO TO 809
      IF(NTRIED.GT.30) GO TO 875
809   CONTINUE
C
C     AVERAGE  VORTEX STRENGTHS
C
      DO   802   J=1, 25
      GOR(J) =  DAMPR(J)*  GR(J) +(1.-DAMPR(J))*GOR(J)
      IF(SYM) GO TO  802
      GOL(J) =  DAMPL(J)* GL(J)  +(1.-DAMPL(J))*GOL(J)
802   CONTINUE
C
C     COMPUTE INDUCED VELOCITIES
C
```

```
      DO    803    I= 1, 25
      DO    804    K=1, 3
      WL(I,K)=0.
804   WR(I,K) = 0.
      DO    805  J=1, 25
      DO    805  K=1, 3
      WR(I,K)= WR(I,K)+ GOR(J)*TRR(I,J,K)
      IF(SYM) GO TO 806
      WR(I,K)= WR(I,K)+ GOL(J)*TLR(I,J,K)
      WL(I,K)= WL(I,K)+ GOL(J)*TLL(I,J,K)
      WL(I,K)= WL(I,K)+ GOR(J)*TRL(I,J,K)
      GO TO 805
806   CONTINUE
      WR(I,K)= WR(I,K) + GOR(J)*TLR(I,J,K)
805   CONTINUE
      IF(.NOT.SYM) GO TO 803
      WL(I,1)=WR(I,1)
      WL(I,2)=-WR(I,2)
      WL(I,3)= WR(I,3)
803   CONTINUE
      DO 841 I=1,25
      IF(WR(I,1).LT.WMIN)WR(I,1)=WMIN
      IF(WL(I,1).LT.WMIN)WL(I,1)=WMIN
841   CONTINUE
C
C      COMPUTE DAMPING FACTORS (FIRST PASS ONLY)
C
      IF(NTRY.NE.1) GO TO 880
```

```
875   CONTINUE
      DO 879 J=1, 25
      DO 876 K=1,3
      CHECK=WR(J,K)
      IF(ABS(CHECK).LT.0.25) GO TO 876
      CHECK=.25*ABS(CHECK)/CHECK
876   TEMP(K)=CHECK+U(K)
      CALL VCROSS( TEMP, ABONDR, TEMP2,  DUMA, DUMC)
      CALL VMAG(TEMP2, DV1, DV2, DNORR, DNORR2)
      CALL VDOT(TEMP,  UNR,  DV1, DNWCP , DUMC)
      DAL =   ASIN(DNWCP/DNORR)
      CJCALL= CJR(J)/DNORR2
      CFCALL=    CFS(J)/FFSR(J)
      CALL CEEL(DAL, CJCALL, DR(J), CFCALL,  0., DCL,  DCM)
      GRR=.5*CHDR(J)*CSSW*DCL*DNORR
      DO 872 K=1,3
      CHECK=WR(J,K)
      IF(ABS(CHECK).LT.0.25) GO TO 872
      CHECK=.25*ABS(CHECK)/CHECK
872   TEMP(K)=CHECK+U(K)+DG*TRR(J,J,K)
      CALL VCROSS( TEMP, ABONDR, TEMP2,  DUMA, DUMC)
      CALL VMAG(TEMP2, DV1, DV2, DNORR, DNORR2)
      CALL VDOT(TEMP,  UNR,  DV1, DNWCP , DUMC)
      DAL =   ASIN(DNWCP/DNORR)
      CJCALL= CJR(J)/DNORR2
      CALL CEEL(DAL, CJCALL, DR(J), CFCALL,  0., DCL,  DCM)
```

```
      GRD=.5*CHDR(J)*CSSW*DCL*DNORR
      DGDG=(GRD-GRR)/DG
      DAMPR(J)= 1./(1.-DGDG)
      DAMPR(J)=ABS(DAMPR(J))
      DO 877 K=1, 3
      CHECK=WL(J,K)
      IF(ABS(CHECK).LT.0.25) GO TO 877
      CHECK=.25*ABS(CHECK)/CHECK
877   TEMP(K)=CHECK+U(K)
      CALL VCROSS(TEMP, ABONDL, TEMP2,  DUMA, DUMC)
      CALL VMAG(TEMP2,  DV1,  DV2,  DNORL, DNORL2)
      CALL VDOT(TEMP, UNL, DV1, DNWCP, DUMC)
      DAL=  ASIN(DNWCP/DNORL)
      CJCALL= CJL(J)/DNORL2
      CFCALL=    CFS(J)/FFSL(J)
      CALL CEEL (DAL, CJCALL, DL(J),  CFCALL,  0.., DCL,  DCM)
      GLR= .5* CHDL(J)*CSSW*DCL*DNORL
      DO 873 K=1, 3
      CHECK=WL(J,K)
      IF(ABS(CHECK).LT.0.25) GO TO 873
      CHECK=.25*ABS(CHECK)/CHECK
873   TEMP(K)=CHECK+U(K)+DG*TLL(J,J,K)
      CALL VCROSS(TEMP, ABONDL, TEMP2,  DUMA, DUMC)
      CALL VMAG(TEMP2,  DV1,  DV2,  DNORL, DNORL2)
      CALL VDOT(TEMP, UNL, DV1, DNWCP, DUMC)
      DAL=  ASIN(DNWCP/DNORL)
      CJCALL= CJL(J)/DNORL2
      CALL CEEL (DAL, CJCALL, DL(J),  CFCALL,  0.., DCL,  DCM)
```

```
      GLD= .5* CHDL(J)*CSSW*DCL*DNORL
      DGDG=(GLD-GLR)/DG
      DAMPL(J)= 1./(1.-DGDG)
      DAMPL(J)=ABS(DAMPL(J))
879   CONTINUE
      DAMREF=DAMPR(1)
880   CONTINUE
C
C     COMPUTE  NEW VORTEX  STRENGTHS
C
      DO  810   I= 1, 25
      DO  811  K=1,3
811   TEMP(K) = WR(I,K) + U(K)
      CALL VCROSS(TEMP, ARONDR, TEMP2,  DUMA, DUMC)
      CALL VMAG(TEMP2, DV1, DV2, VNORR, VNORR2)
      CALL VDOT(TEMP, UNR, DV1,  WNWCP, DUMC)
      DYNPR(I)=VNORR2
      ALF=   ASIN(WNWCP/VNORR) +TW(I)
      CJCALL= CJR(I)/VNORR2
      IF(BLOWDR.GE.0.) CJCALL= CJCALL*CSSW
      ALFIN=ATAN(-2.*WR(I,3)/CSSMB)
      CFCALL = CFS(I)/FFSR(I)
      CALL CEEL(ALF,  CJCALL,  DR(I), CFCALL, ALFIN, CLRR,  CMR(I))
      AJETR(I)= ALFIN-ALF
      GR(I) = .5*CHDR(I)*CSSW*CLRR*VNORR
      CMR(I) = CMR(I)+ CLRR*(1.-FFSR(I))/4.
      IF(SYM)GO TO 810
      DO  812  K=1,3
```

```
812    TEMP(K)= WL(I,K) +U(K)
       CALL  VCROSS(TEMP, ABONDL, TEMP2, DUMA,  DUMC)
       CALL  VMAG(TEMP2,  DV1,  DV2,  VNORL,  VNORL2)
       CALL  VDOT(TEMP,  UNL,  DV1,  WNWCP,  DUMC)
       DYNPL(I) =VNORL2
       ALF=  ASIN(WNWCP/VNORL) +TW(I)
       CJCALL =CJL(I)/VNORL2
       IF(BLOWDR.GE.0.) CJCALL =CJCALL*CSSW
       ALFIN=ATAN(-2.*WL(I,3)/CSSPB)
       AJETL(I)=ALFIN-ALF
       CFCALL = CFS(I)/FFSL(I)
       CALL  CEEL( ALF,  CJCALL,  DL(I),  CFCALL,  ALFIN, CLRL, CML(I,)
       CML(I)= CML(I) + CLRL*(1.-FFSL(I))/4.
       GL(I) = .5* CHDL(I)*CSSW*CLRL*VNORL
810    CONTINUE
       IF(SYM) GO TO 815
       CALL SMOOTH(GL)
815    CALL SMOOTH(GR)
C
C      COMPUTE EXCESS
C
       EXCESS= 0.
       SUMG =0.
       DO  820  I= 1,25
       SUMG = SUMG + GR(I)
       DIF=ABS(GR(I)- GOR(I))
       IF(DIF.GT.EXCESS) EXCESS =DIF
       IF(SYM) GO TO  820
```

```
      SUMG = SUMG + GL(I)
      DIF =ABS(GL(I)- GOL(I))
      IF(DIF.GT.EXCESS) EXCESS =DIF
820   CONTINUE
      GAVE = SUMG/50.
      IF(SYM) GAVE = SUMG/25.
      EXCESS = EXCESS/GAVE
      EXCESS=ABS(EXCESS)
      IF(EXCESS.LT.EXCESO)  GO TO 83
832   ICON=0
      DO 831 I=1,25
      DAMPR(I)=.8*DAMPR(I)
831   DAMPL(I)=.8*DAMPL(I)
      RATIO=DAMPR(1)/ DAMREF
      GO TO 750
830   CONTINUE
833   CONTINUE
      EXCESO=EXCESS
      IF(EXCESS.GT..01) GO TO 801
860   CON= .TRUE.
850   NTRY=NTRY-1
C
C     COMPUTE  VORTEX  FORCES
C
      DO 901   I=1,25
      GR(I)=.5*(GR(I)+ GOR(I))
      DO  902  K=1,3
902   TEMP(K) = U(K)+ WR(I,K)
```

```
      CALL VMAG(TEMP,DV1, DV2, VELR(I), DUMC)
      CALL VCROSS(TEMP, GRITE,  TEMP1,  DUMA, DUMC)
      DO  9010  K=1, 3
      ALFAR(I)=  ASIN(TEMP(3)/SQRT(TEMP(1)**2+TEMP(3)**2))/DTOR
      ALFAR(I)=ALFAR(I)+TW(I)    /DTOR
9010  FOR(I, K) = TEMP1(K) * GR(I) * 2.
901   BETAR(I)=- ASIN(TEMP(2)/VELR(I))/DTOR
      IF(SYM) GO TO 910
      DO 910 I=1,25
      GL(I)=(GL(I)+GOL(I))/2.
      DO  904   K=1, 3
904   TEMP(K) = U(K) + WL(I,K)
      CALL VCROSS(TEMP, GLEFT, TEMP2,  DUMA, DUMC)
      CALL VMAG(TEMP, DV1, DV2, VELL(I), DUMC)
      DO  903  K=1, 3
      FOL(I,K) = TEMP2(K)*  GL(I)*2.
903   CONTINUE
      BETAL(I)= - ASIN(TEMP(2)/VELL(I))/DTOR
      ALFAL(I)=  ASIN(TEMP(3)/SQRT(TEMP(1)**2+TEMP(3)**2))/DTOR
      ALFAL(I)=ALFAL(I)+TW(I)     /DTOR
910   CONTINUE
C
C     SUM  FORCES AND MOMENTS
C
      DO  920  K=1, 3
      TF(K)=0.
      TM(K)=0.
920   TSM(K)=0.
```

```
      DO   921   I=1, 25
      DO   921   K=1, 3
921   TF(K) = TF(K)+ FOR(I,K)
      IF(.NOT.SYM) GO TO 930
      CALL SCALM(TF, DV1, TF, 2., DUMC)
      DO   922   I=1, 25
922   TM(2)=TM(2)+FOR(I,1)*QR(I,3)-FOR(I,3)*QR(I,1)
      TM(2)=2.*TM(2)
      GO TO   94
930   CONTINUE
      DO   931   I=1, 25
      DO   932   K=1, 3
      TEMP(K) = QR(I,K)
932   TEMP1(K) = FOR(I,K)
      CALL  VCROSS(TEMP,TEMP1, TEMP2,  DUMA, DUMC)
      CALL  VPLUS(TEMP2, TM, TM,  DUMA, DUMC)
      DO 933  K=1,3
      TEMP(K) = QL(I,K)
933   TEMP1(K)= FOL(I,K)
      CALL VCROSS(TEMP, TEMP1,  TEMP2, DUMA, DUMC)
      CALL VPLUS(TEMP2, TM, TM,  DUMA, DUMC)
      DO 934  K=1,3
934   TF(K)=TF(K)+FOL(I,K)
931   CONTINUE
940   CONTINUE
C
C     COMPUTE JET FORCES
C
```

```
      IF(BLOWDR.LT.0.) GO TO  945
      DO 941  I=1,25
      STRIPJ=CHDR(I)*CJR(I)*.04
      DO  942  K=1, 3
      FACTOR= -ABONDR(K)*SNSW + CSSW*(SIN(AJETR(I))*UNR(K)
     1 -COS(AJETR(I))* DOWNR(K))
942   FJR(I,K) = STRIPJ*FACTOR
941   CONTINUE
      IF(SYM) GO TO  950
      DO  943  I=1, 25
      STRIPJ= CHDL(I)* CJL(I)*.04
      DO  944  K=1, 3
      FACTOR=  ABONDL(K)*SNSW + CSSW*(SIN(AJETL(I))*UNL(K)
     1 -COS(AJETL(I))* DOWNL(K))
944   FJL(I,K) = STRIPJ* FACTOR
943   CONTINUE
      GO  TO   950
945   CONTINUE
      DO  946   I=1, 25
      STRIPJ= CHDR(I)*CJR(I)*.04
      DO  946   K=1, 3
946   FJR(I,K)=  STRIPJ*(SIN(AJETR(I))*UNR(K) - COS(AJETR(I))*DOWNR(K))
      IF(SYM) GO  TO  950
      DO  947   I=1, 25
      STRIPJ= CHDL(I)* CJL(I)*.04
      DO  947   K=1, 3
947   FJL(I,K)=  STRIPJ*(SIN(AJETL(I))*UNL(K) - COS(AJETL(I))*DOWNL(K))
950   CONTINUE
```

```
C
C     SUM  JET FORCES  AND  MOMENTS
C
      DO 949  K=1, 3
      TJF(K)=0.
949   TJM(K) = 0.
      DO  951   I=1, 25
      DO  952   K=1, 3
      TEMP(K)=  QR(I,K)
952   FJET (K)= FJR(I,K)
      CALL VCROSS(TEMP, FJET , TEMP1,DUMA, DUMC)
      CALL  VPLUS(TJF, FJET, TJF,  DUMA,  DUMC)
      CALL  VPLUS(TJM, TEMP1, TJM, DUMA,  DUMC)
951   CONTINUE
      IF(SYM)  GO  TO  959
      DO 955  I=1,25
      DO 954  K=1,3
      TEMP(K) =QL(I,K)
954   FJET(K) =FJL(I,K)
      CALL  VCROSS(TEMP, FJET,  TEMP1, DUMA,  DUMC)
      CALL  VPLUS (TJM, TEMP1,  TJM,  DUMA,  DUMC)
      CALL  VPLUS (TJF, FJET,   TJF,  DUMA,  DUMC)
955   CONTINUE
      GO  TO  96
959   CONTINUE
      CALL SCALM(TJF, DV1, TJF, 2., DUMA)
      CALL SCALM(TJM, DV1, TJM, 2., DUMA)
960   CONTINUE
```

```
C
C     COMPUTE   MOMENTS  DUE  TO  SECTION  CMS
C
      DO    961    I=1,  25
      DELM =DYNPR(I)*CMR(I)*CSSW*.04*(CHDR(I)**2)
      DO    961  K=1, 3
961   TSM(K) =  TSM(K) +DELM*ABONDR(K)
      IF(SYM) GO TO  965
      DO  962   I=1, 25
      DELM= DYNPL(I) *CML(I) *CSSW *.04 *(CHDL(I)**2)
      DO  962   K=1, 3
962   TSM(K) =TSM(K) + DELM* ABONDL(K)
      GO  TO  97
965   TSM(2) =2.* TSM(2)
      TSM(1) =0.
      TSM(3) =0.
970   CONTINUE
C
C     FIND  FORCE  AND  MOMENT COEFFICIENTS
C
C     1.  RESOLUTION  TO  STABILITY  AXES
C
      SAX(1) =-U(1)/SQRT(U(1)**2 + U(3)**2)
      SAX(2) =0.
      SAX(3) =-U(3)/SQRT(U(1)**2 + U(3)**2)
      SAY(1)=0.
      SAY(2)=1.
      SAY(3)=0.
```

```
      CALL VCROSS(SAX,SAY,SAZ,DUMA,DUMB)
      DO    971  K=1,3
      TOTF(K) = TF(K) + TJF(K)
971   TOTM(K) = TM(K) + TJM(K) + TSM(K)
      ROTORG(1) = XCBAR
      ROTORG(2) = 0
      ROTORG(3) = CBAR
      CALL VCROSS(ROTORG,TOTF,TEMP,DUMA,DUMB)
      CALL VPLUS(TOTM.TEMP.TOTM,DUMA,DUMB)
      CALL  VDOT(SAZ,  TOTF, DV1,  CLIFT, DUMA)

      CALL  VDOT(SAX,  TOTF, DV1,  CDRAG, DUMA)

      CALL  VDOT(SAY,  TOTF, DV1,  CSIDE, DUMA)

      CALL  VDOT(SAZ,  TOTM, DV1,  CYAW , DUMA)

      CALL  VDOT(SAX,  TOTM, DV1,  CROLL, DUMA)

      CALL  VDOT(SAY, TOTM, DV1,  CPITCH,  DUMA)

      CPITCH=CPITCH+TOTF(3)*XCBAR -TOTF(1)*ZCBAR

C

C     ADJUST  NON-DIMENSIONALIZING FACTORS  AND SIGNS

C

      CLIFT=-CLIFT/ESS

      CDRAG=-CDRAG/ESS

      CPITCH= CPITCH/(ESS* CBAR)

      CSIDE= CSIDE/ESS

      CROLL =  CROLL/(2.* ESS)

      CYAW  =  CYAW/(2.* ESS )

C

C     COMPUTE STATION LOADINGS IN OUTPUT FORM

C

      DO   1201   I=1, 25

      DO   1202   K=1, 3

1202  TEMP(K)=FOR(I,K) + FJR(I,K)

      CALL VDOT(TEMP, SAX, DV1,  DLOADR(I), DUMC)

      CALL VDOT(TEMP, SAZ, DV1,  UPLODR(I), DUMC)
```

```
      SLOADR(I)=TEMP(2)
      UPLODR(I)=-UPLODR(I)
      DLOADR(I)=-DLOADR(I)
      SECCLR(I)= UPLODR(I)*25./CHDR(I)
1201  SECCDR(I)= DLOADR(I)*25./CHDR(I)
      IF(SYM)  GO TO 1210
      DO 1203   I=1, 25
      DO 1204   K=1, 3
1204  TEMP(K) =FOL(I, K)   + FJL(I,K)
      CALL  VDOT(TEMP, SAZ, DV1, UPLODL(I), DUMC)
      CALL  VDOT(TEMP, SAX, DV1, DLOADL(I), DUMC)
      SLOADL(I) = TEMP(2)
      DLOADL(I)=-DLOADL(I)
      UPLODL(I)=-UPLODL(I)
      SECCLL(I) = UPLODL(I)*25./CHDL(I)
1203  SECCDL(I) = DLOADL(I)*25./CHDL(I)
1210  CONTINUE
C
C     PRINT  RESULTS
C
      NPAGE=NPAGE+1
      WRITE(6,1001) DATE1,DATE2,TITLE, NPAGE
1001  FORMAT(1H1, A10, A2,27X,10A7/40X,50(1H.),22X,*   PAGE *,
     1I2/* WING CHARACTERISTICS-    ASPECT RATIO        SWEEP ANGLE
     2 TAPER RATIO      DIHEDRAL ANGLE          TWIST*)
      WRITE(6,1002) AR, SWEEP,  TAPER, DIHDRL,TWIST
1002  FORMAT(1H ,28X,F5.2,12X,F5.2,* DEG*,11X,F5.3,10X,F5.2,* DEG*,
     110X,F5.2,* DEG*/)
```

```
      WRITE(6,1003)(I, I=1,NPAN)
1003  FORMAT(* FLAP ARRANGEMENT-    *,6(*       PANEL *, I1)/)
      WRITE(6,1004)(FB(I), I=2, NPANP1)
1004  FORMAT(*      END SPAN*,6X,6(10XF4.2))
      WRITE(6,1005)(CF(I), I=1, NPAN)
1005  FORMAT(*      CHORD RATIO    *, 6(10XF4.2) )
      IF(SYM)  GO TO  1100
      WRITE(6, 1006)(DFR(I), I=1, NPAN)
1006  FORMAT(*      RIGHT     DEFLECTION  *,6(F6.2,* DEG    *))
      WRITE(6, 1007)(FFR(I), I=1, NPAN)
1007  FORMAT(*       WING-    EXTENSION     *, 6(F4.2,10X) )
      WRITE(6,1008)(DFL(I),I=1, NPAN)
1008  FORMAT(*      LEFT      DEFLECTION  *, 6(F6.2,* DEG    *))
      WRITE(6,1007)(FFL(I),I=1, NPAN)
      GO TO 1101
1100  WRITE(6, 1009)(DFR(I), I=1,NPAN)
1009  FORMAT(*      DEFLECTION*, 12X, 6(F6.2,* DEG    *))
      WRITE(6, 1010)(FFR(I),I=1, NPAN)
1010  FORMAT(*      EXTENSION *, 14X, 6(F4.2, 10X)/)
      WRITE(6,1011) (BLOS(I),  I=1, NPAN)
1011  FORMAT(* BLOWING DISTRIBUTION-*, 7X, 6(F5.3, 9X)/)
      GO TO 1102
1101  CONTINUE
      WRITE(6,1012) (BLOR(I), I=1, NPAN)
1012  FORMAT(* BLOWING DISTRIBUTION-*/15(1H ),*RIGHT WING    *,6(F5.3,9X
     1))
      WRITE(6,1013) (BLOL(I), I=1, NPAN)
1013  FORMAT(15(1H ),*LEFT WING     *, 6(F5.3, 9X))
```

```
1102  CONTINUE
      IF(SYM) GO TO 1030
      WRITE(6,1031) (CJPR(I), I=1, NPAN)
1031  FORMAT(* PANEL CJ S-   RIGHT WING   *,6(F6.3,8X))
      WRITE(6,1032) (CJPL(I), I=1, NPAN)
1032  FORMAT(*                LEFT  WING   *,6(F6.3,8X))
      GO TO 1034
1030  CONTINUE
      WRITE(6,1033)(CJPR(I), I=1, NPAN)
1033  FORMAT(* PANEL CJ S-*,16X,6(F6.3,8X))
1034  CONTINUE
      IF(BLOWDR.GE.0.) WRITE(6,1014)
      IF(BLOWDR.LT.0.) WRITE(6,1015)
1014  FORMAT(* BLOWING PARALLEL TO PLANE OF SYMMETRY.*)
1015  FORMAT(* BLOWING NORMAL TO HINGE LINE.*)
      WRITE(6,1016) ALFF(NAS), BETA(NBS),  CJ(NJS)
1016  FORMAT(/* FLIGHT CONDITION-     ANGLE OF ATTACK       SIDESLIP ANG
     1LE         OVERALL CJ*/26X, F6.2,* DEG *,10X,F6.2,* DEG*,12X,F5.2)
      WRITE(6,8001) NTRY, EXCESS
8001  FORMAT(* TRIAL *,I3,*,  EXCESS=*,F10.5)
      IF(SYM) GO TO 1103
      WRITE(6, 1017) CLIFT, CDRAG,CSIDE,  CPITCH, CROLL, CYAW
1017  FORMAT(/* FORCE AND MOMENT            LIFT       DRAG       SIDE FORCE
     1             PITCH          ROLL         YAW*/*   COEFFICIENTS*,12X,
     2F6.3,4X,F8.4, F10.4,14XF8.4,5X,F9.5,3X,F9.5/1H ,125(1H.)//* RIGHT
     3WING DATA-*/)
      GO TO 1104
1103  WRITE(6, 1018) CLIFT, CDRAG, CPITCH
```

```
1018  FORMAT(/* FORCE AND MOMENT COEFFICIENTS-   LIFT-*F7.3,*    DRAG-*,
     1F9.4, *      PITCH-*, F9.4/1H ,125(1H.)//* STATION-BY-STATION DATA-
     2*/)
1104  WRITE(6,1019)
1019  FORMAT(* STA  SPAN  CHORD   CIRCU-    LOCAL  WIND-            LOCA
     1L LOADING-              CHORD      SECTION COEFFICIENTS-*/
     2* NO    LOC    (NOM)    LATION    SPEED     ALPHA  BETA   LIFT    DRA
     3G    SIDE        (EXT)          CL           CD            CJ*)
      DO 1105 I=1, 25
1105  WRITE(6,1020) I, QR(I,2), CNOM(I), GR(I), VELR(I), ALFAR(I), BETAR
     1(I), UPLODR(I), DLOADR(I), SLOADR(I),CHDR(I),SECCLR(I),SECCDR(I)
     2, CJR(I)
      IF(SYM) GO TO 1301
1020  FORMAT(1H ,I2,F6.2,2F9.4,F10.3,F8.2, F7.2, F8.4,2F9.5, F7.4,
     1F12.3, F12.5, F12.3)
      NPAGE = NPAGE+1
      WRITE(6,1021)DATE1, DATE2,  NPAGE
1021  FORMAT(1H1, 98XA10, A2,*   PAGE *,I2/* LEFT WING DATA-*/)
      WRITE(6,1019)
      DO 1106  I=1, 25
1106  WRITE(6,1020) I, QL(I,2), CNOM(I), GL(I), VELL(I), ALFAL(I), BETAL
     1(I), UPLODL(I), DLOADL(I), SLOADL(I),CHDL(I),SECCLL(I),SECCDL(I)
     2 ,CJL(I)
1301  CONTINUE
C
C     SET UP NEXT CASE
C
      NAS= NAS+1
```

```
      IF(NAS.LE.NA) GO TO 500
      NAS=1
      NBS= NBS+1
      IF(NBS.LE.NB) GO TO 500
      NBS=1
      NJS=NJS+1
      IF(NJS.LE.NJ) GO TO 450
      NJS=1
      NEXT=XIN(10)
      GO TO (1, 2, 3, 4, 5, 55, 6, 7, 8, 9, 10, 11, 12, 13), NEXT
13    CALL EXIT
      END
      SUBROUTINE  VICTOR (A, B, C, D, E)
      DIMENSION A(3), B(3),  C(3)
      ENTRY VPLUS
      DO 1  J=1,3
    1 C(J)= A(J)+B(J)
      RETURN
      ENTRY VCROSS
      C(1) = A(2)*B(3)-A(3)*B(2)
      C(2) = A(3)*B(1)-A(1)*B(3)
      C(3) = A(1)*B(2)-A(2)*B(1)
      RETURN
      ENTRY VDOT
      D=A(1)*B(1)+A(2)*B(2)+A(3)*B(3)
      RETURN
      ENTRY VMAG
      E=A(1)**2 +A(2)**2 +A(3)**2
```

```
      D= SQRT(E)
      RETURN
      ENTRY  SCALM
      DO 2 J=1,3
    2 C(J)= D*A(J)
      RETURN
      ENTRY VMINE
      DO 3 J=1,3
    3 C(J)=A(J)- B(J)
      RETURN
      ENTRY SCALD
      DO 4  J=1,3
4     B(J)=A(J)/D
      RETURN
      END
      SUBROUTINE  WASH (P,A, Q, W)
      LOGICAL SEGM
      DIMENSION P(3), A(3), Q(3), W(3),  R(3), AXR(3), VD(3), VDD(3)
     1,RR(3),ELL(3) ,WD(3)
      SEGM=.FALSE.
      COST=-1.
10    PI=3.141593
      CALL VMINE(Q, P, R, X, Y)
      CALL VCROSS(A, R, AXR, X, Y)
      CALL VMAG( AXR, VD, VDD, X, DEN)
      IF(DEN.LT.1.0E-10)GO TO 20
      CALL VMAG( R,  VD,  VDD, RM, X)
       IF(RM.LT.1.0E-10)GO TO 20
```

```
      CALL VDOT(A, R, VD, ADR, X)
      FAC=(ADR/RM-COST)/(4.*PI*DEN)
      CALL SCALM(AXR, VD,  W,  FAC, X)
      IF(SEGM)GO TO 30
      RETURN
      ENTRY SEG
      SEGM=.TRUE.
      DO 3 K=1,3
3     WD(K)=A(K)
      CALL  VMINE (Q, A, RR, X, Y)
      CALL  VMINE (A, P, ELL, X, Y)
      CALL  VMAG(ELL, VDD,VD, AM, Y)
      IF(AM.GT.1.0E-10) GO TO 1
20    CONTINUE
      DO 2 K=1,3
2     W(K)=0.
      IF(SEGM)GO TO 30
      RETURN
1     CONTINUE
      AM=1./AM
      CALL SCALM(ELL, VD,  A, AM, X)
      CALL VDOT(A, RR, VD, ADRR, X)
      CALL VMAG(RR, VD, VDD, RRM, X)
      COST= ADRR/RRM
      GO TO  10
30    CONTINUE
      DO 31 K=1,3
31    A(K)=WD(K)
```

To exit, any number $\geq$ 14. is used for the "next case card number". If a number less than 1. is used, an error return will cause termination of execution.

5. Sample Problem

The externally blown flap problem discussed in Section IV is used as a sample problem here.

Figure 22 is the input keypunch form for cards to run a symmetrical five-panel configuration at three angles of attack and one C_J, then to analyze the same case with the fourth panel on the left wing (representing the area behind the left outboard engine) reduced to zero blowing. (The flap deflection is also changed to reflect the fact that the flap centerline angle did not coincide with the jet deflection.)

Output for the symmetrical 7.5° angle of attack case is shown on Page 99. The printed data is mostly self-explanatory. The blowing distribution factors are given in their normalized form. The "local loading" is the force on the strip divided by the semispan squared and by the freestream dynamic pressure. It includes both "circulation" and jet forces. The "section coefficients" are load per unit span divided by local extended chord and by freestream dynamic pressure.

Output for the same case with engine out is shown on Pages 100 and 101. The same data is given, plus the lateral-directional coefficients, the flap arrangement and blowing data for the other wing, and the station-by-station data for the other wing.

TEN FIELD, SEVEN DIGIT CRD FORMAT

1–7	8–14	15–21	22–28	29–35	36–42	43–49	50–56	57–63	64–70	71	72	IDENT 73–80
EXTERNALLY BLOWN FLAPS				(NASA TN D-6391)								1
7.23	27.5	.336	-3.5	-3.5	1.							2
.16	.28	.36	.48	1.0								3
.28	.28	.28	.28	.28								4
1.16	1.16	1.16	1.16	1.16								5
1.16	1.16	1.16	1.16	1.16								6
1.	0.											7
3.	-5.0	7.5	20.0									8
0.	1.	0.	1.	0.								9
0.	1.	0.	1.	0.								10
49.	49.	40.	49.	40.								11
49.	49.	40.	49.	40.								12
1.	1.55								10.			13
0.	1.	0.	0.	0.								10A
49.	49.	40.	49.	40.								11A
49.	49.	40.	40.	40.								12A
1.	1.162								14.			13A

TITLE NAME DATE PAGE OF

Figure 22: Input Keypunch Form for Externally Blown Flap Problem

JUN 01, 1973 EXTERNALLY BLOWN FLAPS (NASA TN D-6391)

WING CHARACTERISTICS-	ASPECT RATIO	SWEEP ANGLE	TAPER RATIO	DIHEDRAL ANGLE	TWIST
	7.23	27.50 DEG	.336	-3.50 DEG	-3.50 DEG

FLAP ARRANGEMENT-	PANEL 1	PANEL 2	PANEL 3	PANEL 4	PANEL 5	PANEL
END SPAN	.16	.28	.36	.43	1.00	
CHORD RATIO	.23	.23	.23	.28	.26	
DEFLECTION	49.00 DEG	49.00 DEG	40.00 DEG	49.00 DEG	40.00 DEG	
EXTENSION	1.16	1.16	1.16	1.16	1.16	
BLOWING DISTRIBUTION-	0.000	.500	0.000	.500	0.000	
PANEL CJ S-	0.000	5.052	0.000	5.363	0.000	

BLOWING PARALLEL TO PLANE OF SYMMETRY.

FLIGHT CONDITION-	ANGLE OF ATTACK	SIDESLIP ANGLE	OVERALL CJ
	7.50 DEG	0.00 DEG	1.55

TRIAL 36, EXCESS= .00990

FORCE AND MOMENT COEFFICIENTS- LIFT- 4.631 DRAG- -.2402 PITCH- -1.2354

STATION-BY-STATION DATA-

STA NO	SPAN LOC	CHORD (NOM)	CIRCU-LATION	LOCAL SPEED	WIND- ALPHA	BETA	LOCAL LOADING- LIFT	DRAG	SIDE	CHORD (EXT)	SECTION COEFFICIENTS- CL	CD	CJ
1	.02	.4136	.4265	1.134	-25.31	.49	.0316	.02263	-.00744	.4740	1.665	1.19360	0.000
2	.06	.3976	.4447	1.049	-5.43	.75	.0367	.00529	.00650	.4612	1.957	.44909	0.000
3	.10	.3366	.4792	1.054	-6.47	1.15	.0397	.00962	.00021	.4465	2.211	.53565	0.000
4	.14	.3756	.5261	.963	-9.35	-.74	.0563	-.00515	-.00256	.4357	3.226	-.29576	1.367
5	.18	.3545	.5803	.911	-12.30	-3.17	.0757	-.01547	-.00724	.4230	4.475	-.91447	2.316
6	.22	.3536	.6351	.845	-19.61	-5.25	.0991	-.01206	-.01537	.4102	6.039	-.73654	4.355
7	.25	.3426	.6855	.633	-19.51	-6.65	.0799	-.00161	-.01365	.3974	5.024	-.11353	2.997
8	.30	.3316	.7253	.530	-22.96	-7.10	.0603	.01442	-.01200	.3547	3.917	.93715	1.545
9	.34	.3206	.7496	.550	-21.70	-5.67	.0636	.01405	-.01140	.3719	4.272	.94672	1.631
10	.38	.3096	.7576	.657	-15.61	-5.06	.0853	-.00129	-.01313	.3592	5.961	-.09004	3.316
11	.42	.2366	.7461	.593	-13.27	-3.09	.1044	-.02712	-.01005	.3464	7.534	-1.35762	5.157
12	.46	.2376	.7233	.951	-5.39	-.75	.0541	-.02247	-.00260	.3335	6.303	-1.66352	3.570
13	.50	.2766	.5660	1.026	-2.99	1.47	.0672	-.01245	.00256	.3209	5.239	-.97036	1.556
14	.54	.2656	.5411	1.063	2.60	2.65	.0565	.00325	.00504	.3081	4.605	.26555	0.000
15	.58	.2545	.5330	1.062	6.63	2.05	.0522	-.00277	.00611	.2954	4.415	-.23447	0.000
16	.62	.2436	.5457	1.100	11.93	2.16	.0467	-.00529	.00694	.2826	4.304	-.46794	0.000
17	.66	.2326	.5049	1.107	13.25	2.30	.0451	-.00603	.00667	.2699	4.161	-.55562	0.000
18	.70	.2216	.4656	1.102	13.33	2.37	.0417	-.00572	.00627	.2571	4.055	-.55633	0.000
19	.74	.2106	.4370	1.090	12.75	2.35	.0365	-.00499	.00749	.2443	3.943	-.51052	0.000
20	.78	.1996	.4079	1.079	12.13	2.39	.0356	-.00432	.00676	.2315	3.645	-.40597	0.000
21	.82	.1356	.3791	1.073	11.65	2.41	.0329	-.00351	.00622	.2185	3.763	-.44652	0.000
22	.86	.1776	.3500	1.067	11.66	2.47	.0303	-.00356	.00570	.2061	3.673	-.43172	0.000
23	.90	.1666	.3223	1.049	10.22	2.51	.0275	-.00261	.00466	.1933	3.554	-.33757	0.000
24	.94	.1556	.2943	1.031	5.31	2.41	.0240	-.00032	.00326	.1805	3.330	-.04461	0.000
25	.98	.1445	.2257	1.019	6.65	2.57	.0165	-.00135	.00510	.1673	2.799	-.20167	0.000

REFERENCES

1. Spence, D. A., "The Lift Coefficient of a Thin, Jet Flapped Wing." Proceedings of the Royal Society (A), Volume 238, pp 46-48.

2. Spence, D. A., "The Lift on a Thin Aerofoil with a Jet-Augmented Flap," Aeronautical Quarterly, Vol. 9, 1958.

3. Malavard, L., "Recent Developments in the Method of Rheoelectric Analogy Applied to Aerodynamics," Journal of the Aeronautical Sciences, Volume 24, No. 5, May 1957.

4. Maskell, E. C., and Spence, D. A., A Theory of the Jet Flap in Three Dimensions, Royal Aircraft Establishment, Report No. Aero 2612, September 1958.

5. Malavard, L., "Application of the Rheoelectric Analogy for the Jet Flap Wing of Finite Span," Boundary Layer and Flow Control, ed. G. V. Lachmann, Pergamon Press, New York, 1967.

6. Lopez, M. L., and Shen, C. C., Recent Developments in Jet Flap Theory and Its Application to STOL Aerodynamic Analysis, AIAA Paper No. 71-578, June 1971.

7. Lissaman, P. B. S., Analysis of High Aspect Ratio Jet Flap Wings of Arbitrary Geometry, AIAA Paper No. 73-125, January 1973.

8. Helmbold, H. B., "Limitations of Circulation Lift," Journal of the Aeronautical Sciences, Volume 24, No. 3, March 1957.

9. Lockwood, V. E., Turner, T. R., and Riebe, J. M., Wind Tunnel Investigation of Jet Augmented Flaps on a Rectangular Wing to High Momentum Coefficients, NACA TN 3865, December 1956.

10. Wygnanski, I., and Newman, B. G., "The Effect of Jet Entrainment on Lift and Moment for a Thin Aerofoil with Blowing," Aeronautical Quarterly, May 1964.

11. Gainer, T. G., Low Speed Wind Tunnel Investigation to Determine the Aerodynamic Characteristics of a Rectangular Wing Equipped with a Full Span and an Inboard Half Span Jet Augmented Flap Deflected 55°, NASA Memo 1-27-59C, February, 1959.

12. Rauscher, Manfred, Introduction to Aeronautical Dynamics, New York, 1953.

13. Monk, J. R., Lee, J. L., and Palmer, J. P., STOL Tactical Aircraft Investigation - Analysis of Wind Tunnel Data: Vectored Thrust/Mechanical Flaps and Internally Blown Jet Flaps, AFFDL TR-73-19, Volume IV, May 1973.

UNCLASSIFIED
Security Classification

DOCUMENT CONTROL DATA - R&D

(Security classification of title, body of abstract and indexing annotation must be entered when the overall report is classified).

1. ORIGINATING ACTIVITY (Corporate author) Boeing Aerospace Company P.O. Box 3999 Seattle, Washington 98124	2a. REPORT SECURITY CLASSIFICATION Unclassified 2b. GROUP ------

3. REPORT TITLE
STOL Tactical Aircraft Investigation - A Lifting Line Analysis Method for Jet Flapped Wings

4. DESCRIPTIVE NOTES (Types of report and inclusive dates)
Final Technical Report June 1971 to March 1973

5. AUTHORS (First name, middle initial, last name)
Franklyn J. Davenport

6. REPORT DATE	7a. TOTAL NO. OF PAGES	7b. NO. OF REFS
June, 1973	104	15

8a. CONTRACT OR GRANT NO. AF 33615-71-C-1757	9a. ORIGINATOR'S REPORT NUMBERS AFFDL TR-73-19
b. Project No. 643A	
c.	9b. OTHER REPORT NO(S) (Any other numbers that may be assigned this report) Boeing Doc. No. D180-14409-2
d.	

10. DISTRIBUTION STATEMENT
Approved for public release; distribution unlimited.

11. SUPPLEMENTARY NOTES	12. SPONSORING MILITARY ACTIVITY
	Air Force Flight Dynamics Laboratory Wright Patterson Air Force Base, Ohio 45433

13. ABSTRACT

An analytical procedure is developed for jet flapped wings, in which three-dimensional features of the trailing vortex system are represented. More conservative induced drag is predicted than by analyses based on the traditional planar vortex system. Illustrative examples are given showing that this method gives better agreement with measured drag than the planar-vortex methods.

DD FORM 1 NOV 65 1473
DI 4802 1030 ORIG. 3/71
PART 1 OF 3

UNCLASSIFIED
Security Classification

14. KEY WORDS	LINK A		LINK B		LINK C	
	ROLE	WT	ROLE	WT	ROLE	2T
Jet Flaps						
STOL Aerodynamics						
Induced Drag						
Lifting Line						